DOE/ER/10749-1

MASTER

A THEORETICAL STUDY OF ELECTRON CAPTURE IN ION-ION AND ION-ATOM COLLISIONS

Progress Report

For the Period September 1, 1980 - April 30, 1981

M. Lieber
F. T. Chan
Department of Physics
University of Arkansas
Fayetteville, Arkansas

April 1981

Prepared For

The Department of Energy under Contract No. DE-AS05-80ER10749

DISCLAIMER

ABSTRACT

The eikonal approximation has been recently shown to be of significant utility in the study of electron capture cross sections for energetic ion-atom collisions. The method generally gives much better agreement with available experimental data than does the simple OBK approximation without substantially increasing the difficulty of computation.

In the present work we have computed the total cross section for electron capture into an arbitrary $n\ell$ subshell of H^+, C^{+6}, O^{+8}, and Fe^{+24} ions from ground state hydrogen atoms, at energies of 40-200 keV/nuclear (30-100 keV in the H^+ case). These species were selected because of their importance in fusion studies. Interesting variations with ℓ were obtained. Cross sections for capture into an arbitrary final n-shell, or into all final bound states were also obtained.

We have successfully derived an analytic closed form expression for electron capture from an arbitrary initial $n\ell m$ state to an arbitrary final $n'\ell'm'$ state of a hydrogenic target. Numerical results are presented for all $n' = 2,3$ final states in hydrogen, which may be subjected to experimental test in the near future.

Finally, we have studied extension of the eikonal method to multielectron targets. We find that there are ambiguities in the method requiring further analysis. Agreement with experimental data is nevertheless satisfactory, but the high energy results are suspect.

I. Introduction

In recent years the work of Eichler and Chan has shown that the eikonal approximation may be very useful for calculating electron capture cross sections in energetic ion-atom collisions. Since September 1, 1980, Dr. F. T. Chan and Dr. M. Lieber have devoted an estimated 25% of their time to applications and extensions of this method. They were assisted by Mr. T. S. Ho, a full time graduate student.

As a result of this effort three projects have been completed, and papers submitted to Physical Review A for each. (Preprints of those papers are appended.) The three projects are:

A. Eikonal Calculation of Electron Capture Cross Sections in Collisions of H-atoms with Fast Projectiles

B. Eikonal Calculation of Electron Capture Cross Sections from an Arbitrary n&m-shell of a Hydrogenic Target into an Arbitrary n'&'m'-shell of a Fast Bare Projectile

C. Eikonal Approximation for Charge Transfer from a Multi-Electron Atom to Fast Projectiles

Those three projects are described briefly below. (At this writing the work on He^+, described in the original proposal, is in progress.)

II. Eikonal Calculation of Electron Capture Cross Section in Collisions of H-atoms with Fast Projectiles

We have employed the eikonal method to calculate the cross section for the capture, into an arbitrary n&-subshell, of an electron, in collisions between hydrogen atoms and fast projectiles. The projectiles were protons, C^{+6}, O^{+8}, and Fe^{+24}. The energy ranges considered were 30-100 keV in the proton case, and 40-200 keV per nucleon in the other cases. These projectiles

were selected because of their importance in fusion plasmas. For the highly charged case of Fe^{+24} we found that our formulas, while exact, involved a high degree of cancellation and produced unreliable numerical results, so that a numerical integration of the penultimate formula was substituted. In the proton case agreement with recent experimental data is excellent. (See Fig. 1).

For the three heavier projectiles we also calculated the cross section for capture to any bound state (Fig. 1), and to a specific n shell (a typical example, O^{+8}, is shown in Fig. 3) and to a specific nℓ-subshell (O^{+8} case shown in Fig. 4 for one selected energy and several values of n).

III. Eikonal Calculation of Electron Capture Cross Sections from an Arbitrary nℓm Shell of a Hydrogenic Target into an Arbitrary n'ℓ'm' Shell of a Fast Bare Projectile

Using techniques similar to those previously employed the eikonal approximation was applied to the evaluation of the cross section for electron capture from an arbitrary nℓm shell of a hydrogenic target atom into an arbitrary n'ℓ'm' of a fast hydrogenic projectile. The results were obtained in exact analytical closed form. Numerical results were computed for the case $H^+ + H(1s) \rightarrow H(n'\ell'm') + H^+$ when n'=2 and 3 and comparison made with the corresponding OBK results. In Fig. 5 we show the n'=2 results. While no experimental data are available, the experiment may be done in the near future (R. Knize, private communication). Some assistance in this project was provided by Mr. David K. Umberger and Mr. Ray-Long Day.

IV. Eikonal Approximation for Charge Transfer from Multi-Electron Atom to Fast Projectiles

We attempted to extend the eikonal approach developed previously for calculating electron capture cross sections for bare projectiles colliding with hydrogenic targets to allow for multi-electron targets. Both the

impact and wave pictures were employed and their equivalence discussed. As a first approximation, each atomic orbital is specified by the three hydrogenic quantum numbers, an effective nuclear charge Z_t , and an energy eigenvalue in the impact picture, or ionization potential in the wave picture. The Z_t' appearing in the eikonal phase factor is ambiguous because of incomplete information on the many-body target. However, analytic expressions were derived for the theoretical cross sections, and numerical values calculated for simple choices of Z_t'. Those results were compared with existing experimental data for C, Ne, Ar, N_2, O_2, and He targets. As examples, we exhibit Figs. 6. and 7.

In Fig. 6 we show several comparisons of data with the eikonal computations, with $Z_t' = 1$ (which should be a good approximation if large distances from the target are important), $Z_t' = Z_t$ (which should be good if small distances dominate) and the OBK results ($Z_t' = o$). The data appear to lie within the extreme eikonal cases $Z_t' = 1$ and $Z_t' = Z_t$. But Fig. 7 shows data where at the highest energies the data begin to favor the OBK result and generally tend to lie above the eikonal calculations. We conclude that further investigation of the role of Z_t' is needed.

Some assistance with this project was provided by Dr. Kazem Omidvar of NASA.

V. Publications and Presentations

The results described in sections II, III, and IV have been submitted for publication in Physical Review A. Preprints have been appended to this report.

In addition, the results of section II were presented to the American Physical Society meeting at New York on February 1, 1981 (Abstract, published in the Bulletin of the APS, is attached). The results of section III have

been submitted for presentation at the XII I.C.P.E.A.C. meeting in Gatlinburg, Tennessee in July, 1981. In addition, Dr. M. Lieber delivered an invited colloquium address at Louisiana State University (Baton Rouge) where this research was presented and discussed. Dr. Lieber and Dr. Chan attended the D.O.E. Contractors Workshop on April 1, 2 at Argonne National Lab; a summary of the present research was included in the proceedings of that meeting.

On April 7, 1981 Mr. Tak-San Ho successfully defended his Ph.D. dissertation, which was largely based upon the present research. Mr. Ho will receive his Ph.D. degree in May 1981 and will then go to the Hahn-Meitner Institute in West Berlin to do postdoctoral research.

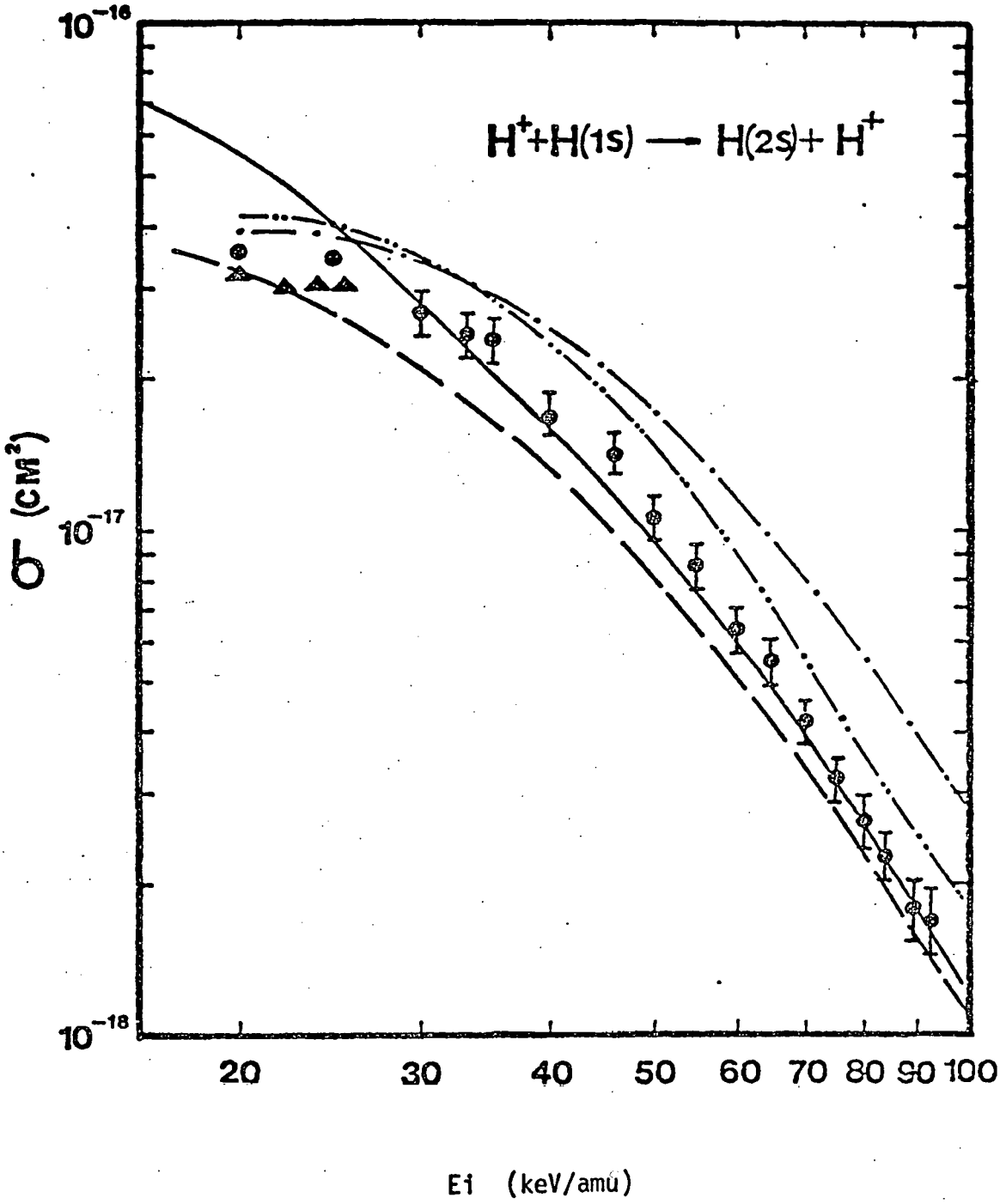

Fig. 1: Cross sections for the process $H^+ + H(1s) \rightarrow H(2s) + H^+$, as a function of the projectile energy. Theory: solid curve, present calculations; dashed curve, Born approximation; dashed-dotted curve, 7-state (4 hydrogenic and 3 pseudostates) close-coupling calculation; dashed-double-dotted curve, 34-state scaled, hydrogenic close-coupling calculation. Experiment: T. J. Morgan et al.; J. Hill et al.

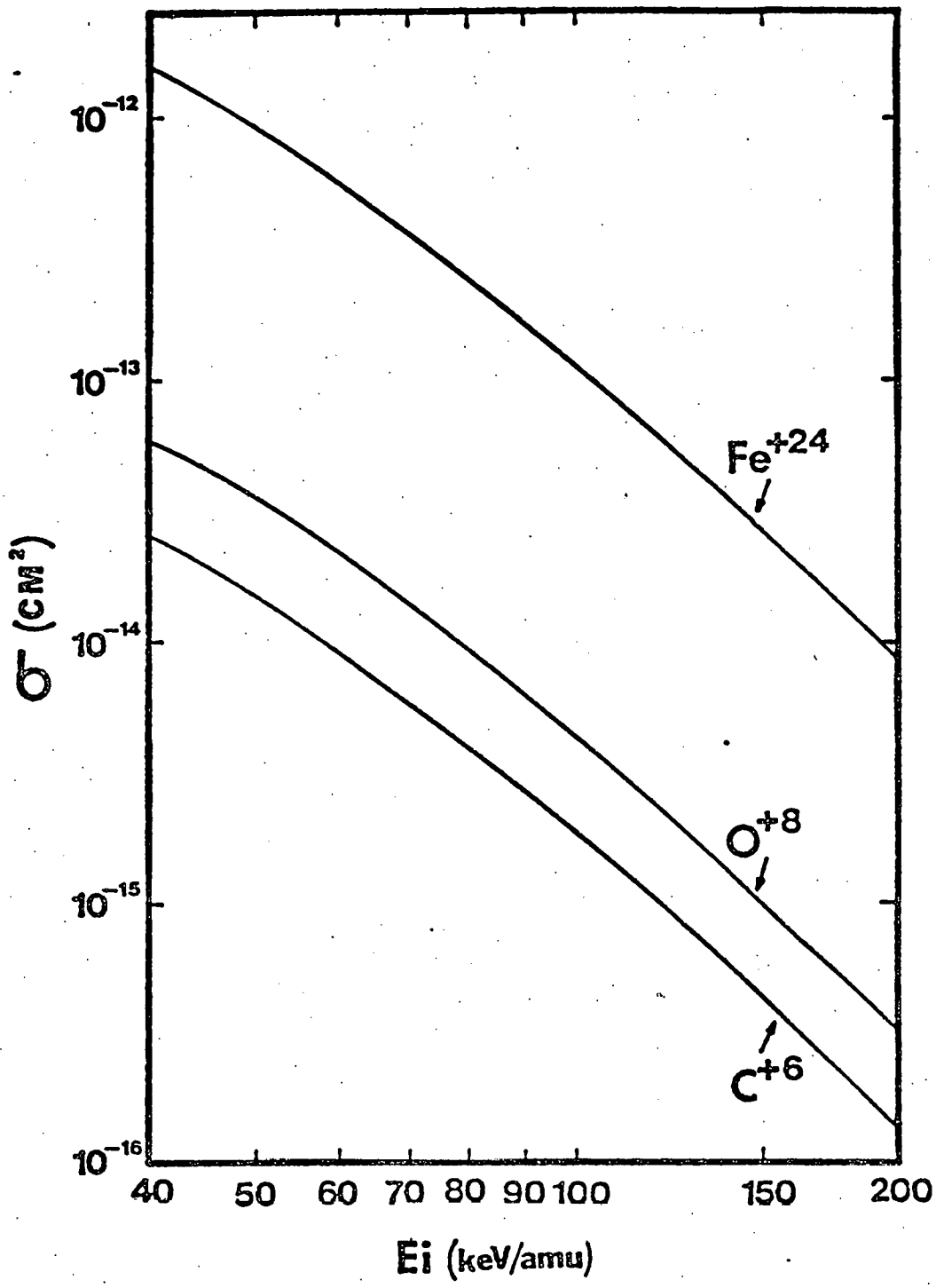

Fig. 2: Total cross sections, as a function of the projectile energy, of the processes: (i) $C^{+6} + H(1s) \rightarrow C^{+5} + H^{+}$; (ii) $O^{+8} + H(1s) \rightarrow O^{+7} + H^{+}$; (iii) $Fe^{+24} + H(1s) \rightarrow Fe^{+23} + H$.

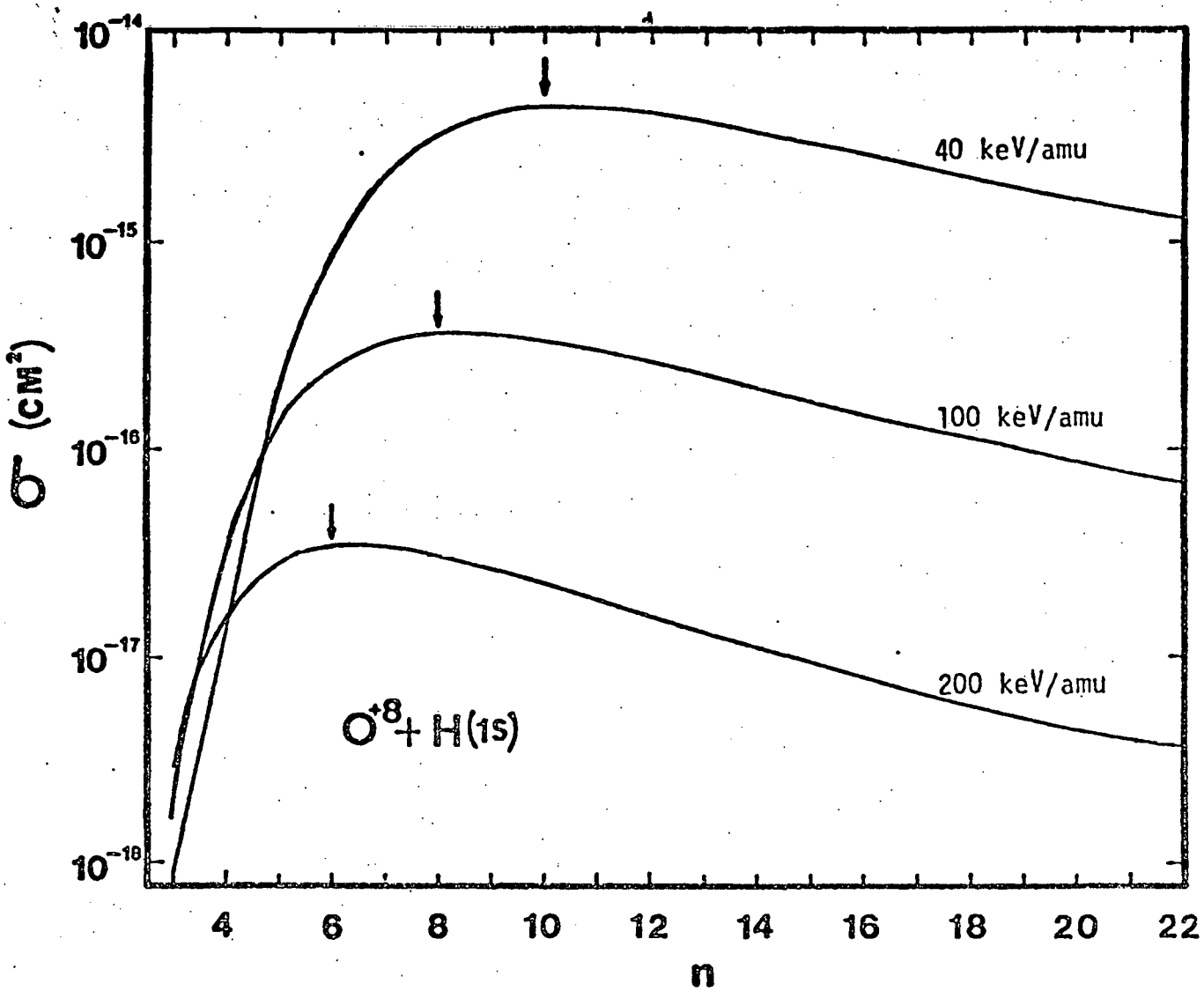

Fig. 3: Capture cross sections into different principal shells as a function of n at energies 40, 100, and 200 keV/amu for the process O^{+8} + H(1s) → O^{+7} (n) + H^{+}.

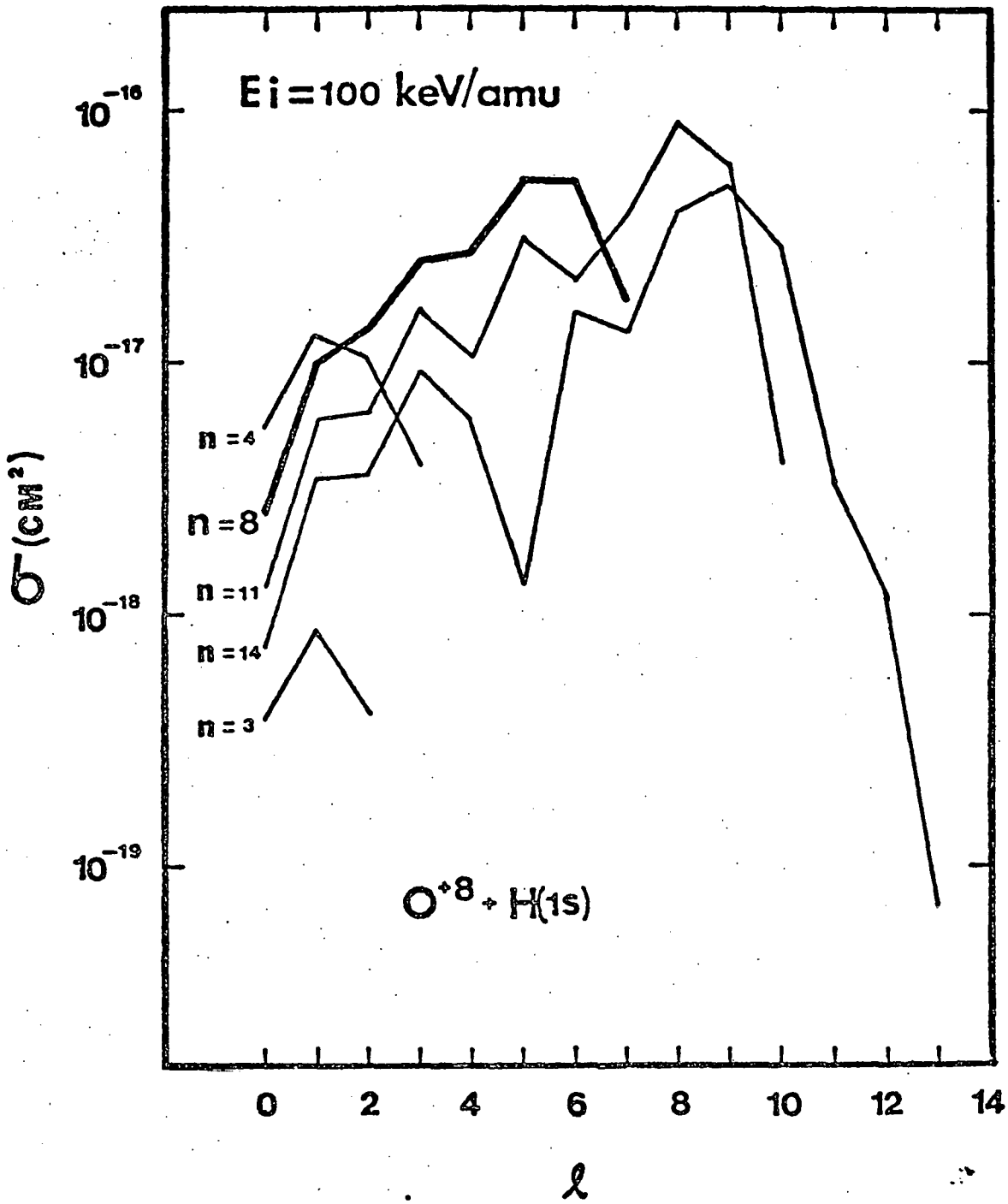

Fig. 4: Capture cross sections into nℓ subshells as a function of ℓ at energy 100 keV/amu for the process $O^{+8} + H(1s) \rightarrow O^{+7}(n\ell) + H^{+}$. The heavy solid line denotes the principal shell n at which the curve peaks when $\sigma_{1s-n}(v)$ is plotted against n.

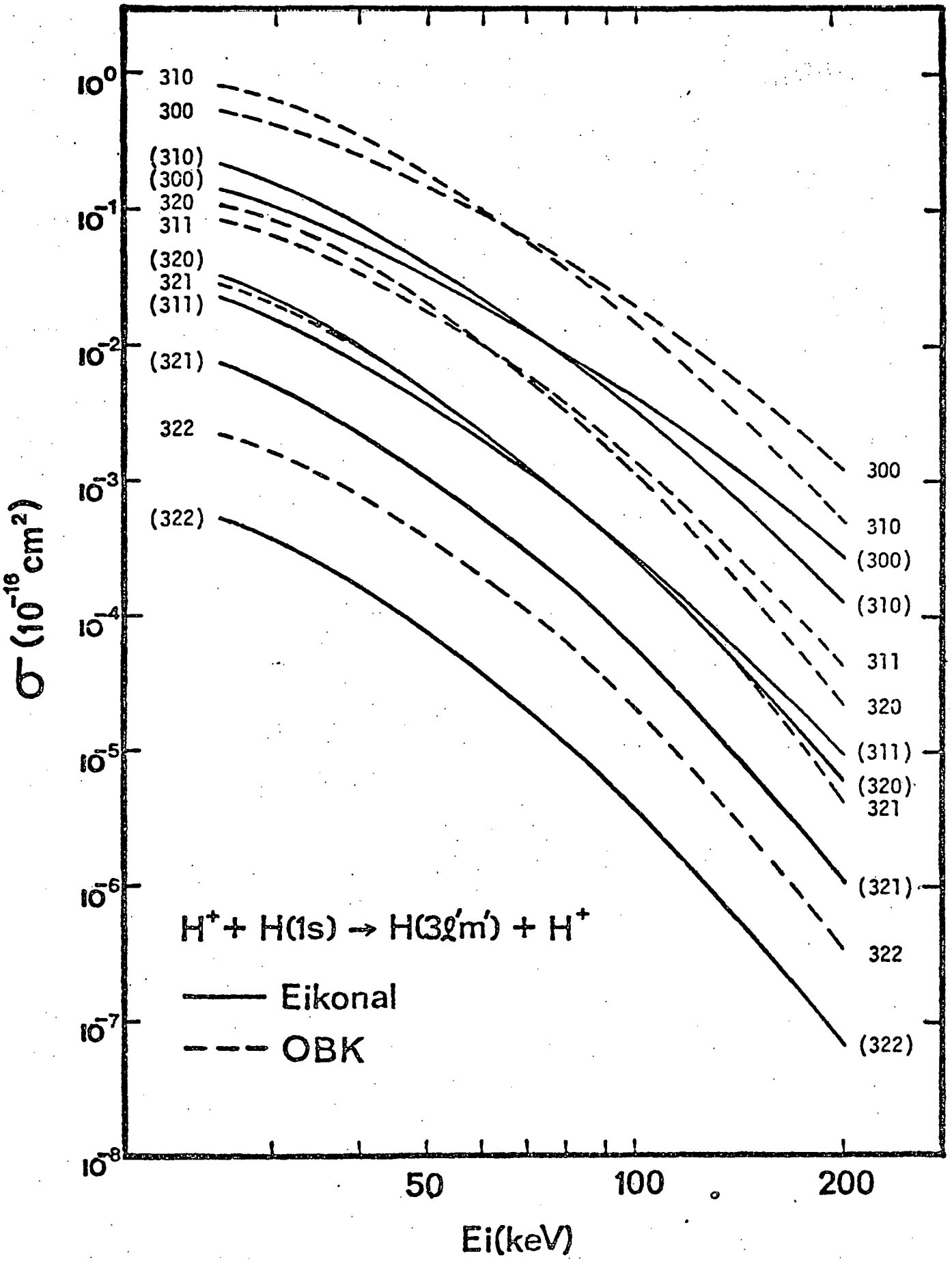

Fig. 5: Eikonal and OBK cross sections for 1s → 3ℓm.

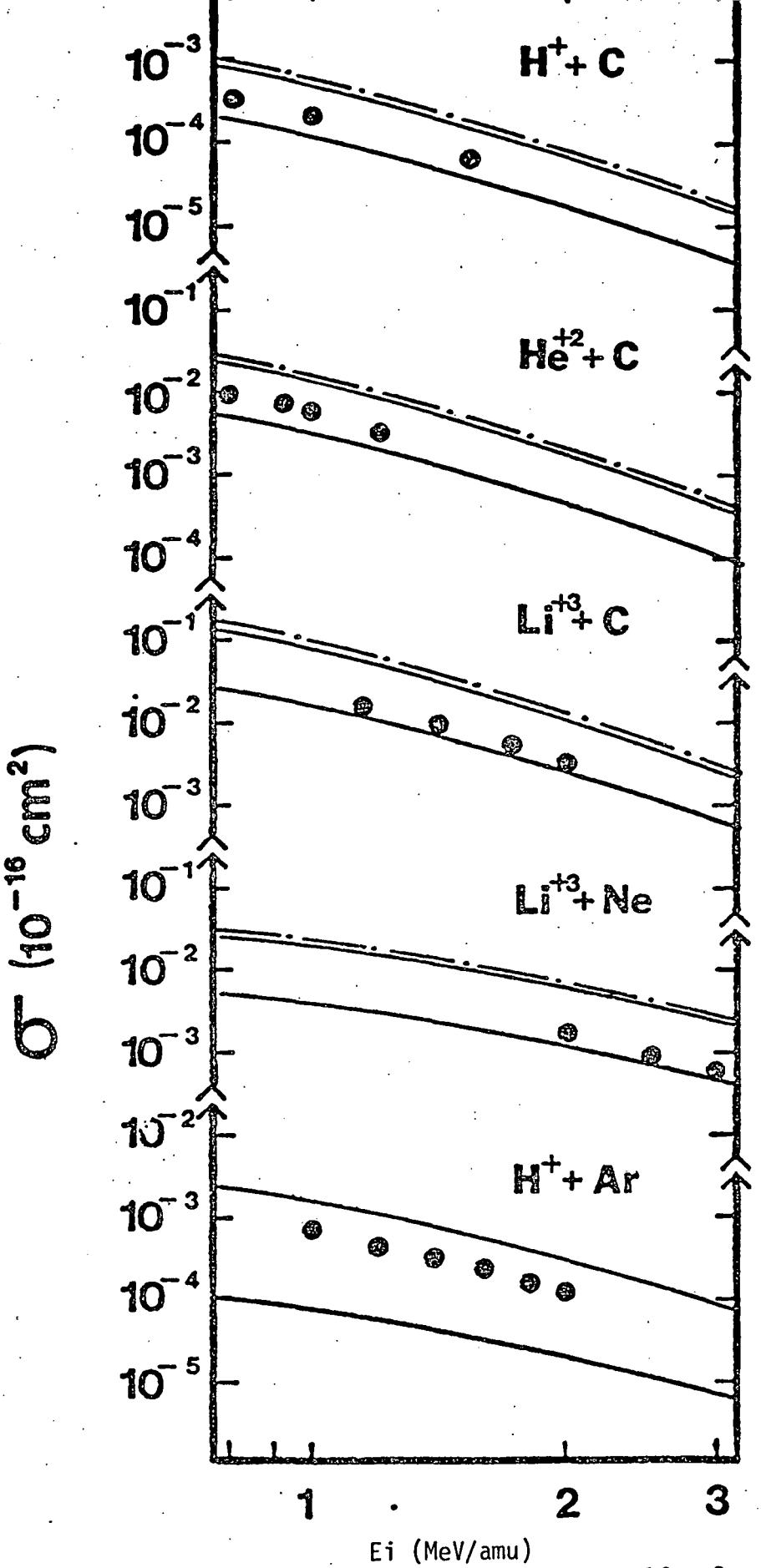

Fig. 6: Total electron capture cross sections (in 10^{-16} cm^2) as a function of energy (in MeV/amu). The electrons are captured from K-shell of atoms C and Ne, but from L-shell of Ar. Theory: upper solid curves, $Z_t' = Z_t$ eikonal results; dashed curves, OBK results. Experiment (dotted)

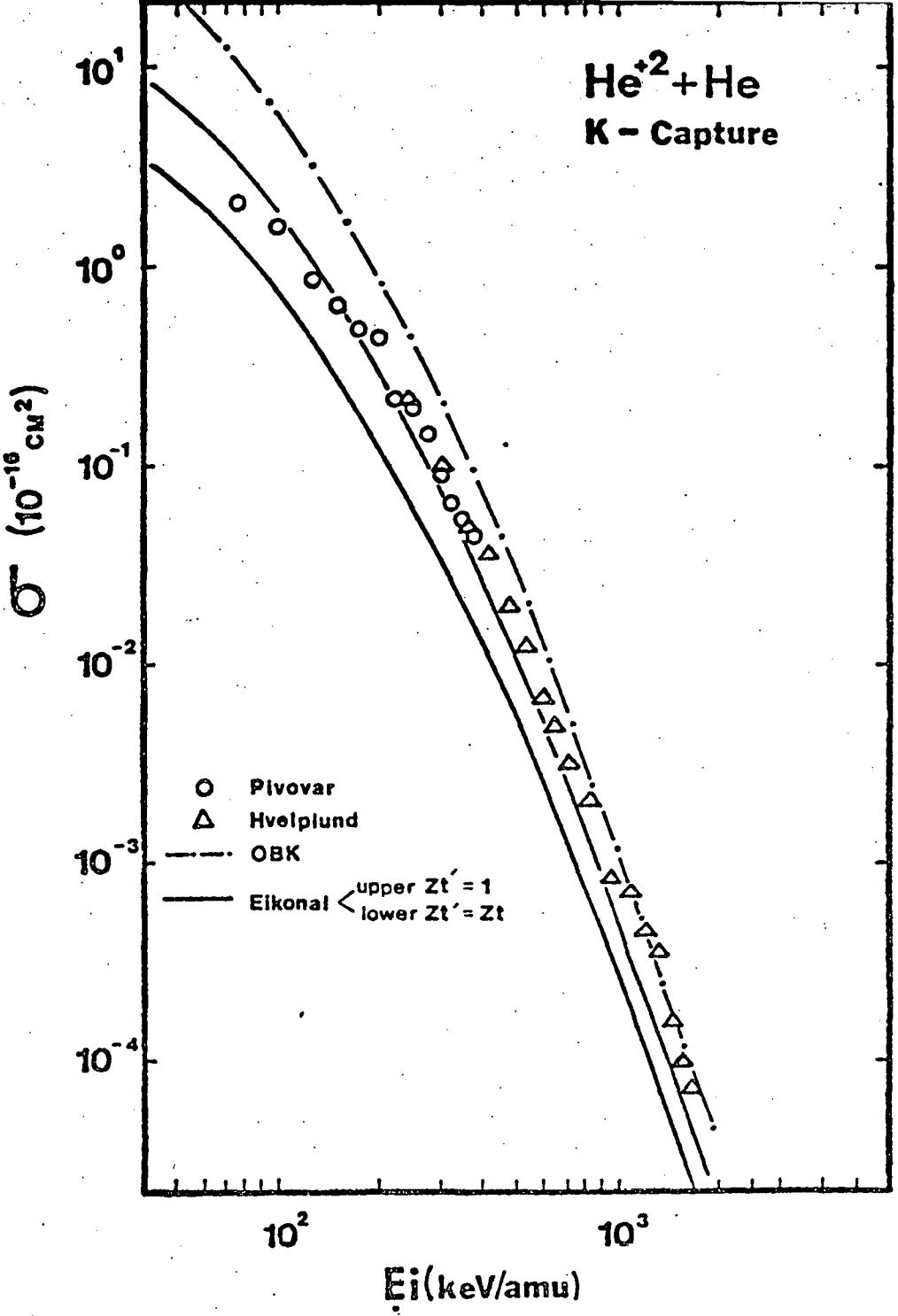

Fig. 7: Total cross sections (in 10^{-16} cm^2), as a function of energy (in KeV/amu), of the electron capture from helium by α-particle. Theory: upper solid curve, $Z_t' = 1$ eikonal results; lower solid curve, $Z_t' = Z_t$ eikonal results; dashed curve, OBK results. Experiment: o , Pivover et al.; Δ, Hvelpund et al.

Abstract Submitted

for the New York Meeting of the

American Physical Society

26-29 Jan. 1981

PACS
Number 34

Suggested Title of session in which paper should be placed:
Atomic Collision Theory

Eikonal Calculation of Electron Capture Cross Section in Collisions of H-atoms with Fast Projectiles.*
M. LIEBER, T. S. HO and F. T. CHAN, Univ. of Arkansas, Fayetteville.--We have employed the eikonal method to calculate the cross section for the capture into an arbitrary $n\ell$-subshell of an electron, in collisions between hydrogen atoms and fast projectiles. The projectiles were protons, C^{+6}, O^{+8}, and Fe^{+24}. The energy ranges considered were 30-100 keV in the proton case, and 40-200 keV per nucleon in the other cases. These projectiles were selected because of their importance in fusion plasmas. In the proton case agreement with recent experimental data[1] is excellent.

*Supported by DOE Contract DEAS05-80ER10749.

[1]T.J. Morgan, J. Stone, and R. Mayo, Phys. Rev. A 22, 1460 (1980).

Prefer regular session

Michael Lieber
Signature of A.P.S. Member

Michael Lieber

Dept. of Physics

University of Arkansas

Fayetteville, AR 72701

Abstract Submitted to XII I.C.P.E.A.C.

(Gatlinburg TN, July 1981)

EIKONAL CALCULATION OF ELECTRON CAPTURE CROSS SECTIONS FROM AN ARBITRARY $n\ell m$ SHELL OF A HYDROGENIC TARGET INTO AN ARBITRARY $n'\ell'm'$ SHELL OF A FAST BARE PROJECTILE*

T. S. Ho, D. Umberger, R. L. Day, M. Lieber, and F. T. Chan

University of Arkansas, Fayetteville, AR 72701

Using techniques similar to those previously employed[1] the eikonal approximation is applied to the evaluation of the cross sections for electron capture from an arbitrary $n\ell m$ shell of a hydrogenic target atom of nuclear charge Z_t into an arbitrary $n'\ell'm'$ of a fast hydrogenic projectile of nuclear charge Z_p. The cross section can be written as a two-dimensional integral

$$\sigma_{n\ell m\to n'\ell'm'}(v) = \frac{2^4\pi^4 Z_p^2}{v^2}\int\left\{|g_{n'\ell'm'}(\vec{P}+\vec{v})|^2 \times |G_{n\ell m}(\vec{P})|^2\right\}_{P_z=P_{0z}} d\vec{P}_b \qquad (1)$$

with

$$P_{0z} = -\frac{1}{2}v + \frac{1}{v}\left(\frac{1}{2}\frac{Z_t^2}{n^2} - \frac{1}{2}\frac{Z_p}{n'^2}\right)$$

and $\vec{P}_b$ projection of $\vec{P}$ onto the plane normal to $\vec{v}$, the constant velocity of the projectile. The quantities $g_{n'\ell'm'}(\vec{\beta})$ and $G_{n\ell m}(\vec{P})$ are two Fourier transforms defined through the following relations

$$g_{n'\ell'm'}(\vec{\beta}) = (2\pi)^{-3/2}\int[\varphi_{n'\ell'm'}(\vec{r}_p)/r_p] \times \exp(i\vec{\beta}\cdot\vec{r}_p)\, d^3r_p \qquad (2)$$

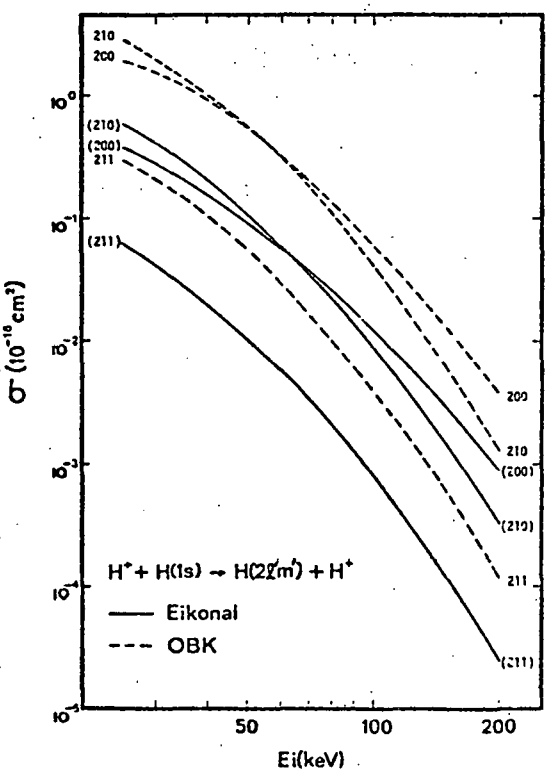

Fig.1. Charge capture cross sections for the process $H^+ + H(1s) \to H(2,\ell',m') + H^+$.

and

$$G_{n\ell m}(\vec{p}) = (2\pi)^{-3/2}\int \varphi_{n\ell m}(\vec{r}_t)\exp\left(-i\int_t^{\infty}\frac{z_t'}{r_t'}dt'\right)\exp(i\vec{p}\cdot\vec{r}_t)\,d^3r_t \qquad (3)$$

with the eikonal phase factor introduced in Eq.(3), and $\varphi_{n\ell m}(\vec{r}_t)$ and $\varphi_{n'\ell'm'}(\vec{r}_p)$ hydrogenic wave functions. We have succeeded in calculating $\sigma_{n\ell m - n'\ell'm'}(v)$ in an exact analytic, closed form. In Figs. 1 and 2, our numerical results are presented for the case $H^+ + H(1s) \rightarrow H(n'\ell'm') + H^+$ when n'=2 and 3. We note that the curvatures of both eikonal and OBK curves for a specific transition are very much alike except the two curves come closer as the energy increases.

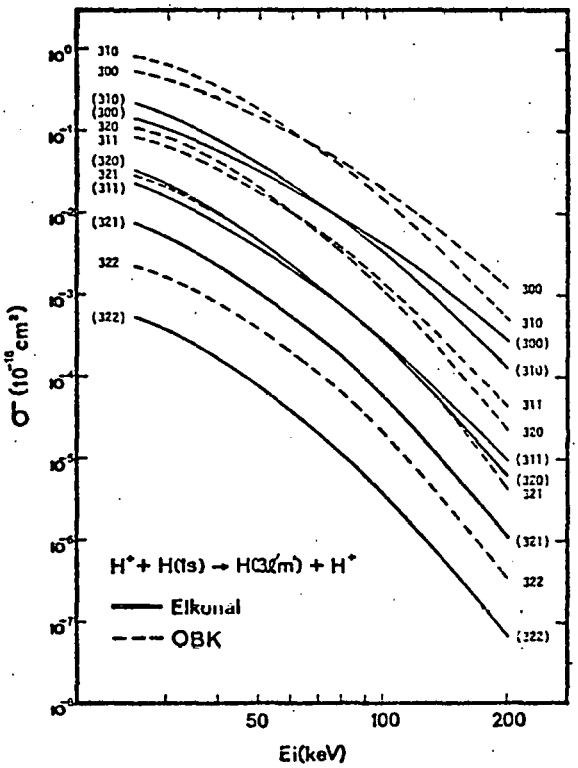

Fig. 2. Charge capture cross sections for the process $H^+ + H(1s) \rightarrow H(3,\ell'm') + H^+$ as a function of the collision energy.

1. F. T. Chan and Jörg Eichler, Phys. Rev. Lett. 42, 58 (1979).

* Research supported in part by DOE under Contract No. DEAS05-80ER10749.

Eikonal Calculation of Electron Capture Cross Section in Collisions of H-atoms with Fast Projectiles

T. S. Ho, M. Lieber, and F. T. Chan

University of Arkansas, Fayetteville, Arkansas 72701

We have employed the eikonal method to calculate the cross section for the capture, into an arbitrary $n\ell$-subshell, of an electron, in collisions between hydrogen atoms and fast projectiles. The projectiles were protons, C^{+6}, O^{+8}, and Fe^{+24}. The energy ranges considered were 30-100 keV in the proton case, and 40-200 keV per nucleon in the other cases. These projectiles were selected because of their importance in fusion plasmas. In the proton case agreement with recent experimental data is excellent.

CONTENTS

INTRODUCTION

Recently there has been recognized a need to study certain charge transfer reactions in controlled thermonuclear fusion research[1,2]. For example, in fusion plasmas, one of the most promising methods of heating and fueling a Tokamak fusion plasma is by injection of fast neutral H^0 and D^0 atoms. However, there is usually a considerable amount of highly stripped impurity ions such as C, O, N, Si, Ar, Fe, Co, Cu, Nb, Mo, or W contained in the plasma. When the injected H^0 or D^0 atom collides with one of these impurity ions, it is quite probable that the injected particle will lose its electron, either by charge exchange or ionization. If this occurs on the outer edge of the plasma, the ionized H or D atom will be magnetically deflected out of the plasma, strike the container walls and therefore produce more impurity atoms. On the other hand the heated plasma may lose its energetic fuel particles (p, d, or t) via charge exchange. Furthermore, the optical spectroscopy of highly charged ions, e. g. iron, provides the means of localized diagnostics of the interior of the plasma which is important in fusion reactor modeling.[3,4] One of the speculations in the observed spectrum is the large rise of the Fe^{+23} light intensity during the high-power neutral beam injection. The most consistent explanation of this phenomenon has been the enhanced recombination of the helium-like Fe^{+24} through charge-exchange with the neutral H^0 or D^0 atoms supplied by the beams. So we need to have a knowledge of cross sections of such charge transfer reactions. In this paper, we carry out, using the eikonal approach[5,6], a detailed study of electron capture

from H (or D) by H^{+1}, C^{+6}, O^{+8}, and Fe^{+24} projectiles in the energy range 40-200 keV/a.m.u. Reliable information on these three reactions[4] is particularly important and is urgently needed for the diagnosis of the role played by impurities in neutral-beam heating of fusion plasmas. Our confidence in the eikonal approach is based on the success already achieved [5,6] in describing a large body of experimental results. In the proton case excellent agreement with recent experimental data[7] is particularly impressive. In summary, we present in this paper calculations on the capture processes listed below,

$$(1) \quad H^+ + H(1s) \longrightarrow H(2s) + H^+ ,$$

$$(2) \quad C^{+6} + H(1s) \longrightarrow C^{+5}(\Sigma, n, n\ell) + H^+ ,$$

$$(3) \quad O^{+8} + H(1s) \longrightarrow O^{+7}(\Sigma, n, n\ell) + H^+ ,$$

and

$$(4) \quad Fe^{+24} + H(1s) \longrightarrow Fe^{+23}(\Sigma, n, n\ell) + H^+ .$$

Here, we remark that (I) the energy ranges from 20 keV to 100 keV for the process (1) while 40 keV/amu to 200 keV/amu otherwise; (II) the symbol Σ inside each parenthesis denotes the summation over all possible final bound states (indexed by the conventional quantum numbers n, ℓ, and m) of the hydrogenic atoms; (III) the ground state (n=1) of Fe^{+23} is excluded among its final states in our calculations because of the previously occupied K-shell of Fe^{+24} (Pauli exclusion principle); and (IV) the ion Fe^{+24} is approximated as a bare projectile because the two K-electrons are so tightly bound by the highly charged nucleus.

METHOD OF CALCULATION

Let M_p be the mass of a bare projectile with nuclear charge Z_p impinging on a hydrogen-like atom with nuclear charge Z_t and mass M_t. We denote the position of the electron with respect to the center of mass, the target, and the projectile nucleus by $\vec{r}$, $\vec{r}_t = \vec{r} + \alpha\vec{R}$, and $\vec{r}_p = \vec{r} - (1-\alpha)\vec{R}$, respectively, with $\alpha = M_p / (M_p + M_t)$ and $\vec{R}$ the relative displacement between two nuclei involved. The propagation of the projectile is defined along a rectilinear trajectory $\vec{R}(t) = \vec{b} + \vec{Z}_R(t) = \vec{b} + \vec{v}t$ with $\vec{b}$ its impact parameter and $\vec{v}$ its incident velocity (assumed to be constant in time). Energies (atomic units are used throughout) $\varepsilon_t = -\frac{1}{2} Z_t^2$ and $\varepsilon_p = -\frac{1}{2} Z_p^2/n^2$ are introduced for the electron, initially bound to the target in the 1s-state, and eventually to the projectile. In evaluating the transition amplitude of the charge transfer process the prior form is adopted for the sake of convenience. We briefly outline the formulae as follows. The transition amplitude is

$$A_{1s\text{-}n\ell m}(\vec{b}, v) = -i\int_{-\infty}^{\infty} dt \left\langle \Psi_{n\ell m}^{(-)} \left| -\frac{Z_p}{r_p} \right| \Psi_{1s} \right\rangle , \tag{1}$$

where

$$\Psi_{1s} = \varphi_{1s}(\vec{r}_t) \exp(-i\varepsilon_t t) \exp(-i\alpha\vec{v}\cdot\vec{r} - \tfrac{1}{2} i\alpha^2 v^2 t) , \tag{2}$$

and

$$\Psi_{n\ell m}^{(-)} \cong \varphi_{n\ell m}(\vec{r}_p) \exp(-i\varepsilon_p t) \exp[i(1-\alpha)\vec{v}\cdot\vec{r} - \tfrac{1}{2} i(1-\alpha)^2 v^2 t] \times \exp\left(-i\int_t^{\infty} \frac{Z_t'}{r_t} dt'\right) . \tag{3}$$

Here $\mathcal{G}_{1S}$ and $\mathcal{G}_{n\ell m}$ are the ground state and arbitrary n,ℓ,m state wave functions of a hydrogenic atom, respectively. The translation factors[8] and the eikonal phase factor[9] are also introduced. The cross section of the capture into arbitrary n,ℓ,m levels of the incident bare ion is then written as

$$\sigma_{1s-n\ell m}(v) = \int |A_{1s-n\ell m}(\vec{b}, v)|^2 \, d^2b \quad . \tag{4}$$

With the help of two well-known sum rules, over m and ℓm, respectively, the capture cross sections into n and nℓ shells, respectively, can be expressed in closed form[5,6], through the relations

$$\sigma_{1s-n\ell}(v) = \sum_{m} \sigma_{1s-n\ell m}(v) \quad , \tag{5}$$

and

$$\sigma_{1s-n}(v) = \sum_{\ell, m} \sigma_{1s-n\ell m}(v) \quad . \tag{6}$$

In computing the total capture cross section (into Σ), we simply sum over n in equation (6) given above, i. e.,

$$\sigma_{1s-\Sigma}(v) = \sum_{n} \sigma_{1s-n}(v) \quad . \tag{7}$$

We remark here that equations (5), (6), and (7) are used in performing calculations for all processes studied in this paper except the case

of $Fe^{+24} + H(1s) \longrightarrow Fe^{+23}(n\ell) + H^+$ with $n \geq 12$. In that situation the computer results from the closed form randomly showed negative signs for some of the $\sigma_{1s-n\ell}(v)$'s, which is obviously physically unacceptable. The reason for this unexpected consequence is believed due to the improper truncation of summands, in the closed form considered, which vary drastically in magnitude and alternate in sign. To circumvent this difficulty in computer summation, we replaced it by performing a numerical integration over $\vec{P}_b$ (the projection on the two-dimensional impact parameter, $\vec{b}$-space of the Fourier counterpart of $\vec{r}_p$ - the position vector of the electron relative to the projectile) rather than using the closed form (which is obtained by analytically performing the $\vec{P}_b$ integration). The integral form employed in numerical work for $\sigma_{1s-n\ell}(v)$ is given below:

$$\sigma_{1s-n\ell}(v) = \frac{2^8 \pi Z_t^5 Z_p^5}{n^3 v^2} \frac{\pi \eta Z_t'}{\sinh(\pi \eta Z_t')} \exp\left[-2\eta Z_t' \tan^{-1}(-P_{oz}/Z_t)\right]$$
$$\times (2\ell+1)\, 2^{4\ell} \frac{(n+\ell)!}{n\,(n-\ell-1)!} \frac{(\ell!)^2}{[(2\ell+1)!]^2} \left(\frac{Z_p^2}{n^2}\right)^\ell$$
$$\times \int_0^\infty d\vec{P}_b^{\,2} \frac{[P_b^2 + (P_{oz}+v)^2]^\ell}{(P_b^2 + P_{oz}^2 + Z_t^2)^{2\ell+2}} \left\{ \frac{1}{4} \left(\frac{\eta Z_t'}{Z_t}\right)^2 \cdot \right.$$
$$\times \frac{1}{(P_{oz}^2 + Z_t^2)(P_b^2 + P_{oz}^2 + Z_t^2)^2} + \frac{\eta Z_t' (P_{oz} - \eta Z_t' Z_t)}{Z_t (P_{oz}^2 + Z_t^2)} \cdot$$
$$\left. \times \frac{1}{(P_b^2 + P_{oz}^2 + Z_t^2)^3} + \frac{(1+\eta^2 Z_t'^2)}{(P_b^2 + P_{oz}^2 + Z_t^2)^4} \right\}$$
$$\times \left\{ {}_2F_1\left(-n+\ell+1,\ n+\ell+1;\ \ell+\tfrac{3}{2};\ \frac{(Z_p^2/n^2)}{(P_b^2 + P_{oz}^2 + Z_t^2)}\right)\right\}^2 \qquad (8)$$

with $\mathcal{E} = \frac{1}{2}\left(Z_t^2 - \frac{Z_p^2}{n^2}\right)$ and $P_{oz} = -\frac{1}{2}v + \eta\mathcal{E}$.

In our case, with a hydrogenic target, the charge Z_t is equal to 1 and the charge Z_t' appearing in the eikonal phase factor is set equal to Z_t in the final computation.

DISCUSSION OF RESULTS

The latest known experimental results[7] along with several theoretical calculations quoted therein for the process $H^+ + H(1s) \longrightarrow H(2s) + H^+$ at energies ranging from 20 keV to 100 keV are compared with our present calculations in Fig. 1. Notice that the eikonal approximation requires that the collision time be small compared with the transition time (i. e. the reciprocal of the transition energy in atomic units). The present results are far superior to other theoretical data in the energy range (greater than 25 keV in this case) in which the eikonal approach is appropriate.

Results for processes (2), (3), and (4) are shown in Figs. 2-8. Figure 2 shows the total cross sections. As expected, it decreases with increasing impact energy. In Figs. 3-5, we present the capture cross section into different principal shells as a function of n (with smooth interpolating curves to guide the eye) at energies of 40, 100, and 200 keV per nucleon. The shift of the peak values (indicated by arrows) toward smaller n as the impact energy is increased illustrates the fact that, as expected on physical grounds, momentum-matching is a dominant mechanism in the capture process when the impact energy is very high, while energy-matching dominates at low energies.

More structural information is shown in Figs. 6-8 where we have plotted the capture cross section into nℓ subshells versus orbital angular quantum number ℓ. The heavy solid line indicates that the "n" indexing the line is the principal quantum number at which the value of σ_{1s-n} peaks for a specific energy when it is plotted versus n (see Figs 3-5). The detailed

structure of the (rapidly) oscillating profiles appearing on these curves may serve as a sensitive test of the eikonal method, if any of these observations is experimentally available. We also tabulate the numerical data for easy reference in tables (1) and (2).

As mentioned, we performed numerical integrations (Eq. (8)) in calculating $\sigma_{1s-n\ell}(v)$ for the case of $Fe^{+24} + H(1s) \longrightarrow Fe^{+23}(n\ell) + H^{+}$ with $n \geq 12$. We believe that the numerical results are as accurate as they would have been had the computer difficulties mentioned previously not prevented our using the exact closed form expressions, because we summed these cross sections over ℓ and obtained agreement with the corresponding σ_{1s-n} obtained from exact closed form expressions.

ACKNOWLEDGEMENTS

We are deeply indebted to Professor Einar Hinnov for suggesting this investigation at the NATO Advanced Study Institute on Atomic and Molecular Processes in Controlled Thermonuclear Fusion, Bonas, France, in 1979. This work was supported in part by the Department of Energy under Contract No. DEAS05-80ER10749.

REFERENCES

1. H. B. Gilbody, in Advances in Atomic and Molecular Physics, edited by D. R. Bates (Academic, New York, 1979), Vol. 15, p.293.
2. Atomic and Molecular Processes in Controlled Thermonuclear Fusion, edited by M. R. C. McDowell and A. M. Ferendeci (Plenum Press, New York, 1979).
3. R. C. Isler, Phys. Rev. Lett. 38, 1359 (1977).
4. E. Hinnov, in Ref. 2, p.449.
5. F. T. Chan and Jörg Eichler, Phys. Rev. Lett. 42, 58 (1979); Jörg Eichler and F. T. Chan, Phys. Rev. A20, 104 (1979).
6. F. T. Chan and Jörg Eichler, Phys. Rev. A20, 1841 (1979).
7. T. J. Morgan, J. Stone, and R. Mayo, Phys. Rev. A22, 1460 (1980).
8. M. R. C. McDowell and J. P. Colemen, Introduction to the Theory of Ion-Atom Collisions (North Holland, Amsterdam, 1970).
9. R. J. Glauber, in Lectures in Theoretical Physics, edited by W. E. Brittin et al. (Interscience, New York, 1959), Vol.1, p.315.

EXPLANATION OF TABLES

All electron capture cross sections are listed in units of 10^{-16} cm^2. The impact energies are specified inside the parentheses; they are all in keV/amu.

n = principal quantum number*

ℓ = orbital angular quantum number

* In the nℓ notation, n's correspond to the peak $\sigma_{1s-n}(v)$ at the energy specified, e. g. in the case of $C^{+6} + H(1s) \longrightarrow C^{+5}(n\ell) + H^+$, the subscript n=8 appearing in $\sigma_{1s-n=8,\ell}(v)$ means that $\sigma_{1s-n=8}$ is peaked at n=8 when σ_{1s-n} is plotted against n (at the energy 40 keV/amu).

Table 1. The cross section of electron capture for $C^{+6} + H(1s) \rightarrow C^{+5}(n\ell) + H^{+}$ at impact energies 40, 100, and 200 keV/amu (in $10^{-16} cm^2$). Subscripts n index peak cross section into the principal shell at different energies.

ℓ	$\sigma_{1s-n=8,\ell}$ (40keV/amu)	$\sigma_{1s-n=6,\ell}$ (100keV/amu)	$\sigma_{1s-n=5,\ell}$ (200keV/amu)
0	2.583(-1)	2.445(-2)	2.933(-3)
1	4.609(-1)	1.087(-1)	1.702(-2)
2	1.357	1.300(-1)	1.899(-2)
3	1.209	3.183(-1)	4.447(-2)
4	2.767	2.671(-1)	1.123(-1)
5	2.545	1.200	
6	5.252		
7	1.054(+1)		

Table 2. The cross section of electron capture for $O^{+8} + H(1s) \rightarrow O^{+7}(n\ell) + H^{+}$ (in 10^{-16} cm^2).

ℓ	$\sigma_{1s-n=10,\ell}$ (40keV/amu)	$\sigma_{1s-n=8,\ell}$ (100keV/amu)	$\sigma_{1s-n=6,\ell}$ (200keV/amu)
0	1.796(-1)	2.667(-2)	3.206(-3)
1	8.291(-1)	1.000(-1)	2.083(-2)
2	9.243(-1)	1.391(-1)	1.698(-2)
3	2.061	2.602(-1)	6.003(-2)
4	1.790	2.784(-1)	3.421(-2)
5	3.692	5.305(-1)	2.105(-1)
6	2.948	5.090(-1)	
7	6.578	1.798	
8	5.165		
9	1.931		

Table 3. The cross section of electron capture for Fe^{+24} + H(1s) → $Fe^{+23}(n\ell)$ + H^+ (in $10^{-16}cm^2$).

ℓ	$\sigma_{1s-n=31,\ell}$ (40keV/amu)	$\sigma_{1s-n=25,\ell}$ (100keV/amu)	$\sigma_{1s-n=19,\ell}$ (200keV/amu)
0	4.121(-1)	1.102(-2)	3.759(-3)
1	1.696	1.352(-1)	1.613(-2)
2	8.867(-1)	5.135(-2)	1.920(-2)
3	1.962	3.272(-1)	3.808(-2)
4	1.923	7.877(-2)	3.555(-2)
5	2.307	5.434(-1)	6.131(-2)
6	2.833	9.191(-2)	5.357(-2)
7	3.409	7.815(-1)	8.699(-2)
8	3.809	1.143(-1)	7.412(-2)
9	4.386	1.005	1.170(-1)
10	4.681	2.138(-1)	9.867(-2)
11	5.655	1.135	1.546(-1)
12	5.422	4.832(-1)	1.309(-1)
13	7.350	1.122	2.071(-1)
14	5.803	9.230(-1)	1.820(-1)
15	9.851	1.093	2.957(-1)
16	5.531	1.336	2.941(-1)
17	1.320(+1)	1.348	5.035(-1)
18	5.252	1.549	7.745(-1)
19	1.677(+1)	2.028	
20	4.700	1.791	
21	2.303(+1)	3.121	
22	1.661	2.580	
23	3.001(+1)	5.350	
24	7.188	5.595	
25	2.447(+1)		
26	2.602(+1)		
27	2.371(+1)		
28	3.676(+1)		
29	4.566(+1)		
30	6.719(+1)		

FIGURE CAPTIONS

Fig. 1: Cross sections for the process $H^+ + H(1s) \rightarrow H(2s) + H^+$, as a function of the projectile energy. Theory: solid curve, present calculations; dashed curve, Born approximation; dashed-dotted curve, 7-state (4 hydrogenic and 3 pseudostates) close-coupling calculation; dashed-double-dotted curve, 34-state scaled, hydrogenic close-coupling calculation. Experiment: ●, T. J. Morgan et al.; ▲ , J. Hill et al. (Ref. 7).

Fig. 2: Total cross sections, as a function of the projectile energy, of the processes: (i) $C^{+6} + H(1s) \rightarrow C^{+5} + H^+$; (ii) $O^{+8} + H(1s) \rightarrow O^{+7} + H^+$; (iii) $Fe^{+24} + H(1s) \rightarrow Fe^{+23} + H^+$.

Fig. 3: Capture cross sections into different principal shells as a function of n at energies 40, 100, and 200 keV/amu for the process $C^{+6} + H(1s) \rightarrow C^{+5}(n) + H^+$.

Fig. 4: Capture cross sections into different principal shells as a function of n at energies 40, 100, and 200 keV/amu for the process $O^{+8} + H(1s) \rightarrow O^{+7}(n) + H^+$.

Fig. 5: Capture cross sections into different principal shells as a function of n at energies 40, 100, and 200 keV/amu for the process $Fe^{+24} + H(1s) \rightarrow Fe^{+23}(n\neq 1) + H^+$.

Fig. 6: Capture cross sections into $n\ell$ subshells as a function of ℓ at energy 100 keV/amu for the process $C^{+6} + H(1s) \rightarrow C^{+5}(n\ell) + H^+$. The heavy solid line denotes the principal shell n at which the curve peaks when $\sigma_{1s-n}(v)$ is plotted against n.

Fig. 7: Capture cross sections into $n\ell$ subshells as a function of ℓ at energy 100 keV/amu for the process $O^{+8} + H(1s) \rightarrow O^{+7}(n\ell) + H^{+}$.

Fig. 8: Capture cross sections into $n\ell$ subshells as a function of ℓ at energy 100 KeV/amu for the process $Fe^{+24} + H(1s) \rightarrow Fe^{+23}(n\ell, n=1) + H^{+}$.

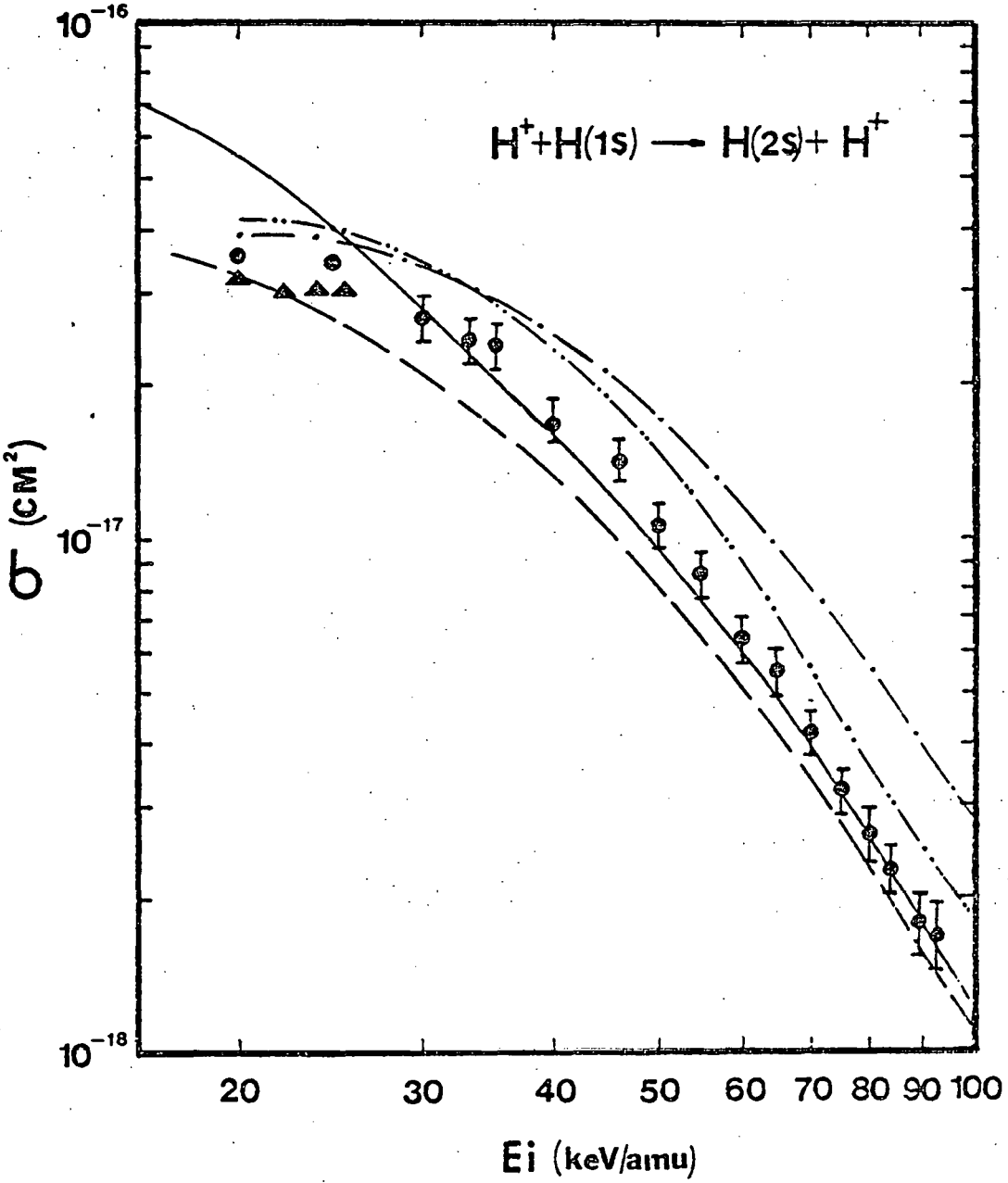
10^{-16}
10^{-17}
10^{-18}
$H^+ + H(1s) \longrightarrow H(2s) + H^+$
σ (CM^2)
20
30
40
50
60
70
80
90
100
Ei (keV/amu)

Fig. 1

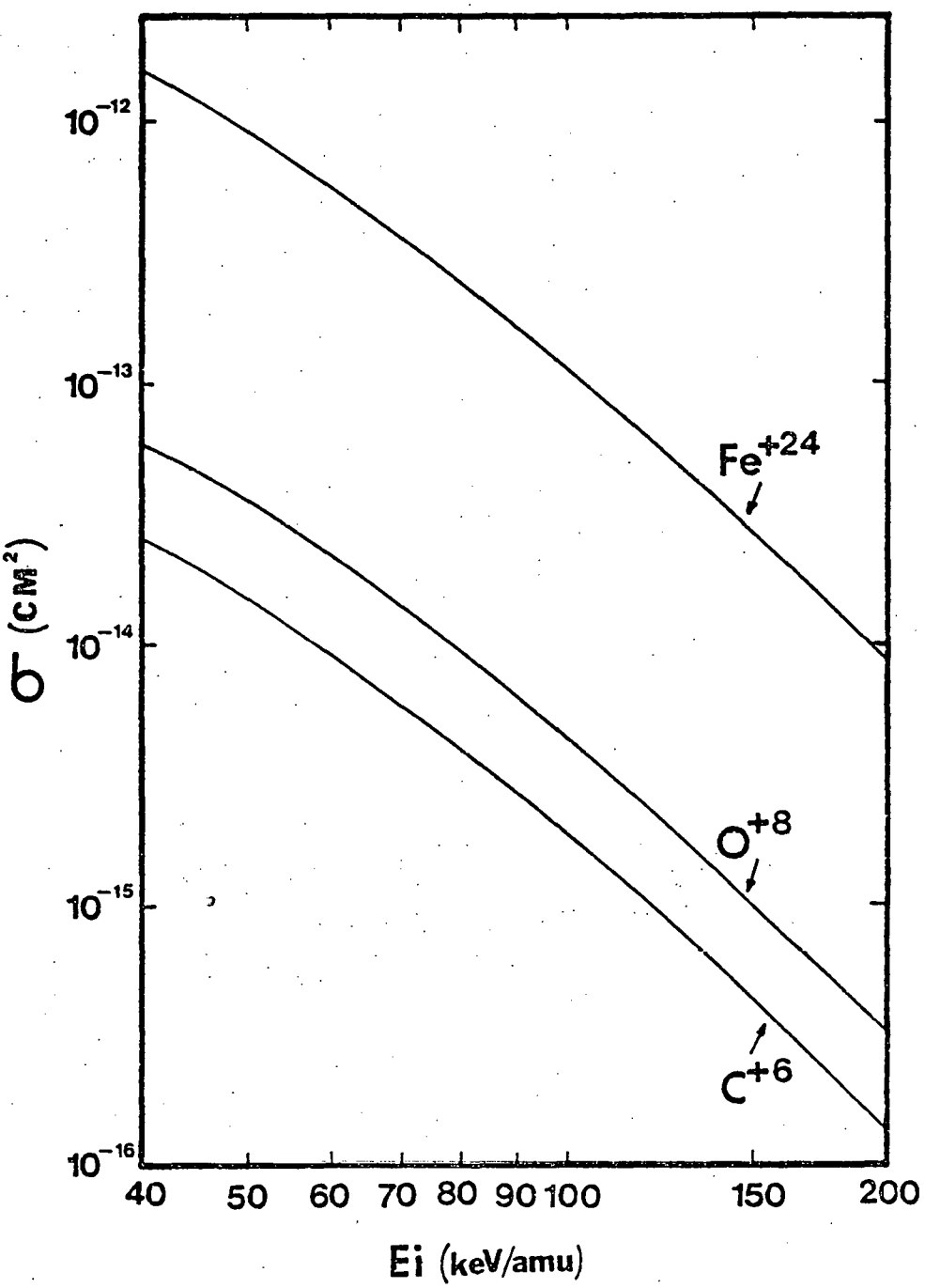
10^{-12}
10^{-13}
10^{-14}
10^{-15}
10^{-16}
σ (cm²)
Fe+24
O+8
C+6
40
50
60
70
80
90
100
150
200
Ei (keV/amu)

Fig. 2

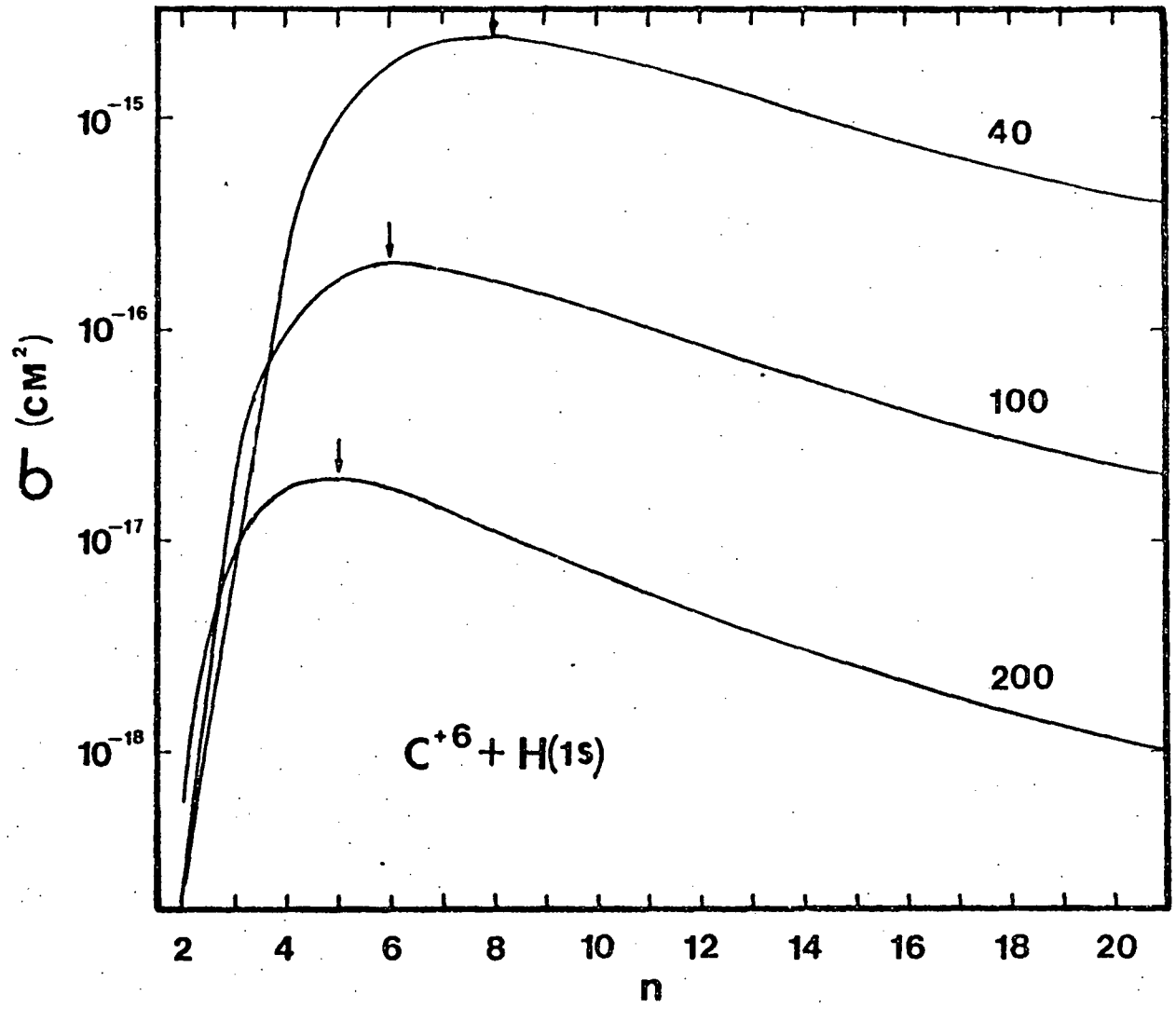
10^{-15}
10^{-16}
10^{-17}
10^{-18}
σ (cm²)
40
100
200
C^{+6} + H(1s)
2
4
6
8
10
12
14
16
18
20
n

Fig. 3

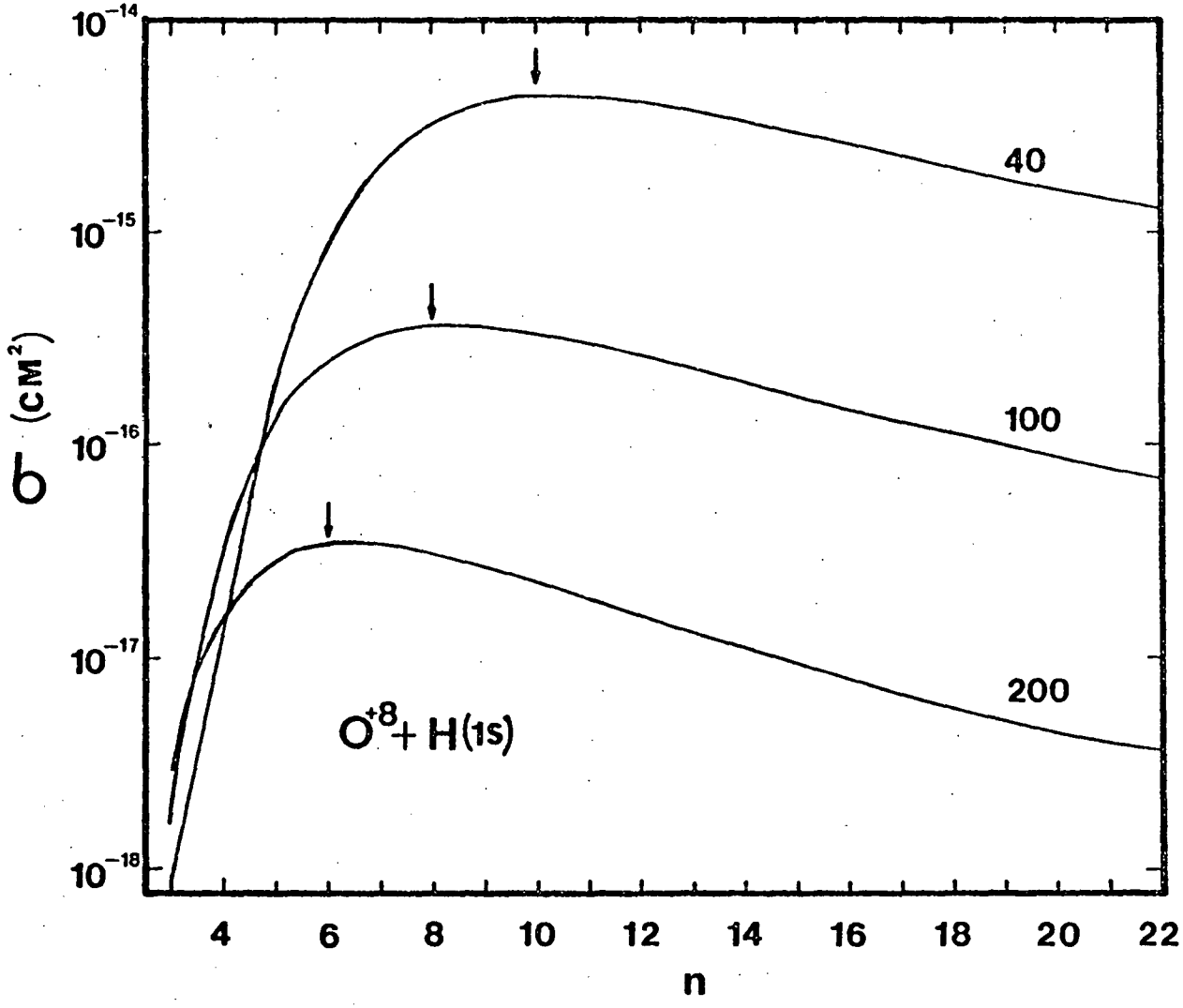
10^{-14}
10^{-15}
10^{-16}
10^{-17}
10^{-18}
σ (cm²)
40
100
200
O^{+8} + H(1s)
4
6
8
10
12
14
16
18
20
22
n

Fig. 4

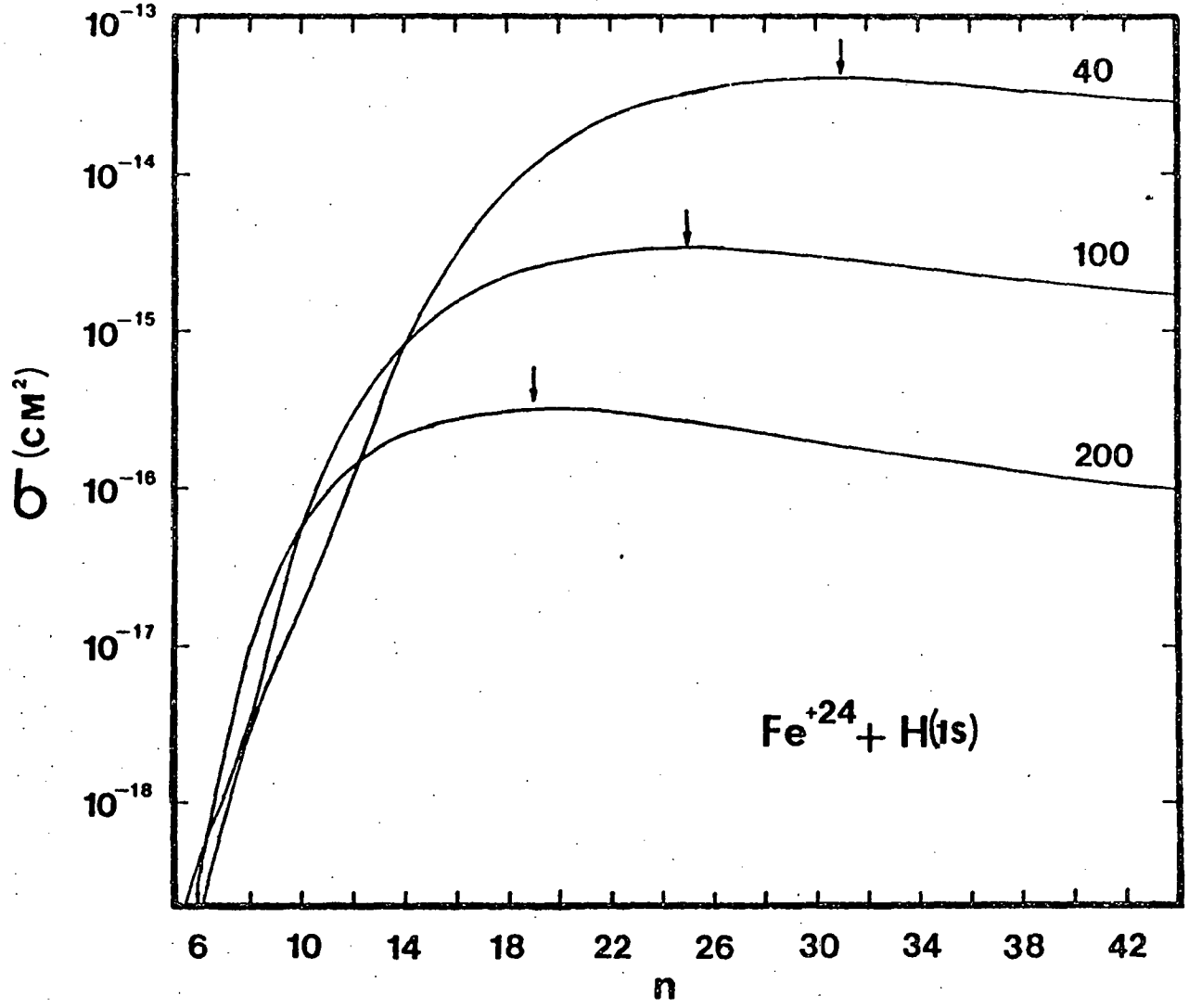
10^{-13}
10^{-14}
10^{-15}
10^{-16}
10^{-17}
10^{-18}
σ (cm²)
40
100
200
Fe^{+24} + H(1s)
6
10
14
18
22
26
30
34
38
42
n

Fig. 5

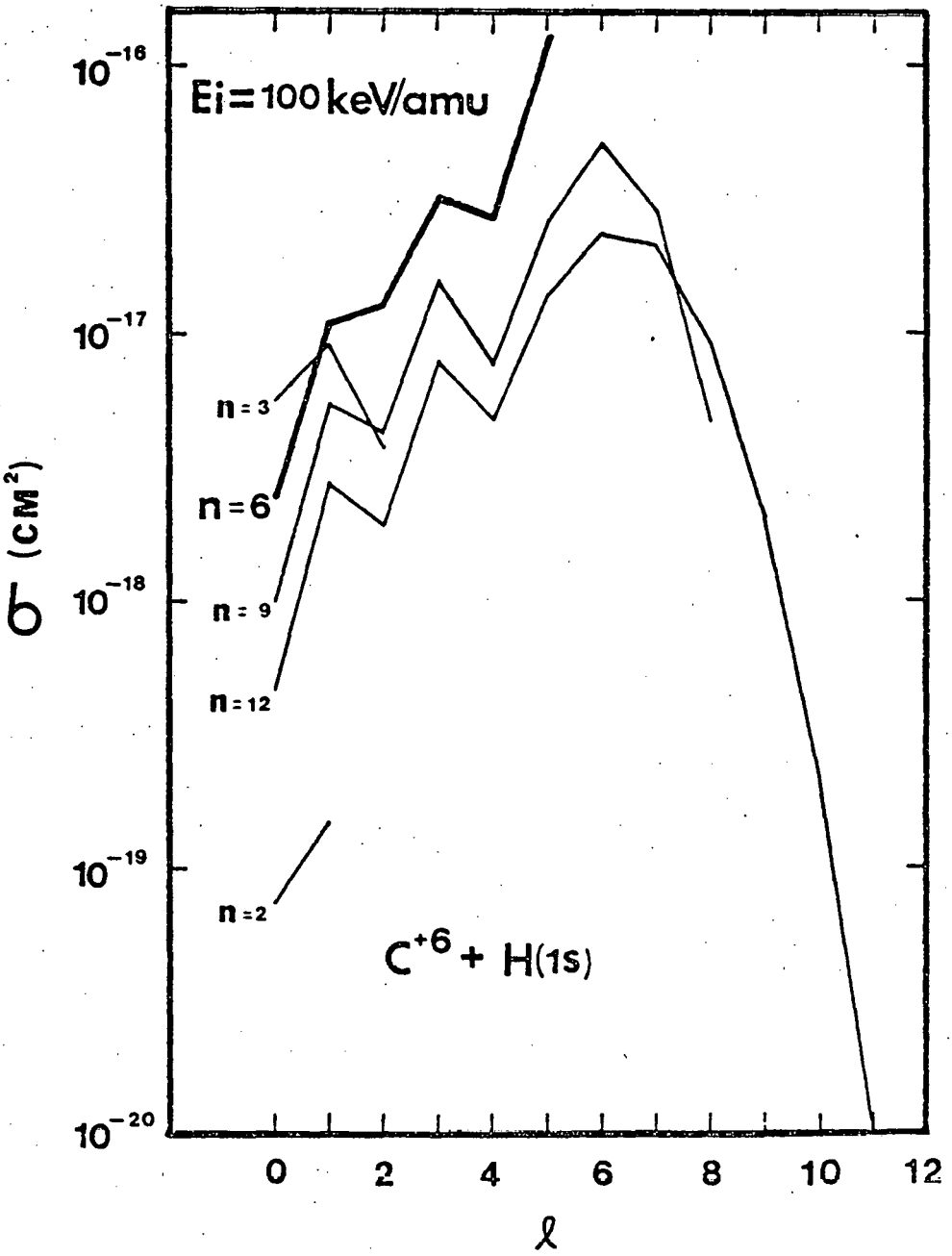
Ei = 100 keV/amu
n = 3
n = 6
n = 9
n = 12
n = 2
C+6 + H(1s)
σ (cm²)
10⁻¹⁶
10⁻¹⁷
10⁻¹⁸
10⁻¹⁹
10⁻²⁰
0
2
4
6
8
10
12
ℓ

Fig. 6

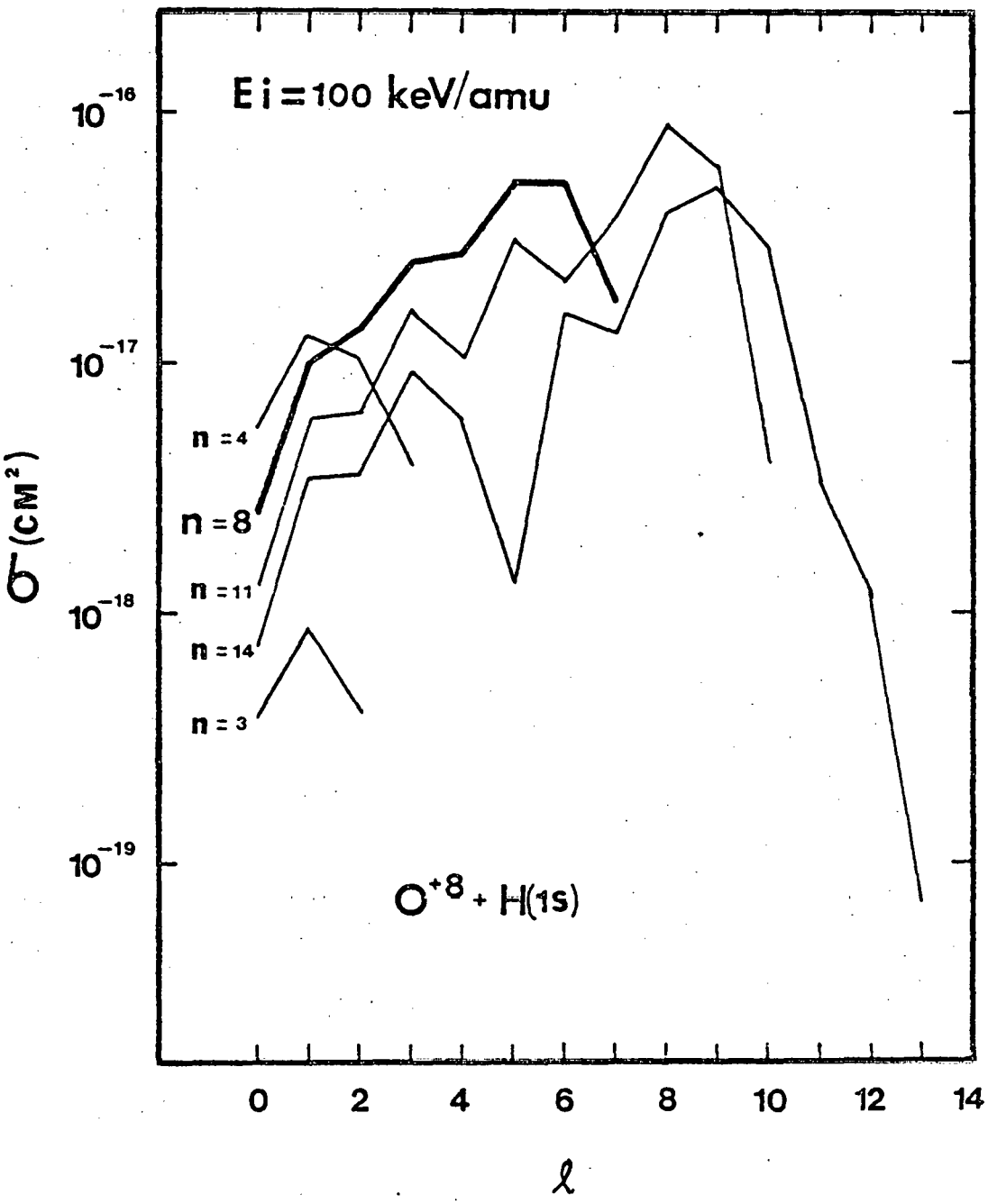
Ei = 100 keV/amu
10^{-16}
10^{-17}
10^{-18}
10^{-19}
σ (CM²)
n = 4
n = 8
n = 11
n = 14
n = 3
O^{+8} + H(1s)
0
2
4
6
8
10
12
14
ℓ

Fig. 7

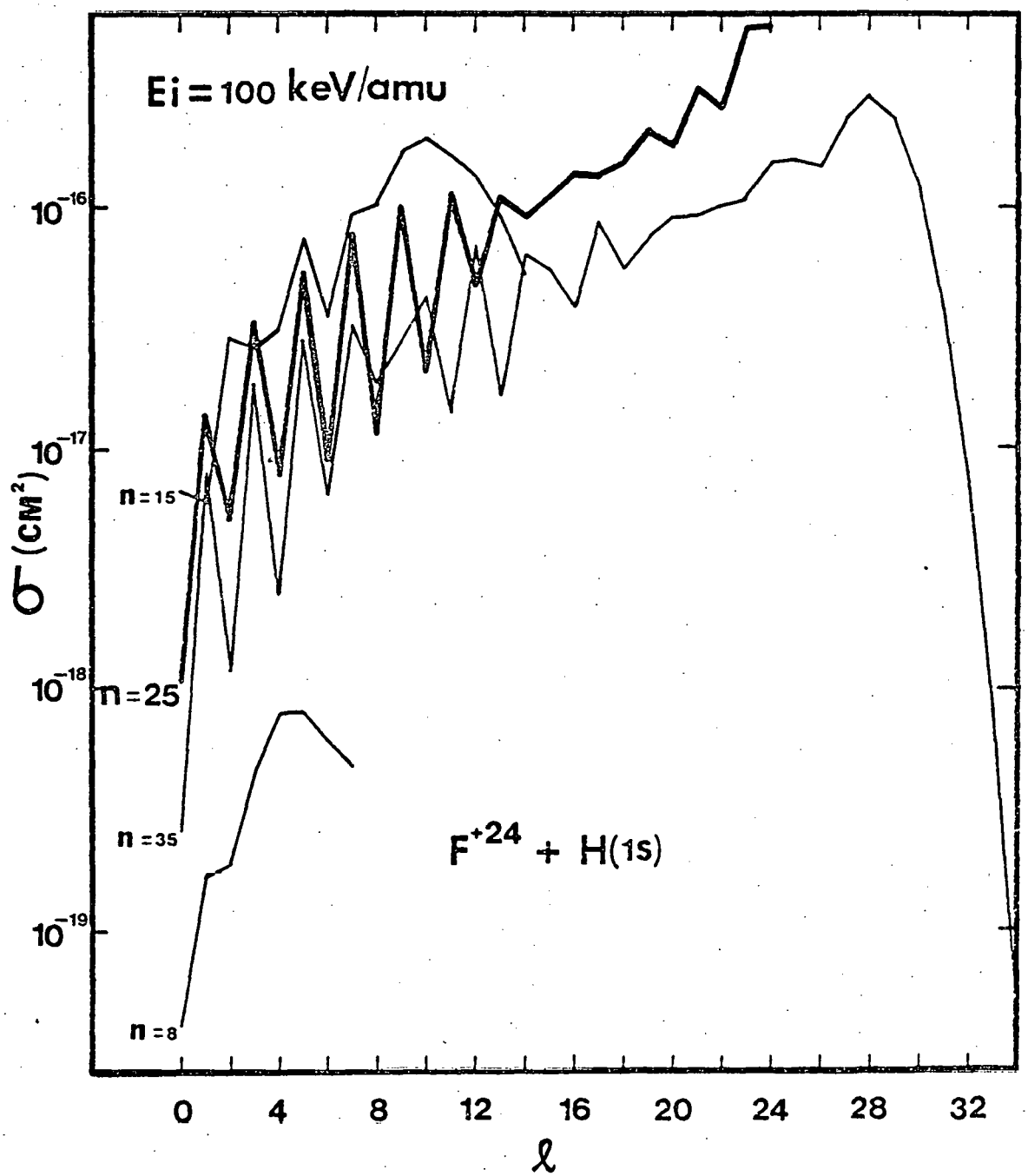
Ei = 100 keV/amu
10^{-16}
10^{-17}
10^{-18}
10^{-19}
σ (cm^2)
n = 15
n = 25
n = 35
n = 8
F^{+24} + H(1s)
0
4
8
12
16
20
24
28
32
ℓ

Fig. 8

Eikonal Approximation for Charge Transfer from Multi-Electron Atom to Fast Projectiles

T. S. Ho, M. Lieber, F. T. Chan

Physics Department, University of Arkansas, Fayetteville, AR 72701

and

K. Omidvar

Laboratory for Planetary Atmospheres
NASA/Goddard Space Flight Center, Greenbelt, MD 20771

The eikonal approach developed previously for calculating electron capture cross sections for bare projectiles colliding with hydrogenic targets is extended here to allow for multi-electron targets. Both the impact and wave pictures are employed and their equivalence is discussed. As a first approximation, each atomic orbital is specified by the three hydrogenic quantum numbers, an effective nuclear charge Z_t , and an energy eigenvalue in the impact picture, or ionization potential in the wave picture. The Z_t' appearing in the eikonal phase factor is left undetermined because of incomplete information on the many-body target. However, analytic expressions are derived for the theoretical cross sections, and numerical values calculated for simple choices of Z_t'. Those results are compared with existing experimental data for C, Ne, Ar, N_2, O_2, and He targets.

I. Introduction

Electron capture processes in ion-atom collisions, e.g., $A^+ + B \longrightarrow A + B^+$, are of great interest both in terms of basic theory and in various practical applications. In particular, capture cross section from atomic oxygen or iron are essential in finding the charge equilibrium of a high-energy beam passing through different gases, or in finding the radiation of cosmic rays passing through intersteller matter.

It is well known that the Oppenheimer-Brinkman-Kramers approximation[1] gives roughly correct shape for the dependence of the total electron capture cross sections upon the collision energy but considerably overestimates the observed data by as much as an order of magnitude. Many efforts have been devoted to obtain a simple semi-empirical formula of the capture cross section by scaling down the OBK results through the comparison with the existing experimental measurements[2]. The physical significance of this scaling behavior was not quite understood until the very recent elegant and instructive illustration furnished by the study within the eikonal approximation[3]. This eikonal approach has been further studied since then and has been very successful in predicting the cross sections of the electron capture for the bare projectile – hydrogenic target systems[4-8]. Among them the cross sections of the capture (i) from $n\ell$ initial state to $n'\ell'$ final state[6], and (ii) from $n\ell m$ initial state to $n'\ell'm'$ final state[8] have been obtained in closed form, a very astonishing consequence considering most of other approaches (other than OBK) are so complicated that one must have recourse to numerical methods.

In this paper, we generalize this eikonal approach to describe, in (i) the impact picture and (ii) the wave picture, the capture process of a single electron from a multi-electron atom into a fast bare projectile. As a first approximation, each atomic orbital is specified by the three hydrogenic quantum numbers, an effective charge, and an energy value (more accurately, an energy eigenvalue in the impact picture or an ionization potential in the wave picture).

In Sec. II, two techniques in formulating the capture cross section are presented, i.e., (i) a straightforward extension from one of our recent papers[8] and (ii) a generating operator (a differential operator, or, for short, a differentiator) and a generating function (an exponential function) are introduced in manipulations. In Sec. III, a discussion on the equivalence of the wave and impact pictures is given. And finally, in Sec. IV, our calculations are compared with the existing experimental data for capture cross sections from C, Ne, Ar, N_2, O_2, and He.

II. The Theory

We shall derive the capture cross section in (A) impact picture and (B) wave picture. Atomic units are used throughout.

(A) Impact picture derivation

In Ref. (8) (hereafter called paper I), we have obtained a closed form for the cross section of the electron capture from an arbitrary nℓm state of a hydrogenic atom to a specific n'ℓ'm' state of a fast bare projectile, starting from the integral

$$\sigma^{(IP)}_{n\ell m - n'\ell'm'}(v) = \frac{2^4\pi^4 Z_P^2}{v^2}\int\left\{\left|g_{n'\ell'm'}(\vec{p}+\vec{v})\right|^2\left|G_{n\ell m}(\vec{p})\right|^2\right\}_{p_z=p_{oz}} d^2p_b \qquad (1)$$

where

$$g_{n'\ell'm'}(\vec{p}) = (2\pi)^{-3/2}\int \frac{\varphi_{n'\ell'm'}(\vec{r}_p)}{r_p}\exp(i\vec{p}\cdot\vec{r}_p)\,d^3r_p \qquad (2)$$

$$G_{n\ell m}(\vec{p}) = (2\pi)^{-3/2}\int\left[\varphi_{n\ell m}(\vec{r}_t)\exp\left(-i\int_t^\infty \frac{Z'_t}{r_t}dt'\right)\right]\exp(i\vec{p}\cdot\vec{r}_t)\,d^3r_t \qquad (3)$$

and

$$p_{oz} = -\tfrac{1}{2}v + \eta\varepsilon\ . \qquad (4)$$

Here, $\varphi_{n\ell m}(\vec{r}_t)$ and $\varphi_{n'\ell'm'}(\vec{r}_p)$ are the hydrogenic wave functions which describe the initial and final bound states of the electron, respectively. The factor $v=\frac{1}{\eta}$ is the impact velocity of the projectile with respect to the target and is kept constant throughout while the quantity $\varepsilon = \varepsilon_p - \varepsilon_t$ with ε_p and ε_t the energy eigenvalues of the initial and final electron

bound states. Furthermore, the eikonal phase factor[9] is introduced in Eq. (3). The effective target charge Z_t' has been introduced in the final state, allowing $Z_t' \neq Z_t$ for multi-electron effects. In the case where the target is a multi-electron atom, the initial $n\ell m$ bound state energy eigenvalue ε_t does not have the form $-\frac{1}{2} Z_t^2/n^2$ and can be calculated through the Hartree-Fock method[10] for each atom of interest, while the final $n'\ell'm'$ bound state energy eigenvalue still keeps the form $-\frac{1}{2} Z_p^2/n'^2$ (because the final bound state is hydrogenic, i.e., bare projectile plus one electron). Consequently, the equality

$$(p_{oz} + v)^2 + \frac{Z_p^2}{n'^2} = p_{oz}^2 + \frac{Z_t^2}{n^2} \tag{5}$$

which holds in the bare projectile — hydrogenic target systems is no longer true in the bare projectile — multi-electron target systems.

Now, let us consider the situation where the active electron is initially in an arbitrary $n\ell m$ state of the target, a multielectron atom, and finally is captured into a specific n' state of the bare projectile. The cross section can then be written as

$$\sigma^{(IP)}_{n\ell m - n'}(v) = \sum_{\ell', m'} \sigma^{(IP)}_{n\ell m - n'\ell'm'}(v) \tag{6}$$

Then Fock's sum rule[11]

$$\sum_{\ell', m'} |g_{n'\ell'm'}(\vec{q})|^2 = \frac{2(Z_p/n')^3}{\pi^2 (q^2 + Z_p^2/n'^2)^2} \tag{7}$$

can be introduced here and the cross section becomes

$$\sigma^{(IP)}_{n\ell m - n'}(v) = \frac{2^5 \pi^2}{v^2} \frac{Z_p^5}{n'^3} \int \left\{ \frac{|G_{n\ell m}(\vec{p})|^2}{[p_b^2 + (p_z + v)^2 + Z_p^2/n'^2]^2} \right\}_{p_z = p_{oz}} d^2 p_b \,. \tag{8}$$

There are two different ways to formulate the quantity $|G_{n\ell m}(\vec{p})|^2$.

(Ai) First Method

In paper I, we have given an analytical expression, having twelve finite summations and depending upon $\vec{p}$ through p_b^2, to the quantity $|G_{n\ell m}(\vec{p})|^2$. Therefore, the integration (8) over $\vec{p}_b$ can be carried out by employing the formula[12]

$$\int_0^\infty \chi^{\nu-1}(\beta+\chi)^{-\mu}(\chi+\gamma)^{-\rho}\,d\chi = \beta^{-\mu}\gamma^{\nu-\rho}B(\nu,\mu-\nu+\rho)\,{}_2F_1(\mu,\nu;\mu+\rho;1-\tfrac{\gamma}{\beta}), \quad (9)$$

and the cross section can be expressed, in closed form, as follows

$$\begin{aligned}
\sigma^{(IP)}_{n\ell m-n'}(v) = {} & \frac{2^4\pi^2 Z_t^5 Z_P^5}{v^2 n^5 n'^3}\,\frac{1}{|\Gamma(-i\eta Z_t')|^2}\exp[-2\eta Z_t' \tan^{-1}(-nP_{0z}/Z_t)] \\
& \times \frac{(n-\ell-1)!\,(2\ell+1)(\ell-|m|)!}{n(n+\ell)!\,2^{2\ell}(\ell!)^2(\ell+|m|)!}\left(\frac{Z_t}{n}\right)^{2\ell}\sum_{\sigma,\sigma'=0}^{n-\ell-1}\ \sum_{\nu,\nu'=0}^{[\frac{\sigma+1}{2}],[\frac{\sigma'+1}{2}]} \\
& \times \sum_{\tau,\tau'=0}^{[\frac{\ell-|m|}{2}]}\ \sum_{\gamma,\gamma'=0}^{\tau+\nu,\,\tau'+\nu'}\ \sum_{\delta,\delta'=0}^{\ell-|m|-2\tau+2\gamma,\,\ell-|m|-2\tau'+2\gamma'}\ \sum_{\alpha,\alpha'=0}^{\sigma+1-2\nu,\,\sigma'+1-2\nu'} \\
& \times \Big\{S_\sigma(n,\ell)\,S_{\sigma'}(n,\ell)\,N_\nu(\ell,\sigma)\,N_{\nu'}(\ell,\sigma')\,T_\tau(\ell,m)\,T_{\tau'}(\ell,m)\,M_\gamma(\tau,\nu) \\
& \times M_{\gamma'}(\tau',\nu')\,D_\delta(\tau,\gamma)\,D_{\delta'}(\tau',\gamma')\,A_\alpha(\sigma,\nu)\,A_{\alpha'}(\sigma',\nu')\Big\}\cdot 2^{\sigma+\sigma'} \\
& \times \frac{\Gamma(2\ell+\sigma+3)\,\Gamma(2\ell+\sigma'+3)}{[\Gamma(\ell+3/2)]^2}\,(-i)^\delta\, i^{\delta'}\left(\frac{Z_t}{n}\right)^{2(\sigma+\sigma'-\nu-\nu')-\alpha-\alpha'} \\
& \times P_{0z}^{\,2(\ell-|m|-\tau-\tau'+\gamma+\gamma')-\delta-\delta'}\left(2\frac{Z_t}{n}-2iP_{0z}\right)^{-\delta-\alpha} \\
& \times \left(2\frac{Z_t}{n}+2iP_{0z}\right)^{-\delta'-\alpha'} B(\delta+\alpha-i\eta Z_t',\ \ell+\sigma+2-\delta-\alpha+i\eta Z_t') \\
& \times B(\delta'+\alpha'+i\eta Z_t',\ \ell+\sigma'+2-\delta'-\alpha'-i\eta Z_t')\cdot(Q')^{-2} \\
& \times Q^{|m|+\tau+\tau'+\nu+\nu'-\gamma-\gamma'-(2\ell+\sigma+\sigma'-\delta-\delta'-\alpha-\alpha')-3} \\
& \times B(|m|+\tau+\tau'+\nu+\nu'-\gamma-\gamma'+1,\ 2\ell+\sigma+\sigma'-\delta-\delta'-\alpha-\alpha'-|m|-\tau-\tau'-\nu-\nu'+\gamma+\gamma'+\cdots \\
& \times {}_2F_1\left(2,|m|+\tau+\tau'+\nu+\nu'-\gamma-\gamma'+1;\ 2\ell+\sigma+\sigma'-\delta-\delta'-\alpha-\alpha'+6;\ 1-\frac{a}{a'}\right), \quad (10)
\end{aligned}$$

where B(x,y) is the usual Beta function,

$$S_\sigma(n,\ell) = (-1)^\sigma \frac{(n+\ell)!}{(n-\ell-1-\sigma)!\,(2\ell+1+\sigma)!\,\sigma!} ,$$

$$N_\nu(\ell,\sigma) = (-1)^\nu \frac{\left(-\frac{\sigma+1}{2}\right)_\nu \left(-\frac{\sigma}{2}\right)_\nu}{\left(\ell+3/2\right)_\nu \; \nu!} ,$$

$$T_\tau(\ell,m) = (-1)^\tau \frac{\ell!\,(2\ell-2\tau)!}{(\ell-\tau)!\,\tau!\,(\ell-|m|-2\tau)!} ,$$

$$M_{\gamma'}(\tau,\nu) = \frac{(\tau+\nu)!}{\gamma'!\,(\tau+\nu-\gamma')!} ,$$

$$D_\delta(\tau,\gamma') = \frac{(\ell-|m|-2\tau+2\gamma')!}{\delta!\,(\ell-|m|-2\tau+2\gamma'-\delta)!} ,$$

$$A_\alpha(\sigma,\nu) = \frac{(\sigma+1-2\nu-\alpha)!}{\alpha!\,(\sigma+1-2\nu-\alpha)!} ,$$

$$Q = P_{oz}^2 + \frac{Z_t^2}{n^2}$$

and

$$Q' = (P_{oz}+v)^2 + \frac{Z_p^2}{n'^2} .$$

Here we have approximated the initial atomic orbital by a hydrogenic wave function.

(Aii) Second Approach

We introduce a generating function $\exp[-\beta r_t + i\vec{\mu}\cdot\vec{r}_t]$ with β a scalar and $\vec{\mu}$ a 3-dimensional vector having components μ_x, μ_y, and μ_z along three rectangular coordinates and a generating operator (a differentiator) $\hat{D}_{n\ell m}(\beta,\vec{\mu})$ which is a linear combination of $\frac{\partial}{\partial\beta}$, $\frac{\partial}{\partial\mu_x}$, $\frac{\partial}{\partial\mu_y}$, $\frac{\partial}{\partial\mu_z}$ and

their higher order counterparts, e.g., $\frac{\partial^2}{\partial\beta^2}$, $\frac{\partial^2}{\partial\mu_x\partial\beta}$, $\frac{\partial^2}{\partial\mu_x^2}$, etc., such that the wavefunction is given by

$$\varphi_{n\ell m}(\vec{r}_t) = \left\{ \hat{D}_{n\ell m}(\beta, \vec{\mu}) \exp[-\beta r_t + i\vec{\mu}\cdot\vec{r}_t] \right\}_{\substack{\beta = \text{const.} \\ \vec{\mu}=0}} \tag{11}$$

In this expression the parameters β and $\vec{\mu}$ are assigned definite constant values after the differentiation. We remark that the scalar β will take the value Z_t/n if the hydrogenic function is chosen for $\varphi_{n\ell m}(\vec{r}_t)$.

Substituting Eq. (11) in Eq. (3) and interchanging the order of the $\vec{r}_x$-integration and differentiator $\hat{D}_{n\ell m}$, we have

$$G_{n\ell m}(\vec{p}) = \left\{ \hat{D}_{n\ell m}(\beta, \vec{\mu}) \Lambda(\vec{p}; \beta, \vec{\mu}) \right\}_{\substack{\beta=\text{const.} \\ \vec{\mu}=0}} \tag{12}$$

with

$$\Lambda(\vec{p}; \beta, \vec{\mu}) = (2\pi)^{-3/2} \int \exp[-\beta r_x + i\vec{\mu}\cdot\vec{r}_x] \exp\left[-i\int_t^\infty \frac{z_x'}{r_x} dt'\right] \exp[i\vec{p}\cdot\vec{r}_x]\, d^3r_x \,. \tag{13}$$

The Eq. (13) can be written in a more convenient way by introducing the integral representation of the eikonal phase factor[13], namely,

$$\exp\left(i\int_t^\infty \frac{z_x'}{r_x} dt'\right) = \frac{1}{\Gamma(-i\eta z_x')} \int_0^\infty \lambda^{-i\eta z_x' - 1} \exp[-\lambda(r_x - z_x)]\, d\lambda \,. \tag{14}$$

Therefore, Eq. (13) becomes

$$\Lambda(\vec{p}; \beta, \vec{\mu}) = \frac{(2\pi)^{-3/2}}{\Gamma(-i\eta z_x')} \int_0^\infty \int \exp(-\beta r_x + i\vec{\mu}\cdot\vec{r}_x)\, \lambda^{-i\eta z_x' - 1} \times \exp[-\lambda(r_x - z_x)] \exp(i\vec{p}\cdot\vec{r}_x)\, d^3r_x\, d\lambda \,. \tag{15}$$

The integral (15) can be carried out by first integrating over $\vec{r}_t$ (radial part follows angular part) and then over λ . Introducing a complex vector

$$\vec{K} = \vec{p} + \vec{\mu} - i\lambda\hat{z} \quad , \tag{16}$$

Eq. (15) can be written as follows

$$\Lambda(\vec{p};\beta,\vec{\mu}) = \frac{1}{(2\pi)^{3/2}\,\Gamma(-i\eta z_t')} \int_0^\infty d\lambda\; \lambda^{-i\eta z_t' - 1} \int_0^\infty dr_t\; r_t^2\; \exp[-(\beta+\lambda) r_t]$$

$$\times \int_0^{2\pi} d\phi \int_{-1}^{+1} d\cos\theta\; \exp(iK r_t \cos\theta) \quad , \tag{17}$$

where the quantity K is defined through the relation

$$K = \sqrt{|\vec{p}_t + \vec{\mu}_t|^2 + (p_z + \mu_z - i\lambda)^2} \quad . \tag{18}$$

The 3-dimensional integral (17) can be easily evaluated and one gets

$$\Lambda(\vec{p};\beta,\vec{\mu}) = \frac{4}{\sqrt{2\pi}\,\Gamma(-i\eta z_t')} \frac{\pi}{\sinh(\pi\eta z_t')} (\beta^2 + |\vec{p}+\vec{\mu}|^2)^{-2-i\eta z_t'}$$

$$\times [2\beta - 2i(p_z + \mu_z)]^{i\eta z_t'} \left\{ i\beta(1 + i\eta z_t') \right.$$

$$\left. + \frac{\eta z_t'}{2} \frac{(\beta^2 + |\vec{p}+\vec{\mu}|^2)}{[\beta - i(p_z+\mu_z)]} \right\} . \tag{19}$$

In this approach (hydrogenic radial wave functions are not required), one first has to find a correct form for the differentiator $\hat{D}_{nsm}(\beta,\vec{\mu})$ (via Eq. (11)), then use Eqs. (12) and (19) to obtain $\mathcal{G}_{nsm}(\vec{p})$. Finally, one can insert this $\mathcal{G}_{nsm}(\vec{p})$ in Eq. (8) to get the capture cross section.

A closed form for the cross section can be expected since we note that the only calculations made in deriving the result are the derivatives of $\Lambda(\vec{P};\rho,\vec{u})$, which is expressed analytically.

We remark here that although the cross section of the capture from an initial $n\ell$ state to a specific n' state can be obtained by directly summing over m (also divided by a quantity $(2\ell+1)$ which accounts for the degeneracy of a specific $n\ell$ state) in Eq. (10), there is another way, presented in Ref. (6) (hereafter called paper II), to carry it out. But we would like to point out here that the extension to the case involving multi-electron targets suggested in paper II is inappropriate because a faulty approximation made in that paper, i.e., the equality (5) was assumed. Further investigation of this point will be postponed to the final section where numerical data are displayed. Nonetheless, we exhibit here the correct final form (using the proper replacement for equality (5)):

$$\sigma^{(IP)}_{n\ell-n'}(v) = \frac{2^4\pi^2 z_t^5 z_p^5}{v^2 n'^3 n^5}\,\frac{1}{|\Gamma(-i\eta z_t')|^2}$$

$$\times \exp[-2\eta z_t' \tan^{-1}(-n P_{0z}/z_t)] \times \frac{(n-\ell-1)!}{2^\ell n\,(n+\ell)!}$$

$$\times \left(\frac{z_t}{n}\right)^{2\ell} \sum_{\sigma,\sigma'=0}^{n-\ell-1} \sum_{\nu,\nu'=0}^{[\frac{\sigma+1}{2}],[\frac{\sigma'+1}{2}]} \sum_{\tau=0}^{[\frac{\ell}{2}]}$$

$$\times \sum_{\alpha,\alpha'=0}^{\sigma+1-2\nu,\,\sigma'+1-2\nu'} \sum_{\beta=0}^{\ell-2\tau} \sum_{\gamma,\gamma'=0}^{\tau+\nu,\,\tau+\nu'} \sum_{\delta,\delta'=0}^{\beta+2\gamma,\,\beta+2\gamma'}$$

$$\times \Big\{ S_\sigma(n,\ell)\, S_{\sigma'}(n,\ell)\, N_\nu(\ell,\sigma)\, N_{\nu'}(\ell,\sigma')$$

$$\times T_\tau(\ell)\, A_\alpha(\sigma,\nu)\, A_{\alpha'}(\sigma',\nu') \cdot \binom{\ell-2\tau}{\beta}$$

$$\times \binom{\tau+\nu}{\gamma}\binom{\tau+\nu'}{\gamma'}\binom{\beta+2\gamma}{\delta}\binom{\beta+2\gamma'}{\delta'} \cdot 2^{\sigma+\sigma'}$$

$$\times \frac{\Gamma(2\ell+\sigma+3)\,\Gamma(2\ell+\sigma'+3)}{[\Gamma(\ell+3/2)]^2}\,(-i)^\delta\, i^{\delta'}$$

$$\times \left(\frac{z_t}{n}\right)^{2(\sigma+\sigma'-\nu-\nu')-\alpha-\alpha'} \cdot P_{0z}^{\,2(\beta+\gamma+\gamma')-\delta-\delta'}$$

$$\times \left(2\frac{z_t}{n} - 2i P_{0z}\right)^{-\alpha-\delta} \left(2\frac{z_t}{n} + 2i P_{0z}\right)^{-\alpha'-\delta'}$$

$$\times B(\alpha+\delta-i\eta z_t',\, \ell+\sigma+2-\alpha-\delta+i\eta z_t')$$

$$\times B(\alpha'+\delta'+i\eta z_t',\, \ell+\sigma'+2-\alpha'-\delta'-i\eta z_t')$$

$$\times (Q')^{-2}\, Q^{g-h}\, B(g,\, 2+h-g)$$

$$\times {}_2F_1\left(2,\, g;\, 2+h;\, 1-\frac{Q}{Q'}\right) \qquad (20)$$

with

$$g = \ell - \beta + \nu + \nu' - \gamma - \gamma' + 1 ,$$

$$h = 2\ell + \sigma + \sigma' + 4 - \alpha - \alpha' - \delta - \delta' ,$$

and

$$T_\tau(\ell) = (-1)^\tau \frac{(2\ell - 2\tau)!}{\tau!\,(\ell-\tau)!\,(\ell-2\tau)!} .$$

(B) Wave Picture Derivation

We now proceed to study the same capture process as that mentioned in Sec. II-A but in a fully wave treatment. Let $\vec{\sigma}$ be the position vector of the projectile with respect to the center of mass of the target, $\vec{\rho}$ be the position vector of the center of mass of the projectile plus the active electron with respect to the center of mass of the target nucleus plus all inactive electrons, and $\vec{k}_i = \mu_i \vec{v}$ and $\vec{k}_f = \mu_f \vec{v}$ are the initial and final relative momenta of the colliding systems, respectively, with μ_i and μ_f the initial and final reduced masses, i.e.,

$$\mu_i = \frac{M_p (M_t + 1)}{M_p + M_t + 1} , \tag{21a}$$

and

$$\mu_f = \frac{(M_p + 1) M_t}{M_p + M_t + 1} . \tag{21b}$$

The capture cross section can then be written as follows[14]

$$\sigma_{i \to f}^{(WP)}(v) = \frac{\mu_i \mu_f}{4\pi} \frac{k_f}{k_i} \int |T_{if}|^2 \, d\Omega , \tag{22}$$

where

$$T_{if} = \langle \Psi_f^{(-)} | -\frac{Z_p}{r_p} | \Psi_i \rangle \tag{23}$$

in the prior form. Here, subscripts i and f denote the initial and final bound states of the system. And if the electron is captured from an arbitrary $n\ell m$ state of the target into a definite $n'\ell'm'$ state of the projectile, the wave functions used in Eq. (23) are specified as follows

$$\Psi_i = e^{i\vec{k}_i\cdot\vec{\sigma}}\, \varphi_{n\ell m}(\vec{r}_t) \tag{24a}$$

while the eikonal final state eigenfunction behaves asymptotically as

$$\Psi_f^{(-)} \cong e^{i\vec{k}_f\cdot\vec{\rho}}\, \varphi_{n'\ell'm'}(\vec{r}_p)\; e^{-i\int_t^\infty \frac{Z_t'}{r_t} dt'} . \tag{24b}$$

Using Eqs. (2), (3), (24a), and (24b), the matrix element T_{if} can be expressed as

$$T_{if} = (-Z_p)(2\pi)^{-3}\int e^{-i\vec{k}_f\cdot\vec{\rho} + i\vec{k}_i\cdot\vec{\sigma} + i\vec{q}\cdot\vec{r}_p - i\vec{p}\cdot\vec{r}_t} \times \varphi^*_{n'\ell'm'}(\vec{q})\, G_{n\ell m}(\vec{p})\, d^3q\, d^3p\, d^3r_p\, d^3r_t . \tag{25}$$

By introducing the momentum changes of the projectile and the target, i.e., $\vec{q'} = a\vec{k}_f - \vec{k}_i$ and $\vec{p'} = b\vec{k}_i - \vec{k}_f$ with $a = M_p/(M_p+1)$ and $b = M_t/(M_t+1)$, we have the following relationship

$$-\vec{k}_f\cdot\vec{\rho} + \vec{k}_i\cdot\vec{\sigma} = \vec{p'}\cdot\vec{r}_t + \vec{q'}\cdot\vec{r}_p . \tag{26}$$

Here the relations $\vec{\sigma} = b\vec{r}_t - \vec{r}_p$ and $\vec{\rho} = \vec{r}_t - a\vec{r}_p$ have been assumed.

After some manipulations, Eq. (25) reduces to

$$T_{if} = -Z_p (2\pi)^3 \, g^*_{n'l'm'}(-\vec{\beta}') \, G_{nlm}(\vec{p}') . \tag{27}$$

The cross section for the $nlm - n'l'm'$ capture then becomes

$$\sigma^{(WP)}_{nlm-n'l'm'}(v) = \mu_i \mu_f (2\pi)^4 Z_p^2 \frac{k_f}{k_i} \int \{ |g^*_{n'l'm'}(-\vec{\beta}')|^2 |G_{nlm}(\vec{p}')|^2 \} d\Omega . \tag{28}$$

Moreover, the cross sections for the $nlm - n'$ and $nl - n'$ captures are given as follows, respectively,

$$\sigma^{(WP)}_{nlm-n'}(v) = \sum_{l',m'} \sigma^{(WP)}_{nlm-n'l'm'}(v)$$
$$= \mu_i \mu_f \, 2^6 \pi^3 \frac{Z_p^5}{n'^3} \frac{k_f}{k_i} \int_0^\pi \left\{ \frac{|G_{nlm}(\vec{p}')|^2}{[(\beta')^2 + \frac{Z_p^2}{n'^2}]^2} \right\} \times \sin\theta \, d\theta , \tag{29a}$$

and

$$\sigma^{(WP)}_{nl-n'}(v) = \frac{1}{2l+1} \sum_m \sum_{l',m'} \sigma^{(WP)}_{nlm-n'l'm'}$$
$$= \frac{1}{2l+1} \mu_i \mu_f \, 2^6 \pi^3 \frac{Z_p^5}{n'^3} \frac{k_f}{k_i} \int_0^\pi \frac{1}{[(\beta')^2 + \frac{Z_p^2}{n'^2}]^2} \sum_m |G_{nlm}(\vec{p}')|^2 \times \sin\theta \, d\theta . \tag{29b}$$

Here, we have used Fock's sum rule and chosen spherical polar coordinates (r, θ, ϕ) with polar axis in the direction of the incident beam. And, furthermore, the analytical forms of $|G_{nlm}(\vec{p}')|^2$ and $\sum_m |G_{nlm}(\vec{p}')|^2$ are already given in papers I and II. We note that, in the wave treatment, energy and momentum must be conserved, and the former gives

$$\frac{k_i^2}{2\mu_i} - \frac{k_f^2}{2\mu_f} = \Delta I$$
$$= I_p - I_t \tag{30}$$

where I_p and I_t are the ionization energies of the electron in its initial and final bound states, respectively. This can be significantly different from the $(\varepsilon_p - \varepsilon_t)$ eigenvalue difference which enters into the impact picture development, as will be discussed below.

III. A Discussion of the Equivalence of the Wave and Impact Pictures

This section is devoted to a demonstration that within the eikonal approximation the capture cross section obtained in the wave treatment is equivalent to that obtained in the impact picture. We remark here that the arguments to be made below utilize the fact that the inequality

$$v^2 >> \frac{2\Delta I}{\mu_i} \tag{31a}$$

holds within our method, which requires that the collision time between the colliding systems be small compared to the typical transition time, i.e.,

$$\frac{1}{\pi} \frac{\Delta I}{Z_t} \frac{1}{v} << 1 \tag{31b}$$

in atomic units. This can be easily seen because of the largeness of the μ_i.

We shall discuss the case of the $n\ell m \to n'$ capture as an example and the generalization can be made without any trouble to other situations. The cross section for this process, i.e., Eq. (29a), can be, after changing the integration variable θ to a new variable $y = 4\mu_i\mu_f v^2 \sin^2\frac{\theta}{2}$ (noticing that $\sin\theta d\theta = 2\, d\sin^2\frac{\theta}{2}$) and, recognizing that the new integration upper limit $y_{max} = 4\mu_i\mu_f v^2$ may be virtually regarded as infinite (μ_i and μ_f are obviously very large and v is always greater than unity within the approximation), further approximated by

$$\sigma^{(WP)}_{n\ell m - n'}(v) \cong \frac{2^5\pi^3 Z_P^5}{v^2 n'^3} \int_0^\infty \frac{|G_{n\ell m}(\vec{p}')|^2}{[q'^2 + Z_P^2/n'^2]^2}\, dy \,. \tag{32}$$

Here we have used the fact that $k_i \cong k_f$. The similarity between $\sigma^{(IP)}_{n\ell m-n'}(v)$ Eq. (8), and $\sigma^{(WP)}_{n\ell m-n'}(v)$ could have been noticed when we used the relation $d^2P_b = \pi\, d P_b^2$ in Eq. (8). Now, we need to evaluate the absolute values of the quantities $\overrightarrow{q'}$ and $\overrightarrow{p'}$, to an accuracy of the order of $\frac{1}{M_p}$ and $\frac{1}{M_t}$. They can be easily derived and are written as follows, namely,

$$(q')^2 = \left(\tfrac{1}{2}v + \eta\,\Delta I\right)^2 + 4\mu_i\mu_f v^2 \sin^2\tfrac{\theta}{2} \quad , \tag{33a}$$

and

$$(p')^2 = \left(-\tfrac{1}{2}v + \eta\,\Delta I\right)^2 + 4\mu_i\mu_f v^2 \sin^2\tfrac{\theta}{2} \quad . \tag{33b}$$

Furthermore, an approximate expression of the z-component of $\overrightarrow{p'}$ can be obtained, by using the inequality (31a) and Eq. (30), namely,

$$\begin{aligned} p'_z &= \vec{p}' \cdot \hat{z} \\ &= b k_i - k_f \cos\theta \\ &\cong \left(-\tfrac{v}{2} + \eta\,\Delta I\right) + \frac{\left(1 - \frac{\Delta I}{\mu_i v^2}\right)}{2\mu_f v}\, y \, . \end{aligned} \tag{34a}$$

Similarly, the z-component of q' is

$$\begin{aligned} q'_z &= \vec{q}' \cdot \hat{z} \\ &= a k_f \cos\theta - k_i \\ &= -\left(\tfrac{v}{2} + \Delta I\right) + \frac{\left(1 - \frac{\Delta I}{\mu_i v^2}\right)}{2\mu_i v}\, y \, . \end{aligned} \tag{34b}$$

The last factors in both Eqs. (34) are much smaller than the integration variable y (because of large μ_i and μ_f) and can be neglected throughout, i.e.,

$$P_z' \cong (-\frac{v}{2} + \eta \Delta I) \ ,$$

and

$$q_z' \cong -(\frac{v}{2} + \eta \Delta I) \ .$$

Therefore, after substituting the above two equations in Eqs. (33), we obtain

$$(p')^2 = (P_b')^2 + (P_z')^2 \tag{35a}$$

and

$$(q')^2 = (P_b')^2 + (P_z' + v)^2 \tag{35b}$$

with the components of $\overrightarrow{p'}$ and $\overrightarrow{q'}$ on the x-y plane

$$(P_b')^2 = 4\mu_i \mu_f v^2 \sin^2 \frac{\theta}{2}$$

$$\equiv y \tag{35c}$$

and the z-component of $\overrightarrow{p'}$

$$P_z' = -\frac{1}{2} v + \eta \Delta I \ . \tag{35d}$$

From Eqs. (35a) - (35d), we can see that $\sigma^{(IP)}_{n\ell m - n'}(v)$ and $\sigma^{(WP)}_{n\ell m - n'}(v)$ would be equivalent to each other if $|E_t|$ (the energy eigenvalue used in

impact picture) were equal to I_t (the ionization energy used in wave picture). We have found that the two quantities $|\varepsilon_t|$ and I_t are close in many practical cases, see Table I. The quantities $|\varepsilon_p|$ and I_p are the same, i.e., $\frac{1}{2} Z_p^2/n'^2$ because the projectile and the captured electron form a hydrogenic system.

IV. Results and Discussion

We have pointed out that in the extension from the case involving the hydrogenic target to that of multielectron target the replacement of the quantity $(p_{oz}+v)^2+\frac{Z_p^2}{n'^2}$ by the quantity $p_{oz}^2+\frac{Z_t^2}{n^2}$ (which is equivalent to assuming that the equality (5) holds) is inaccurate (paper II). In Table II, we list the results of the correct calculation (this work) and the improper calculation (paper II) for the capture of the electron from L-shell of argon atom by a fast proton. For the sake of easy comparison, we adopt the definition from paper II for the ionization energy $I_t=\theta\frac{1}{2}\frac{Z_t^2}{n^2}$ with θ = 0.412 and 0.550 and assign Z_t = 13.85 a.u. for Ar - L-shell. We find that the deviation of the results of paper II from the present exact results is quite significant, especially when the proton energy is low where the difference could be as much as a factor of three.

One of the weaknesses in our approach in formulating the cross section of the electron capture from a multi-electron atom is the indeterminacy of the effective nuclear charge Z_t', which is introduced through the eikonal phase factor, due to the lack of information on the many-body system (i.e., the multi-electron atom in the present case). Nevertheless, we could expect that the value of Z_t' should lie in an interval bounded by unity (when the electron is promptly removed from the target at the time of the capture) and Z_t (when the electron stays in its initial orbit around the target for a very long period of time, compared with the orbital period around the projectile after the capture). In our calculations we consider two extreme cases, Z_t' = 1 and Z_t' = Z_t, and compare the results with the experimental

data for the capture cross sections from C, Ne, Ar, N_2, O_2, and He. One could expect that the experimental data fall in the area enveloped by the curves corresponding to these two limits. The values of Z_t, $|\varepsilon_t|$ [10], and I_t [15] for the individual atomic shells, used in the calculations, are tabulated in Table I. Analytic expressions corresponding to the K- and L-shells electron capture are written explicitly as follows,

$$\sigma_{1s-n'}(v) = \frac{2^8 \pi Z_t^5 Z_p^5}{v^2 n'^3} \frac{\pi \eta Z_t'}{\sinh(\pi \eta Z_t')}$$

$$\times \exp[-2\eta Z_t' \tan^{-1}(-P_{03}/Z_t)]$$

$$\times \frac{5}{4} \frac{Q_1^2}{Q'^2} \left\{ \frac{1}{3}\left(1 + \frac{P_{03}^2}{Z_t^2}\right) \eta^2 Z_t'^2 \right.$$

$$\times {}_2F_1(2, 1; 4; 1 - \frac{Q_1}{Q'}) + \eta Z_t'$$

$$\times \left(\frac{P_{03}}{Z_t} - \eta Z_t'\right) {}_2F_1(2, 1; 5; 1 - \frac{Q_1}{Q'})$$

$$\left. + \frac{4}{5}(1 + \eta^2 Z_t'^2) {}_2F_1(2, 1; 6; 1 - \frac{Q_1}{Q'}) \right\}, \quad (36a)$$

$$\sigma_{2s\text{-}n'}(v) = \frac{2^8 \pi z_t^5 z_p^5}{v^2 2^5 n'^3} \frac{\pi \eta z_t'}{\sinh(\pi \eta z_t')} \exp\left[-2\eta z_t' \tan^{-1}(-2p_{0z}/z_t)\right]$$

$$\times \frac{20}{z_t^2 Q'^2} \left\{ \frac{Q_z^2}{12} \eta^2 z_t'^2 \left(p_{0z}^2 - z_t p_{0z} \eta z_t' + \frac{1}{4} z_t^2 \eta^2 z_t'^2\right) \right.$$

$$\times {}_2F_1(2,1;4;1-\frac{Q_z^2}{Q'^2}) + \frac{1}{4} Q_z z_t \eta z_t'$$

$$\times \left[p_{0z}\left(p_{0z}^2 - \frac{1}{4} z_t^2\right) - \left(\frac{1}{8} z_t^2 - 2 p_{0z}^2\right) z_t \eta z_t' \right.$$

$$\left. + z_t^2 p_{0z} \eta^2 z_t'^2 - \frac{1}{8} z_t^3 \eta^3 z_t'^3 \right] {}_2F_1(2,1;5;1-\frac{Q_z^2}{Q'^2})$$

$$+ \frac{1}{5} z_t^2 \left[Q_z^2 - \frac{1}{2} z_t p_{0z} \left(\frac{1}{4} z_t^2 + 3 p_{0z}^2\right) \eta z_t' \right.$$

$$+ \left(\frac{z_t^4}{16} + \frac{7}{4} z_t^2 p_{0z}^2 + p_{0z}^4\right) \eta^2 z_t'^2 - \frac{1}{4} z_t p_{0z}$$

$$\times \left(\frac{11}{4} z_t^2 + 3 p_{0z}^2\right) \eta^3 z_t'^3 + \frac{1}{8} z_t^2 \left(\frac{3}{4} z_t^2 + p_{0z}^2\right)$$

$$\left. \times \eta^4 z_t'^4 \right] {}_2F_1(2,1;6;1-\frac{Q_z^2}{Q'^2})$$

$$+ \frac{1}{6} z_t^4 \left[-Q_z + \frac{1}{2} z_t p_{0z} \eta z_t' - \left(\frac{3}{8} z_t^2 + p_{0z}^2\right) \eta^2 z_t'^2 \right.$$

$$\left. + \frac{1}{2} z_t p_{0z} \eta^3 z_t'^3 - \frac{1}{8} z_t^2 \eta^4 z_t'^4 \right]$$

$$\times {}_2F_1(2,1;7;1-\frac{Q_z^2}{Q'^2}) + \frac{1}{102} z_t^6 \left(4 + 5\eta^2 z_t'^2 + \eta^4 z_t'^4\right)$$

$$\left. \times {}_2F_1(2,1;8;1-\frac{Q_z^2}{Q'^2}) \right\} , \qquad (36b)$$

and

$$\sigma_{2p-n'}(v) = \frac{2^8 \pi z_t^5 z_p^5}{v^2\, 2^5\, n'^3} \quad \frac{\pi \eta z_t'}{\sinh(\pi \eta z_t')}$$

$$\times \exp[-2\eta z_t' \tan^{-1}(-2P_{0z}/z_t)]$$

$$\times \Big\{ \frac{1}{12} Q_2^2 \eta^2 z_t'^2 (1+\eta^2 z_t'^2)\, {}_2F_1(2,1;4;1-\tfrac{Q_2}{Q'})$$

$$+ \frac{1}{2} Q_2^2 \eta^2 z_t'^2\, {}_2F_1(2,1;5;1-\tfrac{Q_2}{Q'})$$

$$+ \frac{1}{5} z_t \eta z_t' \Big[P_{0z}(\tfrac{1}{2} z_t^2 + 6P_{0z}^2) - z_t$$

$$\times (\tfrac{z_t^2}{4} + 6P_{0z}^2)\eta z_t' + 2 z_t^2 P_{0z} \eta^2 z_t'^2$$

$$- \tfrac{1}{4} z_t^3 \eta^3 z_t'^3 \Big]\, {}_2F_1(2,1;6;1-\tfrac{Q_2}{Q'})$$

$$+ \frac{1}{6} z_t^2 \Big[4Q_2 - 2 z_t P_{0z} \eta z_t' + (\tfrac{3}{2} z_t^2 + 4P_{0z}^2)$$

$$\times \eta^2 z_t'^2 - 2 z_t P_{0z} \eta^3 z_t'^3 + \tfrac{1}{2} z_t^2 \eta^4 z_t'^4 \Big]$$

$$\times {}_2F_1(2,1;7;1-\tfrac{Q_2}{Q'})$$

$$- \frac{1}{28} z_t^4 (4 + 5\eta^2 z_t'^2 + \eta^4 z_t'^4)$$

$$\times {}_2F_1(2,1;8;1-\tfrac{Q_2}{Q'}) \Big\} , \qquad (36c)$$

where

$$Q_1 = z_t^2 + P_{0z}^2 ,$$

and

$$Q_2 = \frac{z_t^2}{2^2} + P_{0z}^2 .$$

In Figs. 1 - 5, we present the results of calculations of the total capture cross section, as a function of the impact energy, and the comparisons with the data available are made. It is found, that the $Z_t' = 1$ eikonal curves are closer to the OBK curves than the $Z_t' = Z_t$ eikonal curves throughout. Furthermore, the first two curves become even closer as the nuclear charge Z_t increases because the electron - target interaction involved in the eikonal phase factor, describing the deviation of the eikonal approximation from the OBK approximation, is virtually equal to zero as the nuclear charge is very large while the quantity Z_t' takes on a small value, e.g., approximately unity. The $Z_t' = 1$ and the $Z_t' = Z_t$ curves become closer as the energy increases, reducing the uncertainty in our results in the large energy limit. Most of the experimental data, Fig. 1 - 3, lie in the region between the two eikonal curves, except for the capture from He (light nucleus) where the data match fairly well with the $Z_t' = 1$ eikonal curves in large part of the energy range and shift toward the OBK calculation as the energy increases (Figs. 4 and 5). The irregularity of the data distribution over various targets illustrates the crucial dependence of the quantity Z_t' on Z_t, and probably also on other parameters, e.g., v and Z_p, and requires rigorous study of the properties of Z_t'.

An alternative approach to reduce the uncertainty discussed in the preceding section is to use the post form formulation of the eikonal method[16]. Here the projectile (proton) - active electron interaction potential is $(-\frac{1}{r_p})$, and consequently the eikonal distortion (due to this potential) is weak. On the other hand, we have $(-Z_t'/r_t)$ in the matrix element of the post form of the transition amplitude. Setting $Z_t' = Z_t$ is now a good approximation

since the main contribution from Z_t' is governed by the initial bound state wave function with an effective charge Z_t. Therefore the uncertainty in Z_t' is reduced in the post form formulation. However, sum rules over final states cannot then be used to simplify calculations. One has to evaluate all capture cross sections $\sigma_{nl-n'l'}$ individually and then average over the initial states and sum over the final states. Such a computation is quite lengthly and time-consuming. We conclude that the present status of the eikonal approximation for charge transfer from multi-electron atom is not entirely satisfactory and further investigation is needed.

Acknowledgements

It is a pleasure to thank Professor Jörg Eichler for interesting discussion and correspondence. Two of us (T. S. H. and F. T. C.) would like to thank NASA Goddard Space Flight Center for support and hospitality in the summer of 1980. This work was supported in part by the Department of Energy under Contract No. DEAS05-80ER10749.

References

1. J. R. Oppenheimer, Phys. Rev. 31, 349 (1928); H. C. Brinkman and H. A. Kramers, Proc. K. Ned. Akad. Wet. 33, 973 (1930).
2. V. S. Nikolaev, Zh. Eksp. Teor. Fiz. 51, 1263 (1966) [Sov. Phys. JETP 24, 847 (1967)]; K. Omidvar, Phys. Rev. A 19, 65 (1979).
3. F. T. Chan and Jörg Eichler, Phys. Rev. Lett. 42, 58 (1979); Jörg Eichler and F. T. Chan, Phys. Rev. A 20, 104 (1979).
4. F. T. Chan and Jörg Eichler, Phys. Rev. A 20, 1841 (1979).
5. Jörg Eichler and H. Narumi, Z. Phys. 295, 209 (1980).
6. Jörg Eichler, Phys. Rev. A 23, 498 (1981).
7. R. L. Day, T. S. Ho, M. Lieber, and F. T. Chan, to be published; T. S. Ho, M. Lieber, and F. T. Chan, to be published.
8. T. S. Ho, D. Umberger, R. L. Day, M. Lieber, and F. T. Chan, to be published.
9. R. J. Glauber, in Lectures in Theoretical Physics, edited by W. E. Brittin et al. (Interscience, New York, 1959), Vol. 1, p. 315.
10. C. Froese Fischer, The Hartree-Fock method for Atoms, (Wiley-Interscience, New York, 1977).
11. V. Fock, Z. Phys. 98, 145 (1935).
12. I. S. Gradshteyn and I. M. Ryzhik, Table of Integrals, Series, and Products, (Academic Press, New York, 1965), p. 286, Eq. 3197-1.
13. J. N. Gau and J. Macek, Phys. Rev. A 10, 522 (1974).
14. M. C. R. McDowell and J. P. Coleman, Introduction to the Theory of Ion-Atom Collisions (North-Holland, Amsterdam, 1970).
15. A. H. Wapstra, G. J. Nijgh, and R. van Leishout, Nuclear Spectroscopy Tables (Amsterdam, 1959), p. 77; F. P. Larkins, Atomic Data and Nuclear Data Tables 20, 316 (1977).
16. We would like to thank Professor J. Macek for this remark.

17. M. Rodbro, E. H. Pedersen, C. L. Cooke, and J. R. McDonald, Phys. Rev. A 19, 1936 (1979).

18. L. H. Toburen, M. Y. Nakai, and R. A. Langley, Phys. Rev. 171, 114 (1968).

19. L. M. Welsh, K. H. Berkner, S. N. Kaplan, and R. V. Pyle, Phys. Rev. 158, 85 (1967).

20. K. H. Berkner, S. N. Kaplan, G. A. Paulikas, and R. V. Pyle, Phys. Rev. A 140, 729 (1965).

21. E. Acerbi et al, Nuovo Cimento, 50B, 176 (1967); 64, 1068 (1969).

22. C. F. Barnett and H. K. Reynolds. Phys. Rev. 109, 355 (1958).

23. U. Schryber, Helv. Phys. Acta 40, 1023 (1968).

24. J. F. Williams, Phys. Rev. 157, 97 (1967).

25. F. J. de Heer, J. Van Eck, and J. Kistemaker, in Proceedings of the Sixth Conference on Ionization Phenomena in Gases, Paris, Vol. I (SERMA, Paris, 1963), p. 73.

26. L. I. Pivovar, M. T. Novikov, and V. M. Tubaev, Zh. Eksp. Teor. Fiz. 42, 1490 (1962) [Sov. Phys JETP 15, 1035 (1962)].

27. P. Hvelplund, J. Heinemeier, E. Horsdal Pedersen, and F. R. Simpson, J. Phys. B 9, 491 (1976).

Tables Caption

Table I: Values of effective nuclear charge Z_t, the energy eigenvalue $|\varepsilon_t|$ (Ref. 10), and the ionization energy I_t (Ref. 15) of the individual atomic shells.

Table II: Comparison of the total (summed over all possible final bound states) cross sections for the electron capture from L-shell of argon by proton between the present exact calculations (σ_1) and the approximated calculations (σ_2) in paper II (Ref. 6) at various energies. The ionization energy is defined as $I_t = \theta \frac{1}{2}(Z_t^2/2^2)$ with $\theta = .412$ and .55, and $Z_t = 13.85$ a.u..

Table I

Target	Configuration	Z_t(a.u.)	$\|\varepsilon_t\|$(a.u.)	I_t(a.u.)
He	$1s^2$	1.618	0.91795	0.90334
C	$1s^2$	5.588	11.32551	10.43733
N	$1s^2$	6.570	15.62905	14.70047
	$2s^2$	4.504	0.94532	0.74696
	$2p^3$	3.547	0.56758	0.53436
O	$1s^2$	7.553	20.66865	19.55163
	$2s^2$	5.254	1.24431	1.04520
	$2p^4$	3.547	0.63190	0.50033
Ne	$1s^2$	9.516	32.77244	31.86328
Ar	$2s^2$	14.533	12.32215	10.65784
	$2p^6$	13.322	9.57146	9.04079

Table II

E_1 (MeV/amu)	θ = .412 σ_1 ($10^{-16}cm^2$)	θ = .412 σ_2 ($10^{-16}cm^2$)	θ = .55 σ_1 ($10^{-16}cm^2$)	θ = .55 σ_2 ($10^{-16}cm^2$)
1.0	1.745(-3)	4.776(-4)	1.433(-3)	5.641(-4)
1.2	1.162(-3)	3.372(-4)	1.002(-3)	4.074(-4)
1.4	7.951(-4)	2.441(-4)	7.108(-4)	2.988(-4)
1.6	5.574(-4)	1.805(-4)	5.120(-4)	2.226(-4)
1.8	3.994(-4)	1.358(-4)	3.745(-4)	1.682(-4)
2.0	2.916(-4)	1.039(-4)	2.780(-4)	1.288(-4)
3.0	7.574(-5)	3.243(-5)	7.555(-5)	3.984(-5)
4.0	2.559(-5)	1.247(-5)	2.559(-5)	1.506(-5)
5.0	1.029(-5)	5.519(-6)	1.054(-5)	6.556(-6)
10.0	4.334(-7)	2.980(-7)	4.455(-7)	3.345(-7)
20.0	1.224(-8)	9.938(-9)	1.248(-8)	1.064(-8)

Figures caption

Fig. 1: Total electron capture cross sections (in 10^{-16} cm^2) as a function of energy (in MeV/amu). The electrons are captured from K-shell of atoms C and Ne, but from L-shell of Ar. Theory: upper solid curves, $Z_t' = 1$ eikonal results; lower solid curves, the $Z_t' = Z_t$ eikonal results; dashed curves, OBK results. Experiment (dotted), Ref. 17.

Fig. 2: Total electron capture cross sections (in 10^{-16} cm^2) as a function of energy (in MeV/amu) from K- and L- shells of molecule N_2. The theoretical values for molecule N_2 are equal to twice of the theoretical values for atom N. Theory: upper solid curves, $Z_t' = 1$ eikonal results; lower solid curve, $Z_t' = Z_t$ eikonal results; dashed curves, OBK results. Experiment: ● , Toburen et al. (Ref. 18); □, Welsh et al. (Ref. 19); △ , Berkner et al. (Ref. 20); ○, Acerbi et al. (Ref. 21).

Fig. 3: Total electron capture cross sections (in 10^{-16} cm^2) as a function of energy (in MeV/amu) from K- and L-shells of molecule O_2. The theoretical values for molecule O_2 are equal to twice of the theoretical values for atom O. Theory: upper solid curves, $Z_t' = 1$ eikonal results; lower solid curve, $Z_t' = Z_t$ eikonal results; dashed curves, OBK results. Experiment: ● , Toburen et al. (Ref. 18); ○, Acerbi et al. (Ref. 21).

Fig. 4: Total cross sections (in 10^{-16} cm^2), as a function of energy (in KeV/amu), of the electron capture from helium atom by proton. Theory: upper solid curve, $Z_t' = 1$ eikonal results; lower solid curve, $Z_t' = Z_t$ eikonal results; dashed curve, OBK results. Experiment: ○ , Barnett et al. (Ref. 22); ● , Toburen et al. (Ref. 18); □, Welsh et al. (Ref. 19); ◇ , Schryber (Ref. 23); ▩ , Williams (Ref. 24); △ , Berkner et al. (Ref. 20).

Fig. 5: Total cross sections (in 10^{-16} cm^2), as a function of energy (in KeV/amu), of the electron capture from helium by α-particle. Theory: upper solid curve, $Z_t' = 1$ eikonal results; lower solid curve, $Z_t' = Z_t$ eikonal results; dashed curve, OBK results. Experiment: O , Pivover et al. (Ref. 26); △ , Hvelplund et al. (Ref. 27).

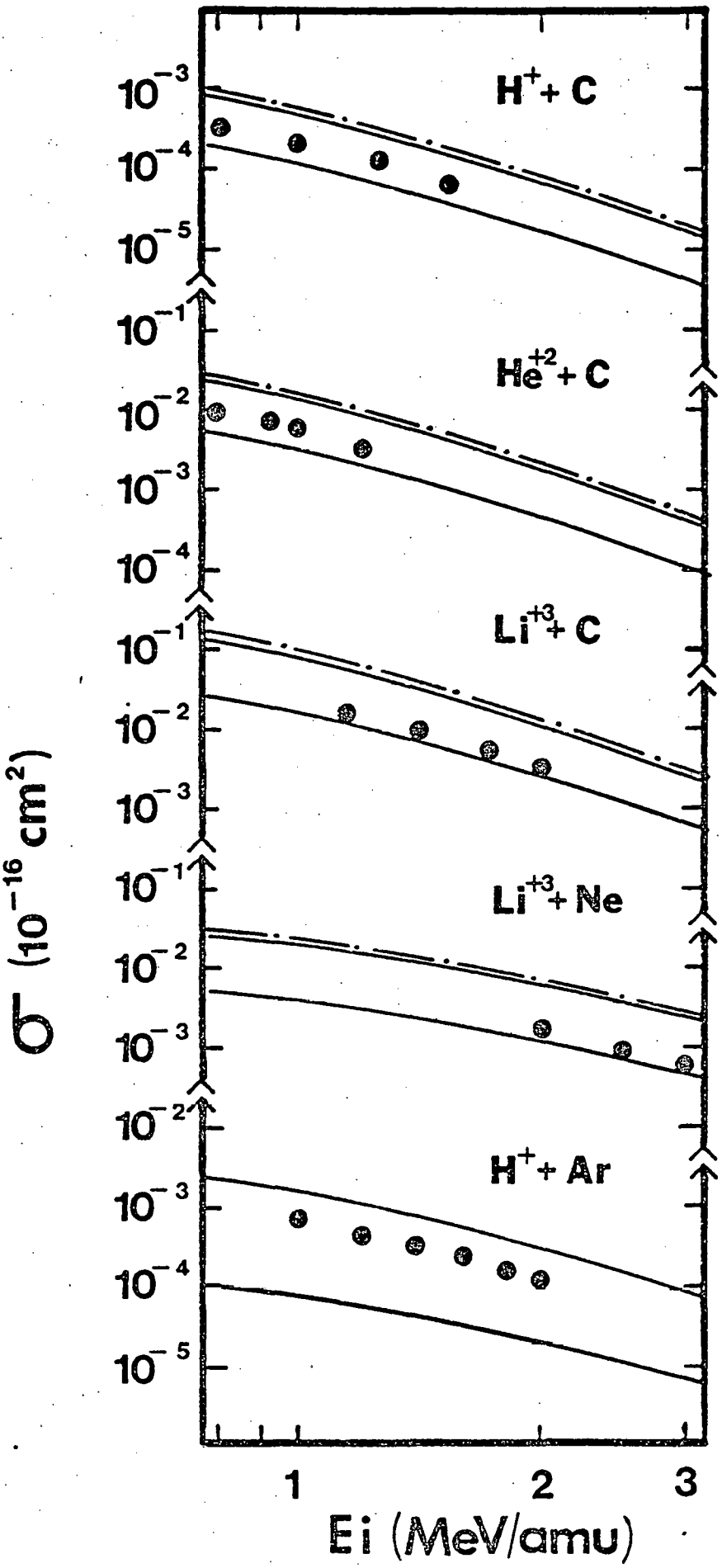
H+ + C
He+2 + C
Li+3 + C
Li+3 + Ne
H+ + Ar
σ (10−16 cm2)
Ei (MeV/amu)
10−3
10−4
10−5
10−1
10−2
10−3
10−4
10−1
10−2
10−3
10−1
10−2
10−3
10−2
10−3
10−4
10−5
1
2
3

Figure 1

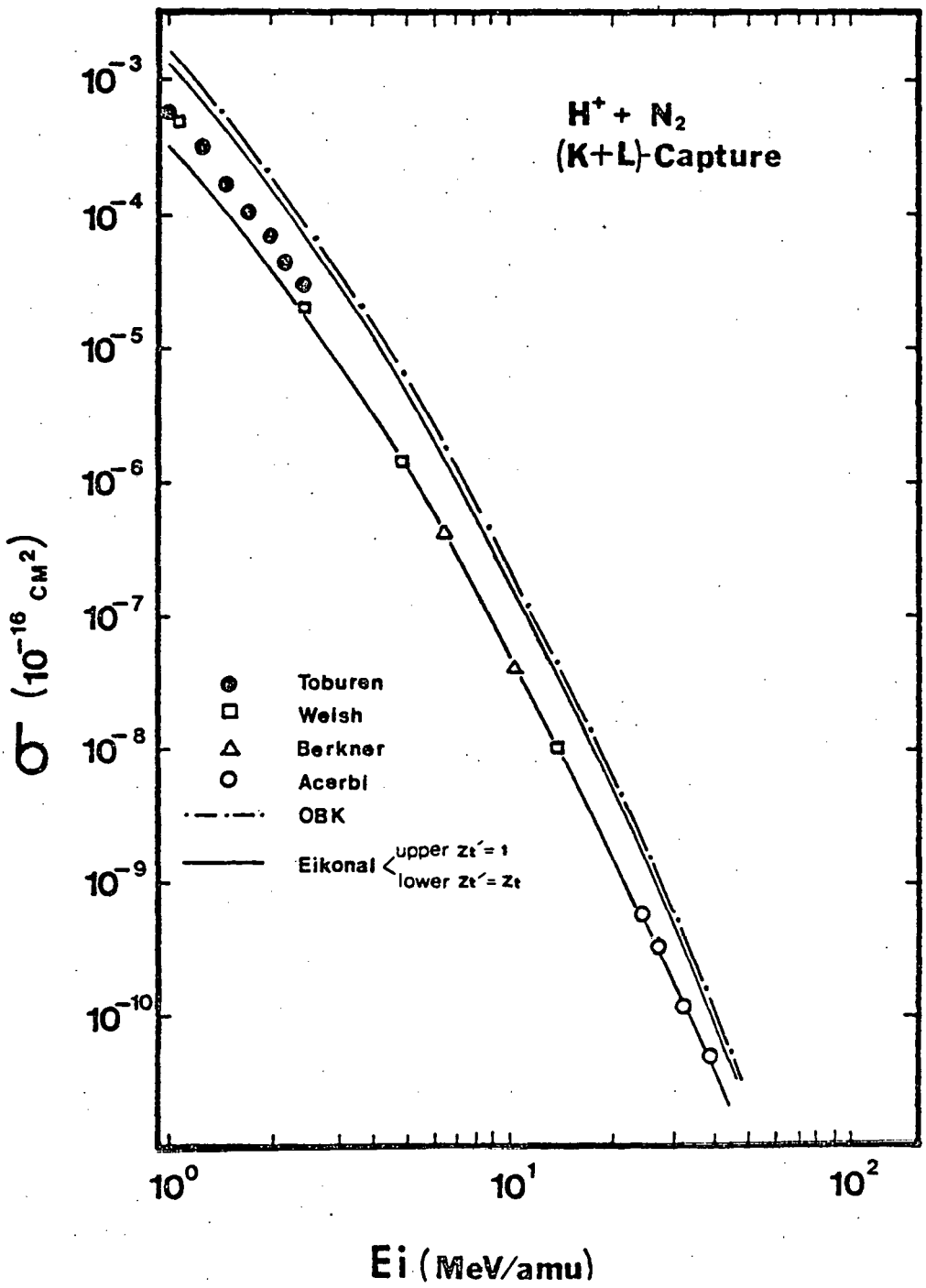
$H^+ + N_2$
(K+L)-Capture
10^{-3}
10^{-4}
10^{-5}
10^{-6}
10^{-7}
10^{-8}
10^{-9}
10^{-10}
σ (10^{-16} cm^2)
Toburen
Welsh
Berkner
Acerbi
OBK
Eikonal
upper $z_t' = 1$
lower $z_t' = z_t$
10^0
10^1
10^2
Ei (MeV/amu)

Figure 2

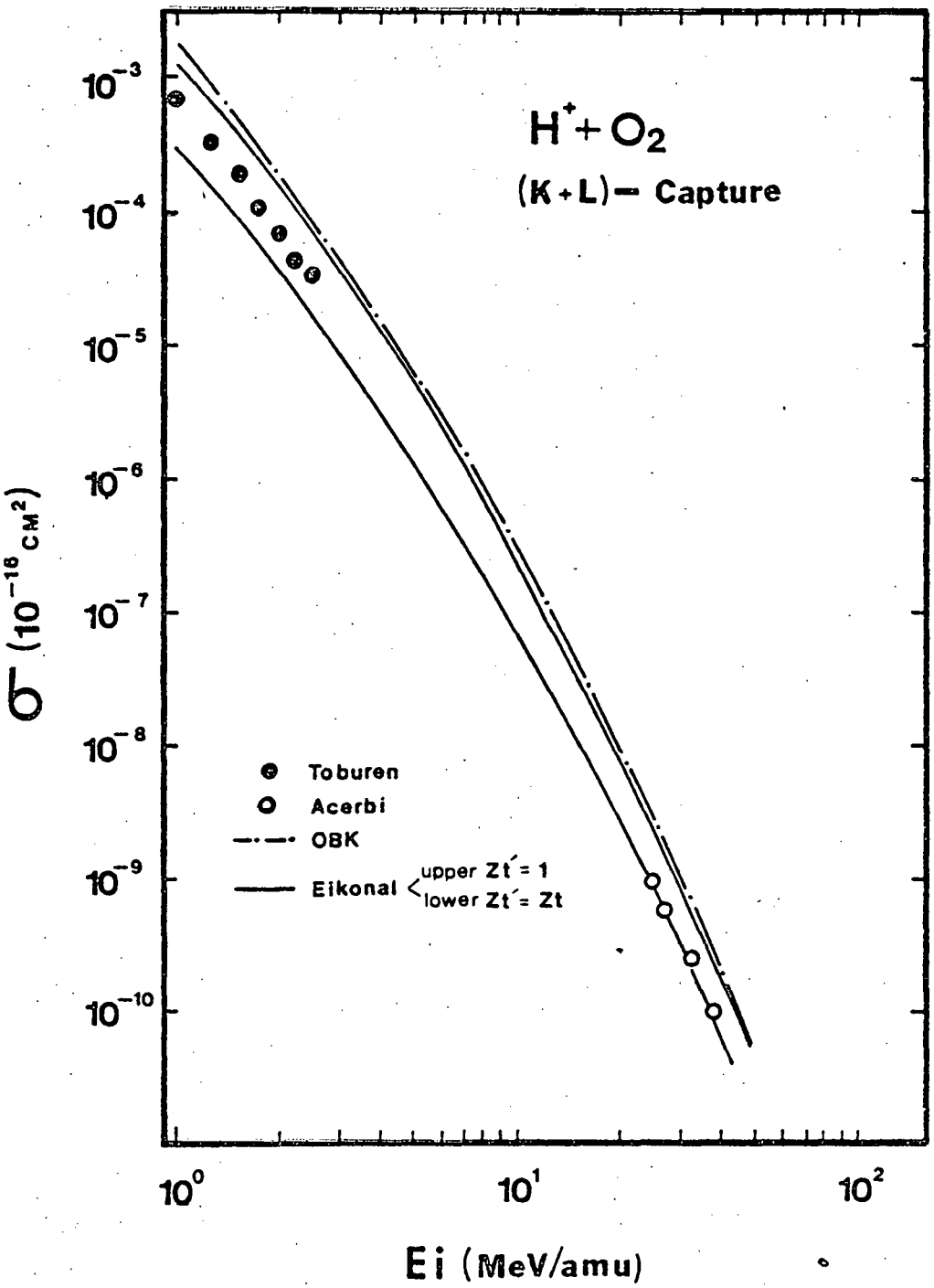
$H^+ + O_2$
(K+L)— Capture
σ (10^{-16} CM^2)
10^{-3}
10^{-4}
10^{-5}
10^{-6}
10^{-7}
10^{-8}
10^{-9}
10^{-10}
10^0
10^1
10^2
Ei (MeV/amu)
Toburen
Acerbi
OBK
Eikonal
upper Zt' = 1
lower Zt' = Zt

Figure 3

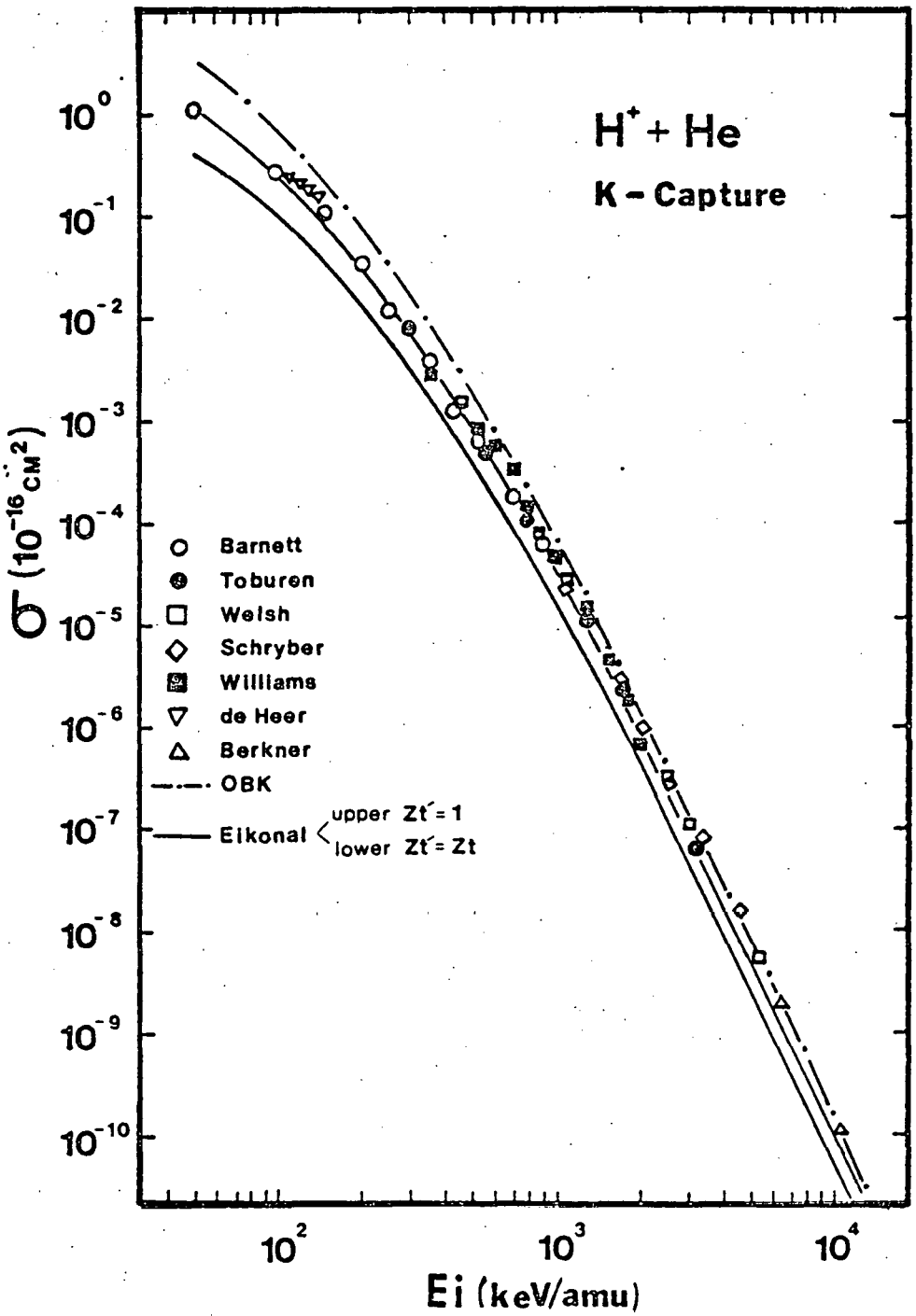
H⁺ + He
K - Capture
σ (10⁻¹⁶ cm²)
Ei (keV/amu)
Barnett
Toburen
Welsh
Schryber
Williams
de Heer
Berkner
OBK
Eikonal
upper Zt' = 1
lower Zt' = Zt

Figure 4

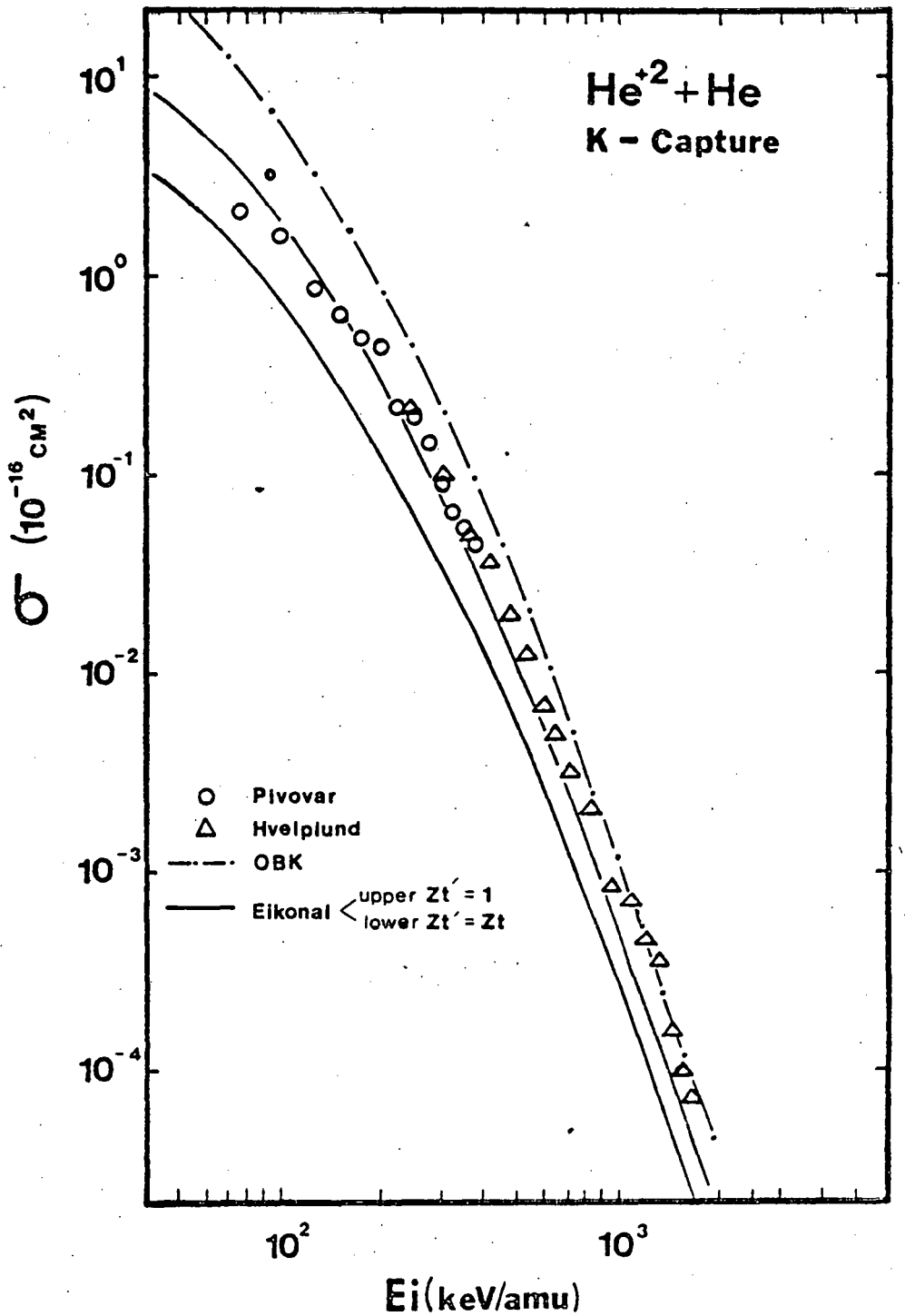
$He^{+2}+He$
K – Capture
10^{1}
10^{0}
10^{-1}
10^{-2}
10^{-3}
10^{-4}
σ $(10^{-16}\ cm^2)$
Pivovar
Hvelplund
OBK
Eikonal
upper Zt´ = 1
lower Zt´ = Zt
10^{2}
10^{3}
Ei(keV/amu)

Figure 5

Eikonal Calculation of Electron Capture Cross Sections from an Arbitrary $n\ell m$ Shell of a Hydrogenic Target into an Arbitrary $n'\ell'm'$ Shell of a Fast Bare Projectile

T. S. Ho, D. Umberger, R. L. Day, M. Lieber, and F. T. Chan
Department of Physics, University of Arkansas, Fayetteville AR 72701

Using techniques similar to those previously employed the eikonal approximation is applied to the evaluation of the cross section for electron capture from an arbitrary $n\ell m$ shell of a hydrogenic target atom into an arbitrary $n'\ell'm'$ of a fast hydrogenic projectile. The results are obtained in exact analytical closed form. Numerical results are presented for the case $H^+ + H(1s) \longrightarrow H(n'\ell'm') + H^+$ when $n'=2$ and 3. Comparison is made with the corresponding OBK results.

I. Introduction

Charge transfer processes have been of interest since the early days of Quantum Mechanics. This interest has increased considerably in the past few years, the focus being on processes relevant to magnetically confined fusion plasmas and astrophysical plasmas. Knowledge concerning the charge transfer from a hydrogenic atom to a bare ion is important not only with regard to these applications but also from a fundamental point of view since such a process is the simplest type of a rearrangement reaction.

An approach for treating electron capture into arbitrary principle shells of energetic projectiles based on the eikonal approximation was developed by Chan and Eichler[1]. They later amended their approach for capture into arbitrary n', ℓ' sublevels of a fast projectile from the ground state[2] as well as from an arbitrary initial n, ℓ sublevel[3] of a hydrogenic target. The results obtained agree well with experimental findings for hydrogen and helium targets. In this paper we extend the eikonal treatment to cover n, ℓ, m contributions. There are at least two reasons why such a study is interesting. First of all, specification of these contributions allow for a sterner test of capture theories. Such a test is realizable since techniques for measuring charge exchange for $p + N_2 \rightarrow N_2^+ + H(n'=3,\ell',m')$ have recently been developed[4] and a corresponding study of charge capture for p + H collisions is now under way at Harvard University[5]. The present study is partly motivated by these experimental interests. Secondly it is the most general case

and it contains all the previous results[1-3] as special cases. In addition, it furnishes information not available from classical trajectory Monte Carlo calculations[6].

In Sec. II, we use the eikonal approximation to calculate the cross section for the capture of an electron into a (n',ℓ',m') state of an energetic projectile from a hydrogenic target initially in the (n,ℓ,m) state. The result is obtained in closed form, and is exact within the eikonal approximation. In Sec. III, we discuss our results and present some theoretical data for the reaction $H^+ + H(1s) \rightarrow H(n'=2,3,\ell',m') + H^+$. The OBK results are obtained as a limiting case and are given in an appendix.

II. The Theory

We consider the process in which an electron, initially in the n,ℓ,m state of a hydrogenic target atom of charge Z_t, is captured into a given n',ℓ',m' state of a bare projectile ion of charge Z_p. We assume that the time which the projectile spends in the vicinity of the target nucleus is samll compared with the transition time of the electron. Let $\vec{r}$, $\vec{r}_t = \vec{r} + \alpha\vec{R}$, and $\vec{r}_p = \vec{r} - (1-\alpha)\vec{R}$ denote the position of the electron with respect to the center of mass, the target nucleus, and the projectile nucleus, respectively, with $\alpha = M_p/(M_p+M_t)$. The projectile is supposed to move rectilinearly and that its trajectory is given by $\vec{R}(t) = \vec{b} + \vec{v}t$ ($\vec{b}\cdot\vec{v}=0$, $|\vec{b}|$=classical impact parameter) with respect to the target nucleus. The cross section can then be written as[7]

$$\sigma_{n\ell m - n'\ell'm'}(v) = \int \left| A_{n\ell m - n'\ell'm'}(\vec{b}, v) \right|^2 d^2b \quad , \tag{1}$$

where the exact eikonal transition amplitude is, in its "prior" form, given by

$$A_{n\ell m - n'\ell'm'}(\vec{b}, v) = -i \int \langle \Psi^{(-)}_{n'\ell'm'} | -\frac{Z_p}{r_p} | \Psi_{n\ell m} \rangle \, dt \quad , \tag{2}$$

with the time-dependent wave functions

$$\Psi_{n\ell m} = \varphi_{n\ell m}(\vec{r}_t) \exp(-i\varepsilon_t t) \exp(-i\alpha\vec{v}\cdot\vec{r} - \tfrac{1}{2}i\alpha^2 v^2 t) \tag{3}$$

and

$$\Psi^{(-)}_{n'\ell'm'} \cong \varphi_{n'\ell'm'}(\vec{r}_p) \exp(-i\varepsilon_p t) \exp[i(1-\alpha)\vec{v}\cdot\vec{r} - \tfrac{1}{2}i(1-\alpha)^2 v^2 t] \times \exp\left(-i\int_t^\infty \frac{Z_t'}{r_t'} dt'\right) \quad . \tag{4}$$

Here, we have introduced the hydrogenic wave functions $\varphi_{n\ell m}(\vec{r}_t)$ and

$\varphi_{n'\ell'm'}(\vec{r}_p)$, and their eigenenergies $\mathcal{E}_t = -\frac{1}{2} Z_t^2/n^2$ and $\mathcal{E}_p = -\frac{1}{2} Z_p^2/n'^2$ (atomic units are used throughout). Furthermore, the translation factors and the eikonal phase factor are included in the wave functions. The effective target charge Z_t' has been introduced in the final state, allowing $Z_t \neq Z_t'$ for multi-electron effects. It is associated with the interaction between the target nucleus and the captured electron. We could also obtain the OBK results by setting $Z_t' = 0$ (Appendix). The approach being used here to obtain the cross section in a closed form is very much the same as that developed in references (1) and (2). First of all, we employ the integral representation of Gau and Macek for the eikonal phase factor[8], namely,

$$\exp\left(i\int_x^\infty \frac{Z_t'}{r_t}\,dx'\right) = \frac{1}{\Gamma(-i\eta z_t')}\int_0^\infty \lambda^{-i\eta z_t'-1}\exp[-\lambda(r_t-z_t)]\,d\lambda \quad , \tag{5}$$

with $\eta = \frac{1}{v}$ and introduce two Fourier transforms $G_{n\ell m}(\vec{p})$ and $g_{n'\ell'm'}(\vec{q})$ by the relations

$$G_{n\ell m}(\vec{p}) = (2\pi)^{-3/2}\int \varphi_{n\ell m}(\vec{r}_t)\left\{\frac{1}{\Gamma(-i\eta z_t')}\int_0^\infty \lambda^{-i\eta z_t'-1}\exp[-\lambda(r_t-z_t)]\,d\lambda\right\} \times \exp(i\vec{p}\cdot\vec{r}_t)\,d^3r_t \tag{6}$$

and

$$g_{n'\ell'm'}(\vec{q}) = (2\pi)^{-3/2}\int \frac{\varphi_{n'\ell'm'}(\vec{r}_p)}{r_p}\exp(i\vec{q}\cdot\vec{r}_p)\,d^3r_p \quad . \tag{7}$$

We can, after introducing $G_{n\ell m}$ and $g_{n'\ell'm'}$ into momentum version of integral (2) and some manipulations involving the Dirac delta function, then reduce a 6-dimensional integral (1) to a two-dimensional integral, over a two-dimensional momentum space which is normal to the incident

velocity $\vec{v}$

$$\sigma_{nem\text{-}n'\ell'm'}(v) = \frac{2^4\pi^4 Z_p^2}{v^2}\int\left\{\left|\mathcal{G}_{n'\ell'm'}(\vec{p}+\vec{v})\right|^2\left|G_{nem}(\vec{p})\right|^2\right\}_{p_z=p_{oz}} d^2p_b \quad , (8)$$

where $p_{oz} = -\frac{1}{2}v+\eta\varepsilon$ with $\varepsilon = \varepsilon_p - \varepsilon_x$. We shall proceed to evaluate these two integrals of Eqs. (6) and (7), exhibiting some detail, and, finally, carry out the $\vec{p}_b$ integration in the remainder of this section. To start with, we consider the integral (7). Although it is well-known[7], we still briefly describe the steps as follows. The Schrodinger equation for a hydrogenic system can be written as

$$-\frac{1}{2}\nabla^2\varphi_{n'\ell'm'} + V\varphi_{n'\ell'm'} = E_{n'}\varphi_{n'\ell'm'} \qquad (9)$$

with $V = -\frac{Z_p}{r_p}$ and $E_{n'} = -\frac{Z_p^2}{2n'^2}$; therefore

$$\frac{\varphi_{n'\ell'm'}}{r_p} = \frac{1}{2Z_p}\left(\frac{Z_p^2}{n'^2}\varphi_{n'\ell'm'} - \nabla^2\varphi_{n'\ell'm'}\right)$$

and

$$\mathcal{G}_{n'\ell'm'}(\vec{q}) = \frac{(2\pi)^{-3/2}}{2Z_p}\int d^3r_p\, \exp(i\vec{q}\cdot\vec{r}_p)\left(\frac{Z_p^2}{n'^2} - \nabla^2\right)\varphi_{n'\ell'm'} \quad , \qquad (10)$$

After integrating by parts twice and some manipulations, we obtain

$$\mathcal{G}_{n'\ell'm'}(\vec{q}) = \frac{q^2+q_{n'}^2}{2Z_p}(2\pi)^{-3/2}\int d^3r_p\, \varphi_{n'\ell'm'}(\vec{r}_p)\exp(i\vec{q}\cdot\vec{r}_p) \quad , \qquad (11)$$

where $q_{n'} = \frac{Z_p}{n'}$ and the Fourier transform of the hydrogenic wave function

$$\tilde{\varphi}_{n'\ell'm'}(\vec{q}) = (2\pi)^{-3/2}\int d^3r_p\, \varphi_{n'\ell'm'}(\vec{r}_p)\exp(i\vec{q}\cdot\vec{r}_p) \qquad (12)$$

is given in closed form[9], namely,

$$\tilde{\varphi}_{n'\ell'm'}(\vec{q}) = \frac{4\, q_{n'}^{\ell+1/2}}{(q^2+q_{n'}^2)^2} N_{n'\ell'}(\sin\alpha)^{\ell'} C_{n'-\ell'-1}^{\ell'+1}(\cos\alpha)\, Y_{\ell'm'}(\hat{q}) \qquad (13)$$

with

$$N_{n\ell}^2 = \frac{n'(n'-\ell'-1)!}{(n'+\ell')!}\,\frac{(\ell'!)^2\,2^{2\ell'+1}}{\pi} \quad ,$$

$$\sin\alpha = \frac{2\beta q_{n'}}{\beta^2+q_{n'}^2} \quad ,$$

and

$$\cos\alpha = \frac{q_{n'}^2-\beta^2}{q_{n'}^2+\beta^2} \quad .$$

Here $C_\mu^\nu(x)$ is the Gegenbauer polynomial[10]. Taking absolute magnitude square of $g_{n'\ell'm'}(\vec{q})$ results in

$$|g_{n'\ell'm'}(\vec{q})|^2 = \frac{2^{2\ell'+2}N_{n'\ell'}^2}{n'^2}\,\frac{q_{n'}^{2\ell'+3}\,\beta^{2\ell'}}{(q_{n'}^2+\beta^2)^{2\ell'+2}}\left[C_{n'-\ell'-1}^{\ell'+1}\left(\frac{q_{n'}^2-\beta^2}{q_{n'}^2+\beta^2}\right)\right]^2 |Y_{\ell'm'}(\hat{q})|^2 \,. \quad (14)$$

Now[11]

$$Y_{\ell'm'}(\vec{q}) = \sqrt{\frac{2\ell'+1}{4\pi}\,\frac{(\ell'-|m'|)!}{(\ell'+|m'|)!}}\;P_{\ell'}^{|m'|}(\cos\theta_{\vec{q}})\,\exp(im'\phi_{\vec{q}}) \,. \quad (15)$$

Its absolute square, when Rodrigues' formula[11] for $P_{\ell'}^{|m'|}(\cos\theta_{\vec{q}})$ is used, results in

$$|Y_{\ell'm'}(\hat{q})|^2 = \frac{2\ell'+1}{4\pi}\,\frac{(\ell'-|m'|)!}{(\ell'+|m'|)!}\,\frac{(\sin\theta_{\vec{q}})^{2|m'|}\,(\cos\theta_{\vec{q}})^{2(\ell'-|m'|)}}{2^{2\ell'}\,(\ell'!)^2}\cdot$$
$$\times\sum_{\mu,\mu'=0}^{\left[\frac{\ell'-|m'|}{2}\right]} H_\mu(\ell',m')\,H_{\mu'}(\ell',m')\,(\cos\theta_{\vec{q}})^{-2(\mu+\mu')} \quad (16)$$

with

$$H_\mu(\ell',m') = (-1)^\mu\binom{\ell'}{\mu}\frac{(2\ell'-2\mu)!}{(\ell'-|m'|-2\mu)!} \,.$$

We can also write the Gegenbauer polynomial as[12]

$$C_{n'-\ell'-1}^{\ell'+1}\left(\frac{q_{n'}^2-\beta^2}{q_{n'}^2+\beta^2}\right) = \frac{(n'+\ell')!}{(n'-\ell'-1)!\,(2\ell'+1)!}\;{}_2F_1\left(n'+\ell'+1,-n'+\ell'+1;\ell'+\tfrac{3}{2};\frac{\beta^2}{\beta^2+q_{n'}^2}\right)$$

$$= \frac{(n'+\ell')!}{(n'+\ell'+1)!\,(2\ell'+1)!} \sum_{k=0}^{n'-\ell'-1} K_k(n',\ell') \frac{q^{2k}}{(\beta_{n'}^2+q^2)^k} \quad , \tag{17}$$

where

$$K_k(n',\ell') = \frac{(n'+\ell'+1)_k\,(-n'+\ell'+1)_k}{(\ell'+3/2)_k\;k!} \qquad \text{with } (a)_k = \frac{\Gamma(a+k)}{\Gamma(a)} .$$

Using Eqs. (15) and (17) with $\vec{q}=(\vec{P}+\vec{v})_{P_3=P_{03}}$ and $\cos\theta_{\vec{q}} = \frac{P_{03}+v}{\sqrt{P_b^2+(P_{03}+v)^2}}$,

we get

$$\begin{aligned} |g_{n'\ell'm'}(\vec{P}+\vec{v})|^2 = {} & \frac{2^{2\ell'+1}\,\beta_{n'}^{2\ell'+3}}{\pi^2} \frac{(n'+\ell')!\,(2\ell'+1)\,(\ell'-|m'|)!}{n'(n'-\ell'-1)!\,[(2\ell'+1)!]^2(\ell'+|m'|)!} \\ & \times \sum_{k,k'=0}^{n'-\ell'-1} \sum_{\mu,\mu'=0}^{[\frac{\ell'-|m'|}{2}]} K_k(n',\ell')\,K_{k'}(n',\ell')\,H_\mu(\ell',m')\,H_{\mu'}(\ell',m') \\ & \times (P_{03}+v)^{2(\ell'-|m'|-\mu-\mu')}\,P_b^{2|m'|} \\ & \times [P_b^2+(P_{03}+v)^2+\beta_{n'}^2]^{-2\ell'-2-k-k'}\,[P_b^2+(P_{03}+v)^2]^{k+k'+\mu+\mu'} . \end{aligned} \tag{18}$$

Here [a] denotes the integral part of the real number a . Next, we compute the integral $G_{n\ell m}(\vec{P})$, i.e. Eq. (6). Inverting the order of integration results in

$$G_{n\ell m}(\vec{P}) = \frac{1}{\Gamma(-i\eta z_x')} \int_0^\infty \lambda^{-i\eta z_x'-1}\, h_{n\ell m}(\vec{P},\lambda)\, d\lambda \quad , \tag{19}$$

where

$$h_{n\ell m}(\vec{P},\lambda) = (2\pi)^{-3/2} \int \varphi_{n\ell m}(\vec{r}_x) \exp[-\lambda(r_x-z_x)] \exp(i\vec{P}\cdot\vec{r}_x)\, d^3r_x . \tag{20}$$

Furthermore, we define a complex vector

$$\vec{K} \equiv \vec{P} - i\lambda\hat{3}$$

and use the relation

$$\varphi_{n\ell m}(\vec{r}_x) = R_{n\ell}(r_x)\, Y_{\ell m}(\hat{r}_x) , \tag{21a}$$

where the radial part given explicitly by[13]

$$R_{n\ell}(r_t) = \left(2\frac{Z_t}{n}\right)^{\ell+3/2}\sqrt{\frac{(n-\ell-1)!}{2n(n+\ell)!}} \times \sum^{n-\ell-1} S_\sigma(n,\ell)\left(2\frac{Z_t}{n}\right)^\sigma \exp\left(-\frac{Z_t}{n}r_t\right) r_t^{\ell+\sigma} \qquad (21b)$$

with

$$S_\sigma(n,\ell) = (-1)^\sigma \frac{(n+\ell)!}{(n-\ell-1-\sigma)!\,(2\ell+1+\sigma)!\,\sigma!} .$$

We also have

$$\exp(i\vec{K}\cdot\vec{r}_t) = 4\pi \sum_{L=0}^{\infty}\sum_{M=-L}^{L} i^L j_L(Kr_t) Y_{LM}(\hat{K}) Y^*_{LM}(\hat{r}_t), \qquad (22)$$

where $j_L(Kr_t)$ is the spherical Bessel function but with complex argument, since

$$K = \sqrt{p^2 - 2i\lambda p_3 - \lambda^2} . \qquad (23)$$

Inserting Eqs. (21a) and (22) in Eq. (20), the orthonormality of spherical harmonic functions gives

$$h_{n\ell m}(\vec{p},\lambda) = i\sqrt{\frac{2}{\pi}}\, Y_{\ell m}(\hat{K}) \int_0^\infty R_{n\ell}(r_t)\exp(-\lambda r_t)\, j_\ell(Kr_t) r_t^2 dr_t . \qquad (24)$$

The use of the explicit form for $R_{n\ell}(r_t)$ enables one to carry r_t-integral (24) out easily. Furthermore, expressing $Y_{\ell m}(\hat{K})$, in the same way as when evaluating $g_{n'\ell'm'}$, in a finite polynomial permits us to perform the λ-integration for the integral $G_{n\ell m}(\vec{p})$. Notice that because the vector $\vec{K}$ is complex we have $\cos\theta_{\vec{K}} = \frac{p_3 - i\lambda}{\sqrt{p^2 - 2i\lambda p_3 - \lambda^2}}$ and $\tan\phi_{\vec{K}} = \frac{p_y}{p_x}$, where $\phi_{\vec{K}}$ is independent of λ. We find then that

$$
\begin{aligned}
G_{n\ell m}(\vec{p}) = {} & \frac{i^{\ell}}{\Gamma(-i\eta z_x')}\, 2\cdot\left(\frac{z_x}{n}\right)^{\ell+3/2}\sqrt{\frac{(n-\ell-1)!\,(2\ell+1)!\,(\ell-|m|)!}{2n\,(n+\ell)!\,4\pi\,(\ell+|m|)!}} \\
& \times \frac{(-1)^{|m|}}{2^{\ell}\,\ell!}\left(2\frac{z_x}{n}-2iP_{0y}\right)^{i\eta z_x'}\left(p^2+\frac{z_x^2}{n^2}\right)^{-i\eta z_x'} \\
& \times \Bigg\{ \sum_{\sigma=0}^{n-\ell-1} \sum_{\nu=0}^{[\frac{\sigma+1}{2}]} \sum_{\tau=0}^{[\frac{\ell-|m|}{2}]} \sum_{\gamma=0}^{\tau+\nu} \sum_{\delta=0}^{\ell-|m|-2\tau+2\gamma} \sum_{\alpha=0}^{\sigma+1-2\nu} \\
& \times S_{\sigma}(n,\ell)\, N_{\nu}(\ell,\sigma)\, T_{\tau}(\ell,m)\, M_{\gamma}(\nu,\tau)\, D_{\delta}(\tau,\gamma)\, A_{\alpha}(\sigma,\nu) \\
& \times (-i)^{\delta}\, 2^{\sigma}\, \frac{\Gamma(2\ell+\sigma+3)}{\Gamma(\ell+3/2)}\left(\frac{z_x}{n}\right)^{2\sigma+1-2\nu-\alpha} \\
& \times P_{0y}^{\ell-|m|-2\tau+2\gamma-\delta}\left(2\frac{z_x}{n}-2iP_{0y}\right)^{-\delta-\alpha} \\
& \times B\left(\delta+\alpha-i\eta z_x',\ \ell+\sigma+2-\delta-\alpha+i\eta z_x'\right) \\
& \times P_b^{|m|+2(\tau+\nu-\gamma)}\left(p^2+\frac{z_x^2}{n^2}\right)^{-(\ell+\sigma+2)+\delta+\alpha}\Bigg\} \\
& \times \exp\left(im\phi_{\vec{p}}\right) \qquad (25)
\end{aligned}
$$

where

$$
S_{\sigma}(n,\ell) = (-1)^{\sigma}\frac{(n+\ell)!}{(n-\ell-1-\sigma)!\,(2\ell+1+\sigma)!\,\sigma!}\ ,
$$

$$
N_{\nu}(\ell,\sigma) = (-1)^{\nu}\frac{\left(\frac{-\sigma-1}{2}\right)_{\nu}\left(-\frac{\sigma}{2}\right)_{\nu}}{(\ell+3/2)_{\nu}\ \nu!}\ ,
$$

$$
T_{\tau}(\ell,m) = (-1)^{\tau}\frac{\ell!\,(2\ell-2\tau)!}{\tau!\,(\ell-\tau)!\,(\ell-|m|-2\tau)!}\ ,
$$

$$M_\gamma(\nu,\tau) = \frac{(\tau+\nu)!}{\gamma!(\tau+\nu+\gamma)!} ,$$

$$D_\delta(\tau,\gamma) = \frac{(\ell-|m|-2\tau+2\gamma)!}{\delta!(\ell-|m|-2\tau+2\gamma-\delta)!} ,$$

$$A_\alpha(\sigma,\nu) = \frac{(\sigma+1-2\nu)!}{\alpha!(\sigma+1-2\nu-\alpha)!} ,$$

$$\tan\phi_{\vec{p}} = \frac{p_y}{p_x} ,$$

and $B(x,y)$ is the usual Beta function[14], defined by

$$B(x,y) \equiv \frac{\Gamma(x)\Gamma(y)}{\Gamma(x+y)}$$

with x and y complex in the present case. We remark, for the case of hydrogenic target, that the following equality holds, namely

$$(p_{0j}+v)^2 + \frac{z_p^2}{n'^2} = p_{0j}^2 + \frac{z_t^2}{n^2} \qquad (26)$$

because of $\varepsilon = -\frac{1}{2}\frac{z_p^2}{n'^2} - \left(-\frac{1}{2}\frac{z_t^2}{n^2}\right)$. Combining Eqs. (18) and (25), and inserting in Eq. (8), the integral over $\vec{p}_b$ may be done immediately via[15]

$$\int_0^\infty x^{\lambda-1}(1+x)^{-\mu+\nu}(x+\beta)^{-\nu}\,dx = B(\mu-\lambda,\lambda)\,{}_2F_1(\nu,\mu-\lambda;\mu;1-\beta).$$

The resulting expression for the cross section is

$$\sigma_{nsm-n'l'm'}(v) = \sigma^{OBK}_{n-n'}\; 2^{-4}\cdot 5\cdot\pi\;\frac{1}{|\Gamma(-i\eta z_f')|^2}\exp\left[-2\eta z_f' \tan^{-1}\left(-\frac{n P_{oz}}{z_f}\right)\right]$$

$$\times\left(\frac{z_p}{n}\right)^{2l'}\;\frac{2^{2l'}(n'+l')!\,(2l'+1)\,(l'-|m'|)!}{n'(n'-l'-1)!\,[(2l'+1)!]^2(l'+|m'|)!}\;\left(\frac{z_f}{n}\right)^{2l}$$

$$\times\frac{(n-l-1)!\,(2l+1)\,(l-|m|)!}{n(n+l)!\,2^{2l}(l!)^2(l+|m|)!}\left(P_{oz}+v\right)^{2(l'-|m'|)}P_{oz}^{\,2(l-|m|)}$$

$$\times\sum_{k,k'=0}^{n'-l'-1}\;\sum_{\mu,\mu'=0}^{\left[\frac{l'-|m'|}{2}\right]}\;\sum_{\sigma,\sigma'=0}^{n-l-1}\;\sum_{\nu,\nu'=0}^{\left[\frac{\sigma+1}{2}\right],\left[\frac{\sigma'+1}{2}\right]}\;\sum_{\tau,\tau'=0}^{\left[\frac{l-|m|}{2}\right]}$$

$$\sum_{\gamma,\gamma'=0}^{\tau+\nu,\,\tau'+\nu'}\;\sum_{\delta,\delta'=0}^{l-|m|-2\tau+2\gamma,\;l-|m|-2\tau'+2\gamma'}\;\sum_{\alpha,\alpha'=0}^{\sigma+1-2\nu,\;\sigma'+1-2\nu'}$$

$$\times K_k(n',l')\,K_{k'}(n',l')\,H_\mu(l',m')\,H_{\mu'}(l',m')$$

$$\times S_\sigma(n,l)\,S_{\sigma'}(n,l)\,N_\nu(l,\sigma)\,N_{\nu'}(l,\sigma')\,T_\tau(l,m)$$

$$\times T_{\tau'}(l,m)\,M_\gamma(\nu,\tau)\,M_{\gamma'}(\nu',\tau')\,D_\delta(\tau,\gamma)\,D_{\delta'}(\tau',\gamma')$$

$$\times A_\alpha(\sigma,\nu)\,A_{\alpha'}(\sigma',\nu')\;(-i)^\delta\,i^\delta\,2^{\sigma+\sigma'}$$

$$\times\frac{\Gamma(2l+\sigma+3)\,\Gamma(2l+\sigma'+3)}{[\Gamma(l+3/2)]^2}\;\left(\frac{z_f}{n}\right)^{2\sigma+2\sigma'-2\nu-2\nu'-\alpha-\alpha'}$$

$$\times\left(P_{oz}+v\right)^{2k+2k'}\;P_{oz}^{\,-2\tau-2\tau'+2\gamma+2\gamma'-\delta-\delta'}$$

$$\times\left(2\frac{z_f}{n}-2iP_{oz}\right)^{-\delta-\alpha}\;\left(2\frac{z_f}{n}+2iP_{oz}\right)^{-\delta'-\alpha'}$$

$$\times B\left(\delta+\alpha-i\eta z_f',\; l+\sigma+2-\delta-\alpha+i\eta z_f'\right)$$

$$\times B\left(\delta'+\alpha'+i\eta z_f',\; l+\sigma'+2-\delta'-\alpha'-i\eta z_f'\right)$$

$$\times\left(P_{oz}^2+\frac{z_f^2}{n^2}\right)^{a+b-c+5}\cdot B(c-b,\,b)$$

$$\times\;{}_2F_1\left(a,\,b;\,c;\,1-\frac{P_{oz}^2+\frac{z_f^2}{n^2}}{(P_{oz}+v)^2}\right)\qquad(27)$$

with

$$a = -(k + k' + \mu + \mu') ,$$

$$b = |m| + |m'| + \nu + \nu' + \tau + \tau' - \gamma - \gamma' + 1 ,$$

and

$$c = 2\ell + 2\ell' + \sigma + \sigma' - \alpha - \alpha' - \delta - \delta' - \mu - \mu' + 6 ,$$

where

$$\sigma^{OBK}_{n-n'}(v) = \frac{2^8 \pi Z_t^5 Z_P^5}{5 v^2 n^5 n'^3} \left(P_{0z}^2 + \frac{Z_t^2}{n^2}\right)^{-5}$$

is the OBK result for capture from the n-th shell of the target to the n'-th shell of the projectile. In particular, the capture cross section for the 1s -(n',ℓ',m') is of current interest and is rather simple, namely

$$\begin{aligned}
\sigma_{1s-n'\ell'm'}(v) = {} & \sigma^{OBK}_{1s-n'}(v) \cdot 5 \cdot \frac{\pi\eta Z_t'}{\sinh(\pi\eta Z_t')} \exp[-2\eta Z_t' \tan^{-1}(-P_{0z}/Z_t)] \\
& \times \frac{(n'+\ell')!\,(2\ell'+1)\,2^{2\ell'}}{n'(n'-\ell'-1)!\,[(2\ell'+1)!]^2} \cdot \frac{(\ell'-|m'|)!}{(\ell'+|m'|)!} \left(\frac{Z_P}{n'}\right)^{2\ell'} \\
& \times (P_{0z} + v)^{2\ell - 2|m'|} \sum_{j=1}^{3} \sum_{k,k'=0}^{n'-\ell'-1} \sum_{\mu,\mu'=0}^{\left[\frac{\ell'-|m'|}{2}\right]} \\
& \times C_j K_k(n',\ell') K_{k'}(n',\ell') H_\mu(\ell',m') H_{\mu'}(\ell',m') \\
& \times (P_{0z} + v)^{2k + 2k'} (P_{0z}^2 + Z_t^2)^{-2\ell' - k - k' + |m'| - j + 3} \\
& \times {}_2F_1\left(-k-k'-\mu-\mu', |m'|+1; 2\ell' + j - \mu - \mu' + 3; \right. \\
& \left. 1 - \frac{P_{0z}^2 + Z_t^2}{(P_{0z} + v)^2}\right) ,
\end{aligned} \tag{28}$$

where

$$C_1 = \frac{\eta^2 z_t'^2}{4 z_t^2 (\rho_{oj}^2 + z_t^2)} \quad ,$$

$$C_2 = \frac{\eta z_t' (\rho_{oj} - \eta z_t' z_t)}{z_t (\rho_{oj}^2 + z_t^2)} \quad ,$$

and

$$C_3 = 1 + \eta^2 z_t'^2 \quad .$$

III. Results and Discussion

In Sec.II we managed to obtain a closed form for the most general capture process, i.e. (n,ℓ,m) - (n',ℓ',m') transition for the bare projectile-hydrogenic target system. Because of the complexity of the results, we have checked several special cases. For example, we summed over the final m' level for a specific n' and ℓ' and compared the resulting expressions with that obtained previously[1,2] for the transitions 1s-1s, 1s-2s, 1s-2p, and 1s-3d; moreover, we compared our calculations with those done independently for the separate transitions, i.e. 2s-(n',ℓ',m') and 2p±1,0-(n',ℓ',m'). For all of these comparisons, complete agreement has been obtained. As mentioned in Sec. I, we are particularly interested in the case where the distinct final sublevels m' could possibly be experimentally distinguished in the near future[4,5], i.e., specifically, the transitions $Z_p + H(1s) \longrightarrow (Z_p + e^-)_{n'\ell'm'} + H^+$ for all n'=2,3 states. The cross sections of these specific processes are as follows,

$$\sigma_{1s-2p_0}(v) = \sigma_{1-2}^{OBK}(v)\, \mathcal{F}_1(\eta z_t', z_t, p_{0_3}) \cdot 5 \cdot z_p^2 (p_{0_3}+v)^2 \cdot \sum_{j=1}^{3} C_j\, A^{1-j}/(4+j) \quad , \tag{29a}$$

$$\sigma_{1s-2p\pm1}(v) = \sigma_{1-2}^{OBK}(v)\, \mathcal{F}_1(\eta z_t', z_t, p_{0_3}) \cdot \frac{5}{2} z_p^2 \sum_{j=1}^{3} C_j \frac{A^{2-j}}{(4+j)(3+j)} \quad , \tag{29b}$$

$$\sigma_{1s-3s}(v) = \sigma_{1-3}^{OBK}(v)\, \mathcal{F}_1(\eta z_t', z_t, p_{0_3}) \cdot 5 \cdot \sum_{j=1}^{3} C_j\, A^{-j} \Big\{ \frac{A^3}{(2+j)} - \frac{2^5}{3}\left(\frac{z_p}{3}\right)^2 \frac{A^2}{(3+j)} + \frac{11\cdot 2^5}{9}\left(\frac{z_p}{3}\right)^4 \frac{A}{(4+j)} - \frac{2^9}{9}\left(\frac{z_p}{3}\right)^6 \frac{1}{(5+j)} + \frac{2^8}{9}\left(\frac{z_p}{3}\right)^8 \frac{A^{-1}}{(6+j)} \Big\} \quad , \tag{29c}$$

$$\sigma_{1s-3p0}(v) = \sigma_{1-3}^{OBK}(v)\mathcal{F}_1(\eta z_t', z_t, P_{0z}) \frac{5\cdot 2^5}{3} \left(\frac{z_p}{3}\right)^2 \sum_{j=1}^{3} C_j A^{-j}$$
$$\times\left\{ \frac{A^2}{(3+j)} - 5\left(\frac{z_p}{3}\right)^2 \frac{A}{(4+j)} + 8\left(\frac{z_p}{3}\right)^4 \frac{1}{(5+j)} - 4\left(\frac{z_p}{3}\right)^6 \frac{A^{-1}}{(6+j)} \right\}, \quad (29d)$$

$$\sigma_{1s-3p\pm1}(v) = \sigma_{1-3}^{OBK}(v)\mathcal{F}_1(\eta z_t', z_t, P_{0z}) \frac{5\cdot 2^4}{3} \left(\frac{z_p}{3}\right)^2 \sum_{j=1}^{3} C_j$$
$$\times A^{-j}\left\{ \frac{A^2}{(4+j)(3+j)} - 4\left(\frac{z_p}{3}\right)^2 \frac{A}{(5+j)(4+j)} + 4\left(\frac{z_p}{3}\right)^4 \frac{1}{(6+j)(5+j)} \right\}, \quad (29e)$$

$$\sigma_{1s-3d0}(v) = \sigma_{1-3}^{OBK}(v)\mathcal{F}_1(\eta z_t', z_t, P_{0z}) \frac{5\cdot 2^7}{9} \left(\frac{z_p}{3}\right)^4 \sum_{j=1}^{3} C_j A^{-j}$$
$$\times\left\{ \frac{1}{2}\frac{A}{(6+j)(5+j)(4+j)} - \frac{P_{0z}+v}{(6+j)(5+j)} + \frac{(P_{0z}+v)^2 A^{-1}}{(6+j)} \right\}, \quad (29f)$$

$$\sigma_{1s-3d\pm1}(v) = \sigma_{1-3}^{OBK}(v)\mathcal{F}_1(\eta z_t', z_t, P_{0z}) \frac{5\cdot 2^6}{3} \left(\frac{z_p}{3}\right)^4 (P_{0z}+v)$$
$$\times \sum_{j=1}^{3} C_j \frac{A^{-j}}{(6+j)(5+j)}, \quad (29g)$$

and

$$\sigma_{1s-3d\pm2}(v) = \sigma_{1-3}^{OBK}(v)\mathcal{F}_1(\eta z_t', z_t, P_{0z}) \frac{5\cdot 2^5}{3} \left(\frac{z_p}{3}\right)^4$$
$$\times \sum_{j=1}^{3} C_j \frac{A^{1-j}}{(6+j)(5+j)(4+j)}, \quad (29h)$$

where

$$\mathcal{F}_1(\eta z_t', z_t, P_{0z}) = \frac{\pi\eta z_t'}{\sinh(\pi\eta z_t')} \exp[-2\eta z_t' \tan^{-1}(-P_{0z}/z_t)],$$

and

$$A = P_{0z}^2 + z_t^2 .$$

In table I, we have listed numerically the capture cross sections of the collision processes $H^+ + H(1s) \rightarrow H(n',\ell',m') + H^+$ with n'=2 and 3 for the proton energy ranging from 25 keV to 200 keV in both the eikonal and OBK calculations. Furthermore, to see the relative roles played by distinct final n', ℓ', m' sublevels, we have also plotted these cross sections, as a function of the proton energy, in Figs. 1 and 2. We notice that the eikonal result is about several times smaller than its OBK counterpart for all these transitions and is almost independent of the collision energy. To be more accurate, the curvatures of both eikonal and OBK curves (the cross section versus the collision energy) for a specific transition, i.e. $1s\text{-}(n',\ell',m')$ with n'=2 or 3, are very much alike except the two curves come a little bit closer as the energy increases.

In conclusion, we would like to point out that although our final expression, $\sigma_{n\ell m\text{-}n'\ell'm'}(v)$ of Eq. (27), is the most general result and is exact within the eikonal approximation, no direct experimental verification involving m'(magnetic quantum state) contribution has been reported yet. Since previous eikonal theoretical results[1-3] which are special cases of our present results agree well with existing experimental data, we have confidence in the theory presented in this paper. Detailed experimental measurement is needed to test the limitations of the general eikonal approach and therefore would be of great value.

Acknowledgement

It is a pleasure to thank Professor Jörg Eichler for stimulating discussion and correspondence. This work was supported in part by the Department of Energy under Contract No. DEAS05-80ER10749.

Appendix: The OBK formula for $\sigma_{n\ell m-n'\ell'm'}(v)$.

The OBK result which corresponds to our exact eikonal form has been previously obtained by Sil[16] only for the n=1 initial target state. By simply setting $Z_t'=0$ in our result, Eq. (27) the general OBK result may be obtained. Because of the complexity of that formula, we present here a simple and more transparent derivation of the OBK result. It should be noted that the OBK result has ten finite summations, whereas the eikonal result has 17, counting the hypergeometric function in each case.

We recall Eq. (8), namely,

$$\sigma_{n\ell m-n'\ell'm'}(v) = \frac{2^4\pi^4 Z_p^4}{v^2}\int\left\{\left|\mathcal{G}_{n'\ell'm'}(\vec{p}+\vec{v})\right|^2\left|G_{n\ell m}(\vec{p})\right|^2\right\}_{p_z=p_{oz}} d^2p_b. \quad (A1)$$

Notice that $G_{n\ell m}(\vec{p})$ in this case is just the Fourier transform of the spatial representation of the hydrogenic wave function $\varphi_{n\ell m}(\vec{r}_t)$, i.e.

$$G_{n\ell m}(\vec{p}) = (2\pi)^{-3/2}\int \varphi_{n\ell m}(\vec{r}_t)\, e^{i\vec{p}\cdot\vec{r}_t}\, d^3r_t \quad (A2)$$

which has been expressed in a closed form, Eq. (13), while $\mathcal{G}_{n'\ell'm'}(\vec{p}+\vec{v})$ is the same as before, Eq. (18). Substituting $G_{n\ell m}$ and $\mathcal{G}_{n'\ell'm'}$ in Eq. (A1) after some manipulations, gives

$$\sigma^{OBK}_{n\ell m - n'\ell'm'}(v) = \sigma^{OBK}_{n-n'} \cdot 5 \cdot 2^{2\ell'} \left(\frac{Z_p}{n'}\right)^{2\ell'} \frac{(n'+\ell')!(2\ell+1)}{n'(n'-\ell'-1)![(2\ell'+1)!]^2}$$

$$\times \frac{(\ell'-|m'|)!}{(\ell'+|m'|)!}\, 2^{2\ell} \left(\frac{Z_t}{n}\right)^{2\ell} \frac{n(n+\ell)!(2\ell+1)}{(n-\ell-1)![(2\ell+1)!]^2}$$

$$\times \frac{(\ell-|m|)!}{(\ell+|m|)!} \sum_{k,k'=0}^{n'-\ell'-1} \sum_{\mu,\mu'=0}^{\left[\frac{\ell'-|m'|}{2}\right]} \sum_{\nu,\nu'=0}^{n-\ell-1}$$

$$\times \sum_{\tau,\tau'=0}^{\left[\frac{\ell-|m|}{2}\right]} \sum_{\alpha=0}^{\nu+\nu'+\tau+\tau'} K_k(n',\ell') K_{k'}(n',\ell')$$

$$\times H_\mu(\ell',m') H_{\mu'}(\ell',m') D_\nu(n,\ell) D_{\nu'}(n,\ell)$$

$$\times T_\tau(\ell,m) T_{\tau'}(\ell,m) A_\alpha(\nu,\nu';\tau,\tau')$$

$$\times (P_{0_3}+v)^{2(\ell'-|m'|+k+k')} P_3^{\,2(\ell-|m|+\nu+\nu'-\alpha)}$$

$$\times \left(P_{0_3}^2+\frac{2\ell^2}{n^2}\right)^{-(2\ell+2\ell'+k+k'+\nu+\nu'-|m|-|m'|-\alpha)}$$

$$\times B(2\ell+2\ell'+\nu+\nu'-\mu-\mu'-|m|-|m'|-\alpha+5,\ |m|+|m'|+\alpha+1)$$

$$\times {}_2F_1\left(-k-k'-\mu-\mu',\ |m|+|m'|+\alpha+1;\ 2\ell+2\ell'+\nu+\nu'-\mu-\mu'+6;\right.$$

$$\left. 1-\frac{P_{0_3}^2+\frac{2\ell^2}{n^2}}{(P_{0_3}+v)^2}\right), \qquad \text{(A3)}$$

where

$$D_\nu(n,\ell) = \frac{(n+\ell+1)_\nu\,(-n+\ell+1)_\nu}{(\ell+3/2)_\nu\ \nu!},$$

and

$$A_\alpha(\nu,\nu';\tau,\tau') = \binom{\nu+\nu'+\tau+\tau'}{\alpha}.$$

References

1. F. T. Chan and Jörg Eichler, Phys. Rev. Lett. 42, 58 (1979); Jörg Eichler and F. T. Chan, Phys. Rev. A20, 104 (1979).
2. F. T. Chan and Jörg Eichler, Phys. Rev. A20, 1841 (1979).
3. Jörg Eichler, Phys. Rev. A23, 498 (1981).
4. R. K. Knize, F. M. Pipkin, and S. R. Lundeen, Abstracts, 7th International Conference on Atomic Physics, August 4-8, 1980, MIT, Cambridge, Mass. (MIT, 1980), p. 131.
5. R. K. Knize (private communication).
6. R. E. Olson and A. Salop, Phys. Rev. A16, 531 (1977); R. E. Olson, K. H. Berkner, W. G. Graham, R. U. Pyles, A. S. Schlachter, and J. W. Stearns, Phys. Rev. Lett. 41, 163 (1978).
7. M. C. R. McDowell and J. P. Coleman, Introduction to the Theory of Ion-Atom Collisions (North-Holland, Amsterdam, 1970).
8. J. N. Gau and J. Macek, Phys. Rev. A10, 522 (1974).
9. B. Podolsky and L. Pauling, Phys. Rev. 34, 109 (1929).
10. I. S. Gradshteyn and I. M. Ryzhik, Table of Integrals, Series, and Products (Academic Press, New York, 1965), p. 1029.
11. J. D. Jackson, Classical Electrodynamics, 2nd ed. (Wiley, New York, 1975), Ch. 3.
12. Ref. 10, p. 1030, Eq. 8932.1.
13. L. I. Schiff, Quantum Mechanics, 3rd ed. (McGraw-Hill, New York, 1968), p. 93.
14. Ref. 10, p. 950, Eq. 8384.1.
15. Ref. 10, p. 287, Eq. 3.197-9.
16. N. C. Sil, Ph.D. Thesis and Ind. J. Phys. 28, 232 (1954).

Table I: Calculated charge capture cross sections $\sigma_{1s-n'\ell'm'}$ (in 10^{-16} cm^2) for the reactions $H^+ + H(1s) \longrightarrow H(n'\ell'm') + H^+$, with n'=2 and 3, as a function of energy. The results for both eikonal (denoted by a) and OBK (denoted by b) are tabulated.

E_i (keV/amu)		25	50	75	100	150	200
n'ℓ'm'							
2 0 0	a	3.88(-1)	9.55(-2)	3.20(-2)	1.28(-2)	2.90(-3)	8.92(-4)
	b	1.84	4.93(-1)	1.62(-1)	6.27(-2)	1.33(-2)	3.87(-3)
2 1 0		6.10(-1)	1.12(-1)	2.80(-2)	8.83(-3)	1.39(-3)	3.25(-4)
		2.76	5.44(-1)	1.33(-1)	4.07(-2)	6.00(-3)	1.33(-3)
2 1 1		6.20(-2)	1.05(-2)	2.49(-3)	7.56(-4)	1.14(-4)	2.59(-5)
		3.05(-1)	5.73(-2)	1.35(-2)	3.99(-3)	5.66(-4)	1.23(-4)
3 0 0		1.35(-1)	3.26(-2)	1.07(-2)	4.23(-3)	9.40(-4)	2.85(-4)
		5.12	1.52(-1)	5.09(-2)	1.98(-2)	4.19(-3)	1.21(-3)
3 1 0		2.17(-1)	4.23(-2)	1.07(-2)	3.35(-3)	5.23(-4)	1.21(-4)
		8.01(-1)	1.86(-1)	4.78(-2)	1.48(-2)	2.20(-3)	4.87(-4)
3 1 1		2.04(-2)	3.70(-3)	8.93(-4)	2.73(-4)	4.11(-5)	9.34(-6)
		8.04(-2)	1.82(-2)	4.54(-3)	1.38(-3)	1.99(-4)	4.34(-5)
3 2 0		3.05(-2)	4.98(-3)	1.01(-3)	2.64(-4)	3.03(-5)	5.54(-6)
		1.10(-1)	2.12(-2)	4.38(-3)	1.12(-3)	1.23(-4)	2.14(-5)
3 2 1		6.92(-3)	1.08(-3)	2.14(-4)	5.46(-5)	6.11(-6)	1.10(-6)
		2.65(-2)	5.04(-3)	1.02(-3)	2.58(-4)	2.77(-5)	4.77(-6)
3 2 2		5.28(-4)	7.77(-5)	1.49(-5)	3.71(-6)	4.05(-7)	7.19(-8)
		2.13(-3)	3.98(-4)	7.94(-5)	1.98(-5)	2.09(-6)	3.56(-7)

Figures Caption

Fig. 1: Charge capture cross sections into a specified $n'=2,\ell',m'$ shell of the impact proton from the K-shell of a hydrogen atom, i.e. $H^+ + H(1s) \rightarrow H(n'=2,\ell',m') + H^+$, as a function of the impact energy. Solid curves are the eikonal calculations while dashed curves are the OBK calculations. Each curve is indexed at both ends by a set of three digits representing the hydrogenic quantum numbers n', ℓ', and m', respectively.

Fig. 2: Charge capture cross sections for the process $H^+ + H(1s) \rightarrow H(n'=3,\ell',m') + H^+$ as a function of the impact energy. Solid curves are the eikonal calculations while dashed curves are the OBK calculations. Each curve is indexed at both ends by a set of three digits representing the hydrogenic quantum numbers n',ℓ', and m', respectively.

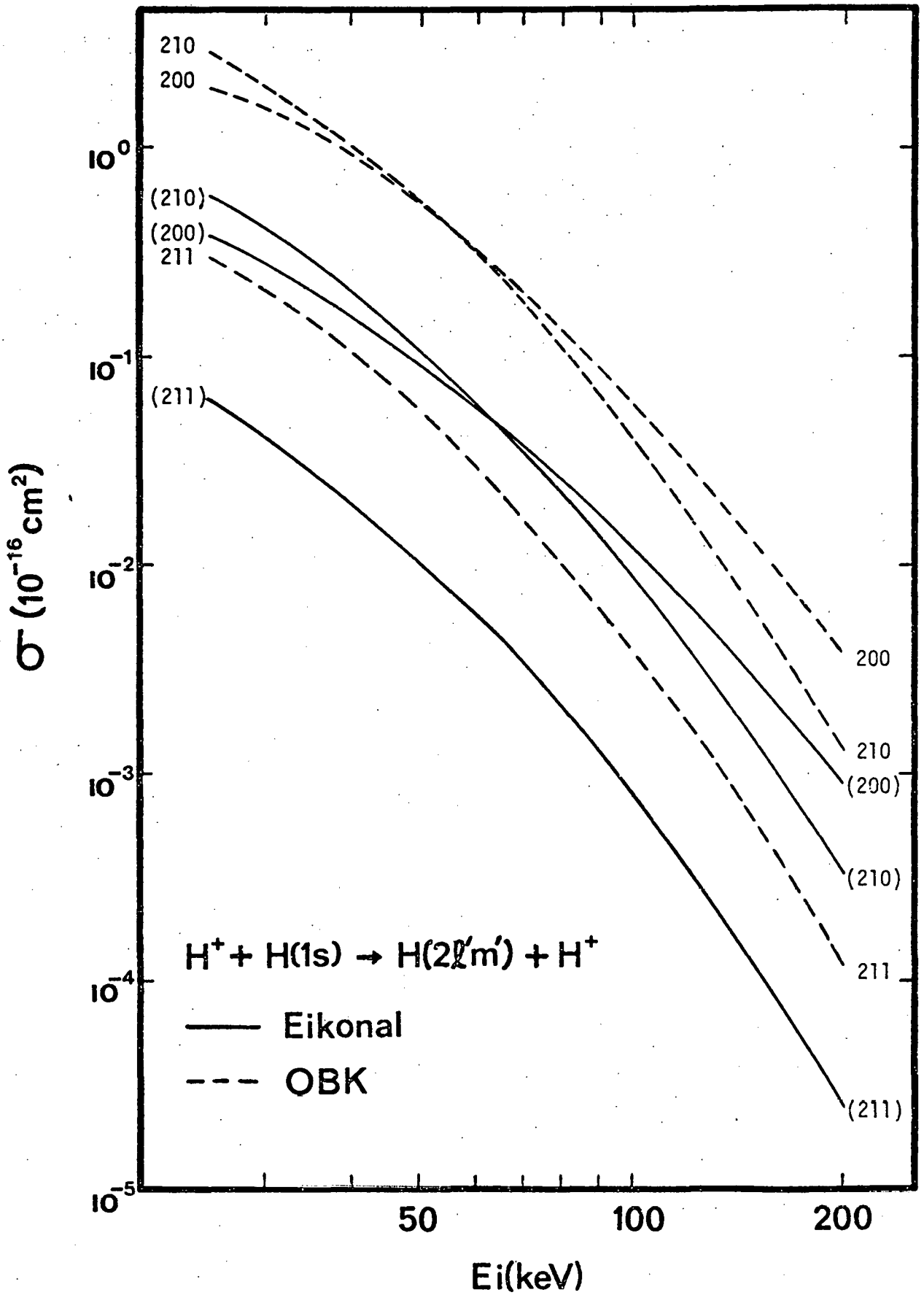
210
200
(210)
(200)
211
(211)
200
210
(200)
(210)
211
(211)
$H^+ + H(1s) \rightarrow H(2\ell'm') + H^+$
Eikonal
OBK
10^0
10^{-1}
10^{-2}
10^{-3}
10^{-4}
10^{-5}
$\sigma\ (10^{-16}\ cm^2)$
50
100
200
Ei(keV)

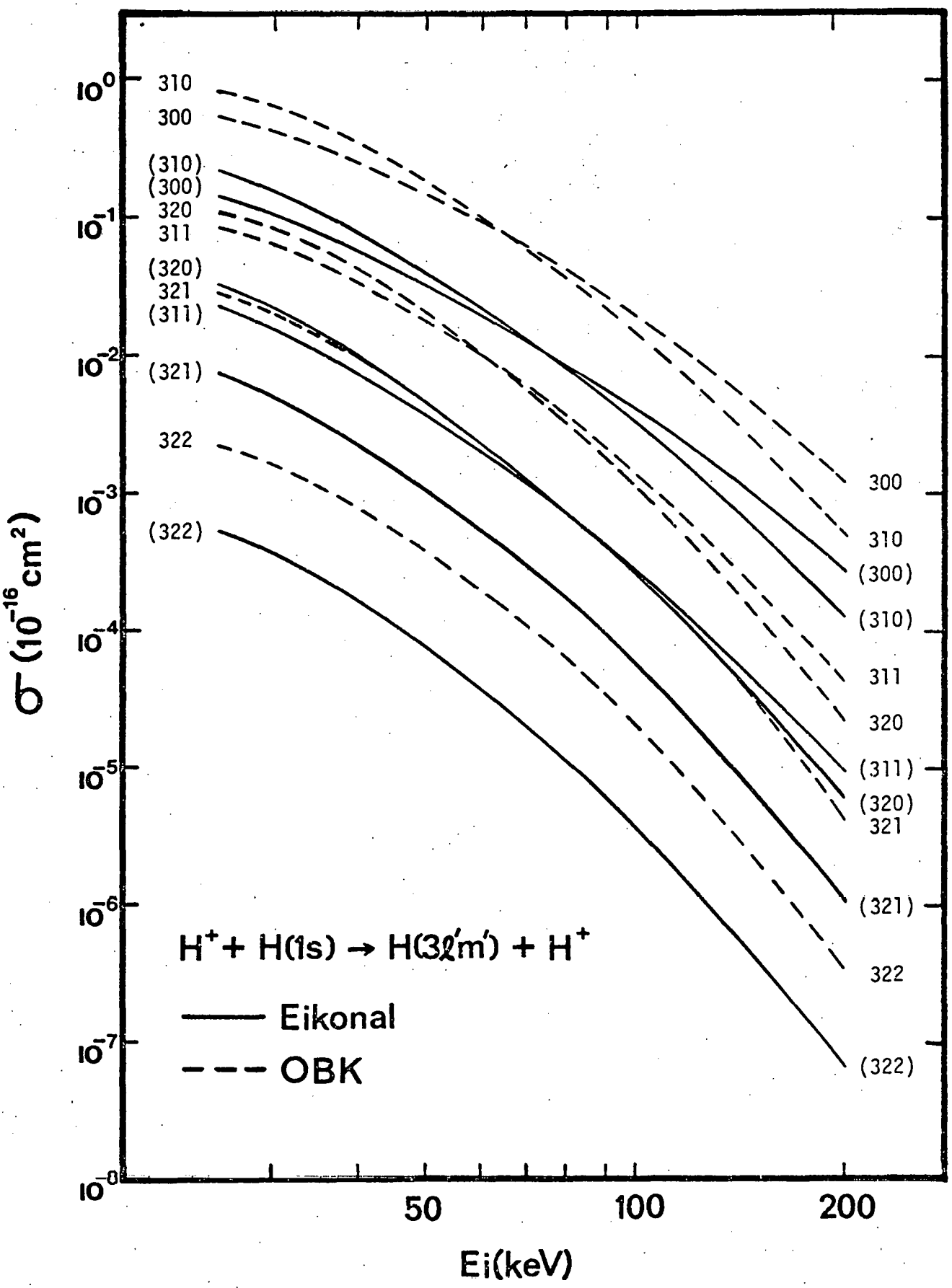
10^{0}
10^{-1}
10^{-2}
10^{-3}
10^{-4}
10^{-5}
10^{-6}
10^{-7}
10^{-8}
$\sigma\ (10^{-16}\,cm^2)$
310
300
(310)
(300)
320
311
(320)
321
(311)
(321)
322
(322)
300
310
(300)
(310)
311
320
(311)
(320)
321
(321)
322
(322)
$H^+ + H(1s) \rightarrow H(3\ell'm') + H^+$
Eikonal
OBK
50
100
200
Ei(keV)